ABSTRACT

CLEVELAND, THOMAS HILBURN. Effective Energy Metering of Solar Domestic Hot Water Systems for Inclusion in Green Power and Renewable Portfolio Standards. (Under the direction of Dr. Richard Johnson)

The goal of this metering experiment was to construct and validate a methodology to meter accurately, reliably, and affordably the amount of electrical energy offset by the collection of solar thermal energy in a solar domestic hot water (SDHW) system. Currently there are thermal energy meters on the market, but no generally accepted method for metering the thermal energy gain supplied by solar thermal collectors. An experimentally proven metering methodology that instills confidence in both consumers and policy makers would help open the door for the participation of domestic solar thermal energy in state or national Green Power and Renewable Portfolio Standards (RPS) programs. SDHW inclusion in such programs could significantly increase its use.

The experimental setup was a thermocouple-monitored three-meter metering system installed on a SDHW system in the NC Solar House. An electric energy meter recorded the energy supplied to the tank via the electric heating elements. The other two meters were thermal energy meters. One was positioned on the solar loop to measure solar energy collection. The other was attached across the water heater to measure the useful thermal energy in the hot water delivered to the house. Three separate months of data were collected, and extensive heat transfer analysis was carried out to model the system thermal losses. Then a TRNSYS model of the system was validated with the recorded data.

TRNSYS simulations indicated that the hot water load, as measured with a thermal meter, minus the electric energy input, as measured by an electric meter, plus the amount of energy lost by the tank (based on a standard experimental daily loss) is equal to the daily amount of energy offset by the use of the solar system. Even with extreme hot water draw profiles, this methodology worked exceptionally well for metering the amount of electric energy offset by the solar energy gain.

EFFECTIVE ENERGY METERING OF SOLAR DOMESTIC HOT WATER SYSTEMS FOR INCLUSION IN GREEN POWER AND RENEWABLE PORTFOLIO STANDARDS

by
Thomas Hilburn Cleveland III

A thesis submitted to the Graduate Faculty of
North Carolina State University
in partial fulfillment of the
requirements for the Degree of
Master of Science

MECHANICAL ENGINEERING

Raleigh

2004

APPROVED BY:

_____ _____

_____
Chair of Advisory Committee

Personal Biography

Tommy Cleveland was born and raised in Lumberton, North Carolina. As a youth, he was always interested in how things work and always wanted to "make something." These two interests led to a study of mechanical engineering at NC State University. His interests in energy, the environment, and the future of our planet led to his study of renewable energy. While a graduate student at NC State, Tommy became involved at the North Carolina Solar Center and was connected with this SDHW metering project while working there. He strongly believes in reducing the amount of energy used by humankind, particularly Americans, and in increasing the fraction provided by renewable sources.

Table of Contents

List of Figures

List of Tables

List of Symbols

Q	heat transfer rate
Cp	specific heat
ΔT	temperature difference
U	internal energy
u	specific internal energy
ρ	density
V	volume
q	heat transfer rate
r	radius
l	length
k	thermal conductivity
D	diameter
L	length
Gr_L	Grashof number
g	acceleration due to gravity
β	coefficient of thermal expansion
m	mass
ν	kinematic viscosity
Ra_L	Rayleigh number
Pr	Prandalt number
$\bar{h}_{air}$	average heat-transfer coefficient
$\overline{Nu}_l$	overall Nusselt number
α	thermal diffusivity
ε	emissivity
σ	Stefan-Boltzmann constant
E	energy
R_{insu}	thermal resistance
ΔIE	change in internal energy

Chapter ONE INTRODUCTION

Domestic hot water (DHW) systems consume about 3.5% (3.4 quadrillion Btus) of the total energy used in the United States each year, and make up 17% of the residential energy use [1]. This is more than the total annual energy use of the entire countries of Sweden and Switzerland, combined [2]. In the U.S., 39% of DHW systems are heated with natural gas and 54% are heated by electricity [3]. However, in North Carolina the majority of DHW systems are electric 59% [4]. About 65% (U.S. and NC) of the electric energy they use is produced by burning coal, oil, or gas at a power plant [2]. In North Carolina, almost all of the remaining 35% of electricity production is from nuclear power [4]. Less than one tenth of one percent of DHW systems in the US are solar domestic hot water systems (SDHW) That figure drops below 0.01% if you consider only the continental U.S. In a typical household, a solar domestic hot water (SDHW) system can supply most of the energy needed to heat hot water for the home each year. Of these three sources of energy for DHW, solar is the least polluting and the only one that is renewable.

The use of SDHW systems can be beneficial, even profitable, to both the end user and the utility serving the end user. Yet, there are still very few SDHW systems in use. The number has been rising at an increasing pace over the last few years, but is still barely scratching the surface of the DHW market. The factors that account for the low numbers are numerous, but leading the list are concerns about payback periods, reliability, and aesthetics. Federal and State incentives (refunds and tax credits primarily) have been

implemented to encourage the use of SDHW systems, but still the systems are few and far between here in North Carolina and in most of the rest of the country. Such policies do have a positive affect on the desirability of SDHW systems.

1.1 Renewable Incentives

The primary renewable incentives currently offered by the U.S., states, and even utilities, are partial purchase refunds and tax credits. Numerous such incentives are available for SDHW. There are currently no national refunds or tax credits, but this may change in the near future with the passing of a new energy bill that is currently in the works. North Carolina offers a 35% tax credit (capped at $1,400) on the purchase and installation price of a SDHW system. No North Carolina utilities offer a refund, but there are several utilities across the country that have had success with refund programs for SDHW systems. The refund program of SMUD, the utility in the Sacramento area in California, saw the installation of 2,800 SDHW systems in its first three years. However, many other types of renewable energy sources are eligible for another entire class of incentives, which is currently not available to SDHW systems. This other class of incentives is performance-based, or production-based. This type of incentive is awarded per unit of energy actually produced, as opposed to a flat award for each system installation or an award based on the system capital cost. These incentives are paid on top of the financial savings that occur naturally from the energy savings due to the use of the SDHW system.

The reason SDHW is not typically included in these types of programs is because it produces only thermal energy and other renewable energy sources produce electrical energy. A unit of electrical energy is always the same and can be readily transported long distances, easily used by countless devices, and metered very cheaply and accurately. This means that the electric energy produced in one location is valuable to anyone in the region, or even farther away, but this is not the case with the thermal energy produced by the SDHW system. Its use is limited to heating water or air for the building. It cannot be sent even down the street easily or efficiently, and it has no cheap and proven metering method. With all of this said, it does work great to heat water for house/building use, thus displacing the use of electricity or natural gas.

1.2 Benefits of Solar Domestic Hot Water Systems

The benefits of SDHW are numerous. Its environmental benefits are perhaps the most obvious. There are significant avoided emissions when solar energy is used in place of fossil fuels. Most water heaters are electric units and therefore get their power from the local utility, in North Carolina 63% comes from coal, 34% from nuclear, and about 2% from renewable (hydroelectric) [5]. According to Cragan, Klein, and Beckman [6] a three square meter SDHW system can save annually over 2 tons of pollution (3863 lbs of CO2, 25 lbs SO2, 0.05 lbs of N2O, 8 lbs of NOX, 0.06 lbs of CH4, and 0.5 lbs of particulates). Common non-electric water heaters are powered by natural gas, which also produces harmful emissions. However, SDHW systems have a tough time competing with natural

gas water heaters on a cost basis. Although, gas prices have been steadily rising, closing the gap in operating costs between them and electric water heater.

Environmentally, the benefits go beyond just these avoided emissions. There is also a potential for environmental damage caused by the mining and shipping of fossil or nuclear fuels that is avoided when utility power is not used. A more subtle, but notable, benefit is the effect of SDHW systems bringing a consciousness of energy production, use, and conservation. Consumers' mindfulness of these energy issues can bring about meaningful changes in their energy use. SDHW systems may serve as a device to increase public awareness of and interest in these important basic energy issues.

The benefits to some utilities of adding and using large numbers of SDHW systems may be the driving force behind many future performance incentives. If they are not the driving force, the benefits may be substantial enough for the utilities to view government directed incentives agreeably. There has been considerable research conducted on the benefits of SDHW systems to utilities. The main benefit to the utility is a peak demand reduction caused by the fact that almost all utilities hit their peak demand during the daytime, which is when SDHW systems are supplying energy to hot water. This means that those homes with SDHW systems need less energy from the utility at the time of the peak demand. This peak demand reduction is incredibility important to utilities at or near there maximum possible production level. In North Carolina, our utilities have a 12% to 15% reserve capacity [5]. As a utility approaches its production capacity, the cost to produce the next kWh of power increases. Therefore, when many utility customers are using SDHW systems at times of peak demands, the SDHW systems are essentially supplying that premium extra power to the utility grid in a decentralized manner.

Here in North Carolina, depending on the weather that year, the utilities can experience either a winter and summer annual peak. Winter peaks occur in the morning as everyone wakes up and turns up the thermostat and takes hot showers that cause electric water heaters to turn on as well. This tends to occur on very cold mornings, which in NC are usually clear nights and mornings. It is on these same days of clear weather that SDHW systems work well because there are no clouds to block the sun. However, the sun does not rise early enough to provide much of a morning peak reduction, unless the electric backup is programmed strategically to avoid morning energy use. This means in NC, in the winter, SDHW systems can offer peak demand reduction, but only with the right auxiliary strategy. A similar matching of summer peak and SDHW functionality occurs in the summer. In the summer, the peak is in the afternoon of a very hot weekday. Again, the same weather that causes the hottest days of the summer is also great for SDHW. On such days, although the hot water demand is not very high, many SDHW systems are able to provide all of the needed energy. This can mean meaningful peak demand reduction.

Engineering studies have found that when utility customers are using a significant number of SDHW systems each system offers a peak demand reduction of 0.2 kW to 1.0 kW [6, 7]. A large component of the cause of the wide range of peak demand reduction values is the difference in peak demand reduction in the summer versus the winter. The reductions seen in the winter are larger for two reasons. People use more hot water in the winter and the water mains are at a significantly lower temperature.

1.3 A Utility SDHW Metering Project

Still other benefits can be experienced by utilities that encourage their customers to use SDHW systems. These benefits include public image, increased market share, and possibly profitability. There are numerous utilities around the country, primarily in California, Florida, and Hawaii, that have active SDHW programs. Most of these programs consist of marketing and an initial rebate to the SDHW purchasing customer. So far, only one utility in America, Lakeland Electric in Florida, has a SDHW program that involves any energy metering. Under their program, interested customers must have their site approved by Lakeland Electric, and then the utility will come and install a utility owned SDHW system. The system includes a new 80-gallon solar storage tank with an electric heating element, an electric energy meter, and a thermal energy meter. For the life of the system, Lakeland Electric will monitor its performance and perform any needed maintenance, while the customer pays each month for the energy provided by the SDHW system.

With the help of the Florida Solar Energy Center (FSEC), Lakeland Electric designed a metering scheme to measure the energy provided by the SDHW system each month. To do this, each SDHW is fitted with a thermal energy meter that measures the amount of useful energy provided, in the form of hot water, to the home (reads in kWh) and an electric meter (kWh) that records the amount of electricity used to heat hot water. Both of these meters are read monthly and the customer is charged for the difference (kWh) between the two meters (at the same price per kWh as his/her electricity). This metering scheme means that the customers are not charged for the losses of the water heater tank.

These losses typically amount to around 15% of the energy consumption of a hot water heater. As a result, participating customers pay less than their neighbors who have electric water heaters [8].

1.4 Green Power and Renewable Portfolio Standard (RPS)

Even though some benefits of SDHW to utilities exist, implementing aggressive programs to promote them may not make good economic sense for many utilities. This is true partially because the cost of the pollution caused by the utilities is not fully included in the price of the power they produce. The same situation is the case for other renewable energy sources. In order to encourage the growth of renewable energy production Green Power programs have been developed by various utilities and Co-Ops. These programs allow customers to voluntarily pay a premium each month to have a portion of their energy come from renewable energy sources. This extra money is then used to purchase renewable energy at premium prices. Most of these programs are designed to offer different premiums, or incentives, for different energy sources based on the "greenness", the cost of production of the energy, and other factors.

A Renewable Portfolio Standard (RPS) is a program that requires all electricity providers to include a minimum percent of renewable electricity in the electric power supply portfolio they offer to their customers. Electricity providers may meet this requirement in a number of ways. They can generate the necessary amount of renewable electricity themselves; they can purchase it from someone else; or they can buy credits

from other providers who have exceeded the standard. They choose the option that is cheapest for them. Through credit trading, the RPS relies on the initiative of businesses to ensure that the standard is met at the lowest possible cost. Several states have implemented a RPS, and more have bills pending [9]. However, most of these programs do not include any credits for SDHW, although SDHW offsets other energy production. A convenient and affordable metering option would significantly increase its chances of being included in more RPSs.

North Carolina has recently started a statewide performance-based renewable energy program entitled NC GreenPower. It is the first statewide green energy program in the nation supported by all the state's utilities and administered independently by a nonprofit organization [10]. Under the program, utility customers are able to voluntarily purchase blocks of 100 kWh of green energy for $4. Commercial customers are able to purchase blocks of "less-green" energy for $2.50 per 100 kWh. The money collected through the voluntary monthly payments is then used to pay generators of renewable energy a premium on top of what they are receiving from their local utility. Just how premium of a price, or incentive, is paid depends on the type of power generation. The predicted premiums range from 18¢ per kWh for photovoltaic produced power to 2.5¢ per kWh for micro hydroelectric power. Wind, PV, micro-hydro, landfill methane, and biomass all claim a premium through the program, but SDHW is not eligible for the program, because it is not electricity based.

The program is still in its infancy and will surely change in the coming years as the program grows. There will be over a year delay between the first money collections and the actual purchase and use of green power. As the demand for more renewable energy

increases in NC, new renewable energy producers will arise. The goal of this paper is to provide an experiment based evaluation of methodologies to meter SDHW systems in North Carolina. The optimum metering scheme would be accurate, reliable, affordable, and easy to use. With a well-defined and validated metering methodology the author hopes NC GreenPower will consider including SDHW in its program. Because NC GreenPower is the first statewide green power program, its inclusion of SDHW would set a positive national precedent for future green power programs.

1.5 Solar Domestic Hot Water Systems

Before going into the details of the project work, a general description of the recent history and the state of the art of SDHW systems here in the United States and North Carolina will be given. Solar hot water systems have been available for many years. Their popularity peaked in the late-70s and early-80s due to federal tax credits and the scare of a national oil shortage. This heyday for SDHW systems crumbled rather quickly when the Reagan administration revoked the tax breaks in 1986. The large tax breaks and quick popularity of SDHW may have hurt the SDHW U.S. market in the long run. Hundreds of small SDHW system manufacturers and installers popped up across the country rushing to make a profit on the rapidly growing market in SDHW. Unfortunately, many of these manufacturers and installers did a rather poor job. So when the tax credits were revoked and homeowners no longer wanted to install solar hot water systems most of the companies went under, thus leaving thousands of orphaned SDHW systems on roofs across the

country. As these water heater systems malfunctioned often no one was available to fix them, and most users did not know enough to diagnosis and fix the problem. This trend of some low quality products, poor installations, and then no service infrastructure worked together to give the SDHW industry a bad name in many Americans' minds. Also unfortunately, many of these systems were not as aesthetically pleasing as many of today's SDHW systems. Because so many of these older less attractive systems were installed, and have been visible for many years, this is the image many American adults think of when they hear 'solar water heater.'

Over the years, various styles and types of SDHW systems have come and gone from the forefront of the market. However, they can all be put into one of two categories, active and passive. Passive systems have no moving parts and are therefore much simpler. Water is circulated through them using only natural convection. They are not as flexible as active systems because the water storage must be above or near the collector. These systems are common in more tropical climates. Here is North Carolina they do not offer adequate freeze protection, but in the proper climate zone they can be quite effective and economical. Because passive collectors do not work well here in North Carolina, they will not be further addressed in this paper. Active systems, which involve some controls and some type of pump, are able to collect a significant amount of energy, but the capital costs are often significant as well. They work well in every area of the state. They consist of a flat plate collector or rows of evacuated tubes, one or two storage tanks, a pump to move the fluid through the collector, valves, controls, and usually a backup source of energy.

All solar hot water heaters can also be easily characterized as either direct or indirect. The system tested in this experiment was a direct system. In all but very warm

climates, direct systems need some form of freeze protection to avoid costly damage to the system when the temperature drops below freezing. The system studied was a draindown system, the only common direct system. Draindown refers to how the water in the collector is drained out to a house drain in the evenings, or during other times when the sunlight falls below the required intensity. So, unfortunately, this design must allow a small amount (about 9 liters in our system) of heated water go unused and down the drain each day. However, the advantage of this system is that it is simpler, and therefore less prone to malfunction (although the primary valve is this system malfunctioned on several occasions), and less expensive, than the other common active system options. Today new draindown systems are quite uncommon, the most similar system is known as a drainback system.

Indirect systems collect the solar energy in a separate fluid from the potable hot water. These systems must include a heat exchanger to transfer the collected energy from the collecting fluid to the potable water. The main advantage of this type of system is that a collecting fluid other then potable water can be used. This is usually distilled water or propylene glycol. The freezing point of glycol is much less than that of water, so this fluid provides excellent freeze protection. Both of these fluids protect the collector and other system components from damage and/or scaling caused by hard water. A drainback system uses distilled water at atmospheric pressure. The system would empty the collector at similar times to a draindown system, but instead of going to a drain the water would be sent to a small insulated holding tank. Another common indirect system is the pressurized glycol system. Because this is a pressurized closed loop, a small expansion tank is required.

Although not a potable domestic hot water heater, pool heaters are usually a passive solar water heating system that is very popular, here in North Carolina and in other states with climates where pools are common. About 95% of solar water heaters produced in 2001 in America were solar pool heaters. Although they are not specifically considered is this study, they hold a potential for production based incentives. However, in the absence of the solar pool heater it is unlikely any other heater would be used in its place, thus bringing up the question of its value in the eyes of most incentive programs.

When replacing an electric water heater, a SDHW system typically has a payback period of 5 – 10 years. At current gas prices, the payback period when the solar energy is offsetting natural gas usage is somewhat higher. The exact payback period obviously is a function of many factors, but perhaps the greatest is how much hot water the household consumes. The more hot water consumed the faster the payback, but also the more money spent on backup heat for the system. Water conservation can have a huge impact on household hot water expenses. Wise use practices and flow restrictors in showerheads and faucets can limit the amount of hot water used. The set point of the thermostat in the water heater also plays an important role in the amount of energy used for hot water. Often hot water heaters come from the factory set at 135°F or 140°F, but this high temperature is not needed unless the house has a dishwasher without an automatic heater, which requires 140°F water. Otherwise, setting the thermostat at 120°F will reduce standby losses in the tank and still supply adequate hot water. In the case of a single-tank SDHW system, the benefits of a lower thermostat setting goes even further. In the case of a draindown system, the water sent to the collector is cooler and therefore is able to experience higher net energy

gains per pass through the collector. Similarly, in indirect systems, the heat exchanger is able to pass energy more effectively the lower the temperature of the potable water.

1.6 Project Summary and Goals

The experimental system in this paper attempted to represent a typical SDHW system in a North Carolina home. The system was retrofitted to a conventional low-cost electric water heater. The flat plate collector used measures 4' by 8', has a single glazing, and a selective surface coating. The pump used is a small DC Eic pump, powered by a 5W PV panel positioned on the roof with the flat plate collector. The system was outfitted with two thermal meters, an electric meter and a controlling datalogger in June of 2003. Readings from the three energy meters, seven thermocouples, and two flow meters were averaged and recorded every five minutes by the datalogger. The datalogger also controlled the draw profile enforced on the system. An analysis using this data, radiation and weather data, and the characteristics of the system was performed to understand the dynamics of the system and the meters. From this analysis and from information on commercially available energy meters and other sensors, several metering methodologies were evaluated. The goal of this experimentation, analysis, and evaluation was to provide an accurate, reliable, robust, and affordable metering scheme for SDHW systems in North Carolina. It is hoped that validation of such a metering scheme will lead to the inclusion of SDHW systems in NC GreenPower and other renewable energy incentive programs.

Chapter TWO EXPERIMENTAL SETUP

2.1 Original System

The experiments in this study were performed on a working draindown SDHW heater in the North Carolina Solar House (Fig. 2.1). This house is open to the public six days a week in Raleigh, North Carolina. The SDHW system that was studied was installed by the NC Solar Center staff over 5 years ago. The level of use was very low before the author applied a water draw profile. The house is occupied daily by a house manager and one to three graduate students during working hours, but it has been many years since anyone has resided in the house. This means that typically the only hot water used is for hand washing. Prior to the author's experiment, electricity had not been wired to the tank because the solar energy alone had been enough to supply all of the hot water

Figure 2.1 Original System (collector not shown).

demand.

The solar system installed at the Solar House was chosen to represent an affordable system that was readily available and would work well in North Carolina. However, since its installation, this system model (controls and valves) has been discontinued. The system is a Solar Sidebar, manufactured by Heliotrope General. It will likely be replaced at the Solar House in the near future in order to display to the public solar products which are currently on the market. The Solar Sidebar is a PV-powered pumping module for active solar water heating systems with draindown freeze protection. The assembly is mounted to the side of an existing gas, propane, or electric water heater and includes all of the working parts of the solar system except for the actual collector, the 10 Watt PV panel to power the pump, and the air release valve. The fact that this system can be retrofitted to an existing hot water system is very attractive for some because it significantly reduces the cost of adding a SDHW system.

The control portion of this valve assembly is located next to the spool valve. It contains a wax phase-change thermostat heated by a tiny electric resistive heater powered solely by the PV panel. Before any sunlight begins to hit the small PV panel the thermostat is at room temperature. Then as the sun comes up and hits the PV panel the resistive heater slowly begins to warm up the thermostat, which starts to expand. This expansion moves a spool valve, which after moving a certain distance opens a pathway for the warm water at the bottom of the hot water tank to rush up into and fill the solar collector. This filling of the system occurs rapidly without the use of any pumps because the water in the tank is at the system water pressure and there is an air release valve at the highest point in the system. With adequate sun, the thermostat continues to expand after the filling of the

collector, and a short time later, it reaches full extension, closing the switch to supply power to the solar pump. The solar pump is a small 12 Volt DC PV-powered static impeller driver (Sid) pump that has no moving parts apart from the actual impeller.

When the power is supplied to the solar pump it is usually enough to keep the pump pumping at its maximum flow rate, but at low irradiation levels the pump may operate at a reduced flow rate. At the end of the day when the sun is low in the sky, or during overcast periods, the insolation will not be intensive enough to keep the control switch closed. At this time the pump stops, but the water remains in the solar loop. The system was designed so that when there is enough sunlight to provide a net energy gain to the water the pump will run. If the solar intensity continues to fall, eventually it will not be enough to keep the thermostat warm enough to keep the spool valve open. At this time, the valve will close off the connection between the solar loop and the tank and will open a connection between the solar loop and a drain. With the help of the air valve at the top of the collector, all of the water in the collector is drained, about 2.25 gallons total. This cycle of filling and draining typically occurs just once each day, but a several times each year on days of dynamic weather, this cycle will happen more than once.

The collector that the water is pumped through is a typical flat plate collector. It measures 4' by 8' and contains a single layer of glazing. Alternate Energy Technologies from Florida produced the collector and Solar Rating & Certification Corporation (SRCC) certified it. The frame is made of anodized aluminum, the cover is low iron tempered glass, the absorber materials are copper, and the absorber has a selective black coating. The insulation on the sides and back is polyisocyanurate. The linear efficiency equation given by SRCC shows the collector has an $F_R\tau\alpha$ value of 0.706 and a F_RUL value of -

4.9099 $W/m^2 \cdot °C$. The collector is mounted on the south facing roof, which faces exactly south. The pitch of the roof is 35°, which is effectively equal to the latitude of Raleigh, NC, 36.1°. The piping to the collector is 61 feet long and passes through one entire living floor and partially through the unconditioned attic. Three quarter inch thick rubatex insulation covers most of the pipe, but over 6 feet are uninsulated. The uninsulated sections are mainly in tight quarters where its installation would be difficult. The return pipe is about 50 feet long with less than 2 feet left uninsulated.

Also included in the Solar Sidebar assembly is a rotameter flow meter and a digital thermometer. The rotameter is a transparent ½" flow meter that allows the user to read the volumetric flow rate of the water passing through the solar loop as indicated by the height of the bob in the meter. This flow provides an otherwise unavailable means for the owner to determine the speed of the water flow in the solar loop. The function of the digital thermometer is also to give the user or maintenance worker a view of the operation of the system. The thermometer measures the temperature of the water returning from the solar loop and the temperature of the water near the center of the tank.

This assembly connects with the existing hot water heater via the drain on the front of the bottom of the tank. The supply and return lines of the solar loop are concentric where they enter the tank and in this way share the single opening in the tank. The hot water supplied to the house leaves from the top of the tank. The cold makeup water enters the shell of the tank at the top, but then flows through a dip tube allowing it to enter the tank at the bottom as to not cool the soon-to-be-used hot water at the top of the tank. The tank is an off-the-shelf 50 gallon electric water heater produced by U.S. Craftmaster. This water heater is not a top-of- the-line high efficiency heater, but rather one of the cheapest

models. It has a rated Energy Factor of 0.86, which means when standardized testing was conducted on this unit, 86% percent of the energy input was returned in the form of hot water and the rest was lost. At the start of this project, 0.86 was the minimum allowable Energy Factor for a 50 gallon tank, however, as of January 2004 new standards took affect that required all new electric water heaters to have an Energy Factor of no less than 0.90. The tank in this system is covered with an insulating blanket that slightly raises the Energy Factor of the tank. The losses affecting the energy factor occur from not only the tank itself, but also the pipes near the tank. There is essentially no energy loss transferring the electric energy into thermal energy by the heating elements. This can be misleading because there are significant losses producing the electric energy at the power plant and as much as 10% lost in its transmission from the plant to the point of use.

The tank has two resistive heating elements, each able to provide 4500 Watts to the hot water. The elements are at different heights in the tank, approximately 1/3 and 2/3's of the height of the tank. Connected to each element is an operable thermostat. Each thermostat may be set independently, but like most electric water heaters, it is wired so that power is only sent to one element at a time. From the factory, both of the thermostats came set at 135°F. Although both thermostats are set to the same temperature, they do not work exactly the same. The dead band (the temperature difference between the set point and the temperature at which it receives power) of the top thermostat is much larger than the dead band of the bottom thermostat. The top element almost never provides any heating. This is because besides having the larger dead band, hot water use causes cold makeup water to enter the tank at the bottom and drastically drop the temperature near the bottom thermostat

while having very little affect on the temperature of the water at the top of the tank. Moreover, the natural buoyancy of hot water causes the tank to stratify.

2.2 Metering System

The metering system added to the original system described above was designed to test possible SDHW metering methodologies. The goal of the metering/monitoring system was to closely monitor the system and the metering values simultaneously in order to understand each metering method as fully as possible. The brain of the monitoring system was a Campbell Scientific CR-10X datalogger. All of the data probes in the system connected to the CR-10X. It collected each data point every 2 seconds and then averaged each temperature reading and summed each pulse counter variable every five minutes. This 5-minute data was then written to internal storage in the datalogger where it could be downloaded to a computer for collection and analysis. Three energy meters and seven thermocouples performed the data collection. Two of the energy meters were thermal energy meters, also known as BTU meters. These meters determine how much energy was added to a stream of water. One meter was located across the water tank. This meter measured the energy used by the house in the form of hot water. This meter is referred to as the house meter or the load meter, and the pipes carrying the water through this meter are referred to as either the house pipes or the load pipes. The other thermal energy meter was located in the solar loop and measured the solar energy collected. This meter is referred to as the solar meter. The third meter was an electric energy meter, which measured how

much electric energy was used by the heating elements. The diagram below shows the monitoring/metering system which is explained in detail in the following sections.

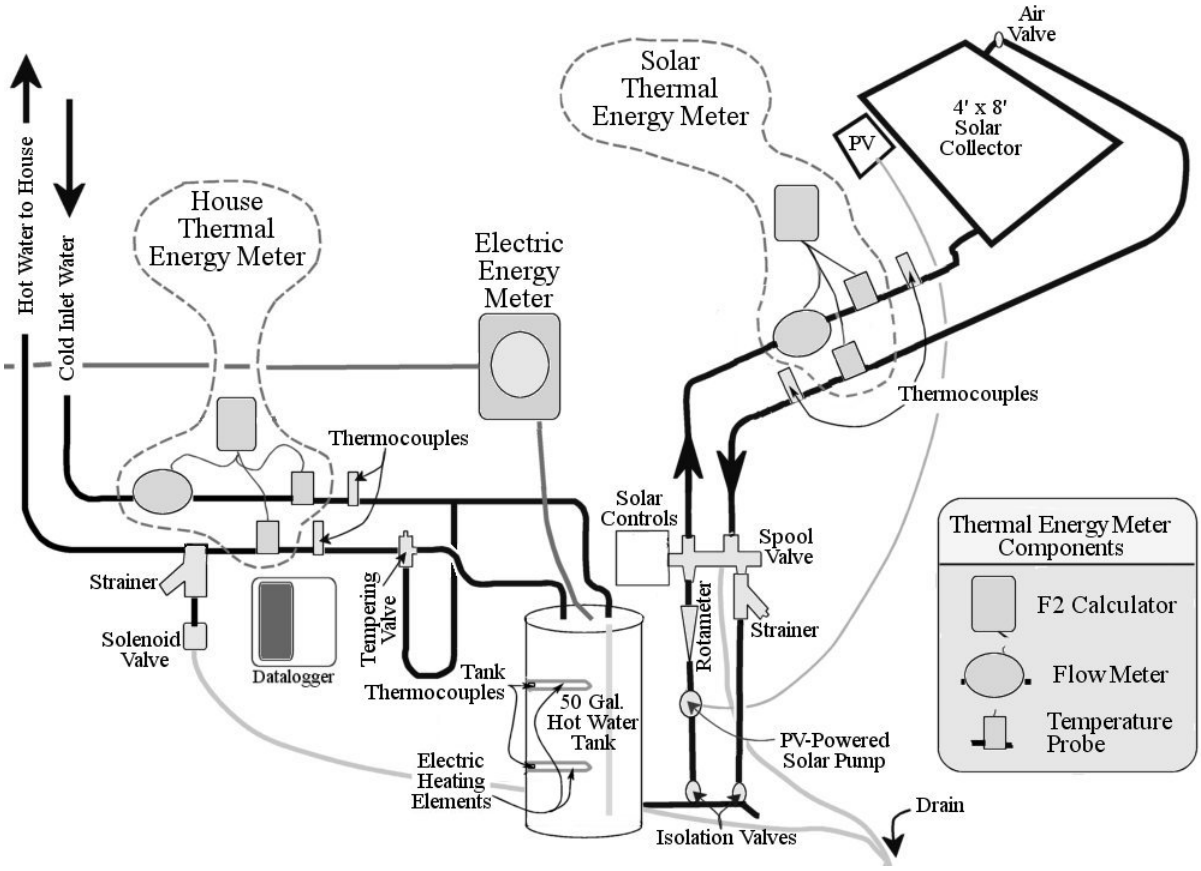

Figure 2.2 System monitoring diagram

2.2.1 System Meters

A thermal meter, or BTU meter as they are often known, is able to meter the energy added to a fluid. Each meter must take three different measurements, calculate the energy

flux, and then integrate these energy flux readings to give an energy meter reading. Each meter measures the temperature of the fluid entering the heating system, the temperature of the fluid leaving the heating system, and the volumetric flow rate of the fluid. The energy flux can then be calculated if the type of fluid is known. (The meters used only work with water) With this information, the specific heat of the fluid, at the average temperature of the two flows, may be looked up. The energy flux is then calculated as shown below,

$$Q = Cp \cdot \frac{m}{s} \cdot \Delta T \qquad (2.1)$$

where ΔT is the difference in temperature of the two fluid flows. Each thermal meter recorded these three readings every few seconds, integrated them, and added the result to the total energy metered so far.

Small thermal meters of the size that would work well for a solar system are sold typically to sub meter hot water use. This may be done in an apartment building, an industrial facility, or anywhere there is a large central water heater. They are commonly used in Europe in apartment buildings where a central water heater is common. They are not as common in the United States where the tendency is for each apartment to have its own hot water heater, therefore negating the need to sub meter the hot water. The product name of the thermal meters used in this project is F2 Thermal Calculator. The two flow meters are different sizes because the house pipes are all ¾ inch pipe and the solar pipes are all ½ inch pipe. The calculator of this meter is shown in Figure 2.3. The flow meter and the temperature probes of the house meter are shown in Figure 2.4. Both of the system meters were made by ABB, a Swedish company. However, Elster-Amco recently bought ABB.

Figure 2.3 Thermal Energy Calculator

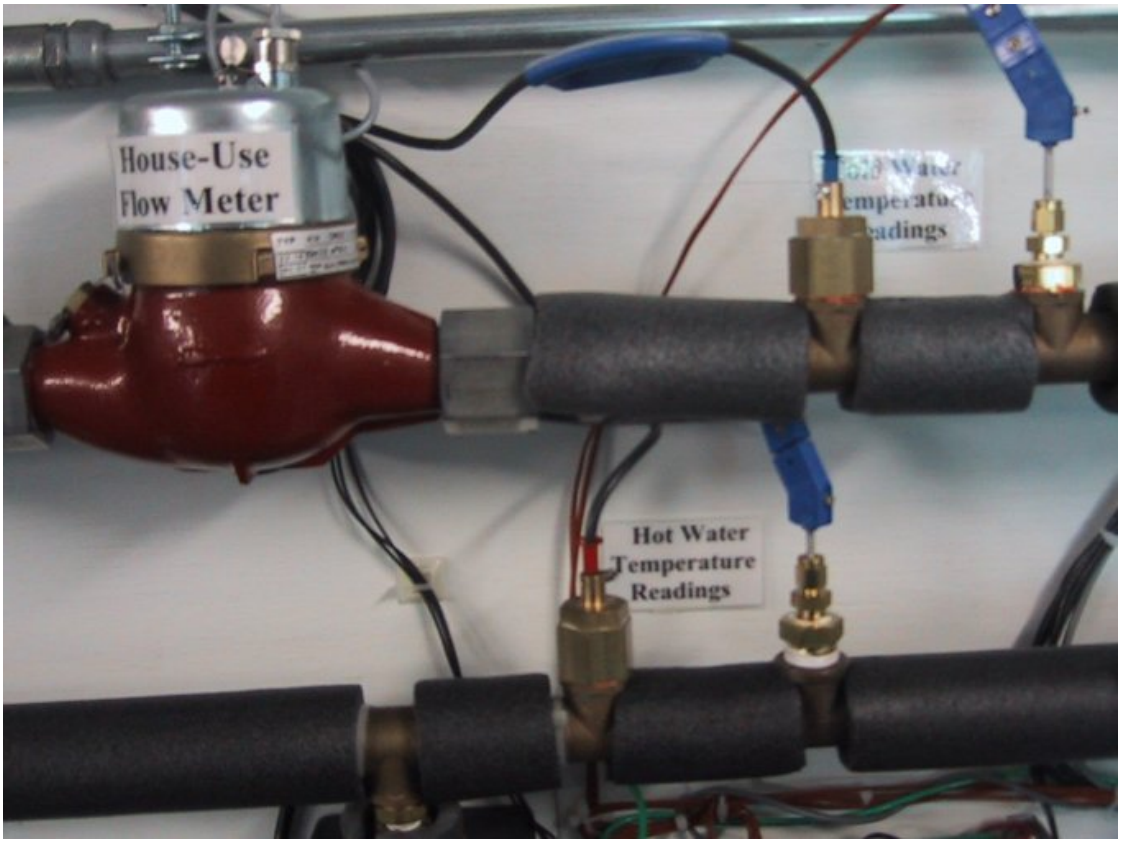

Figure 2.4 House Flow Meter and Temperature Probes

As with most any technical product there is a tradeoff between accuracy and cost with thermal meters. Because there are three discrete readings and an integration required to produce the final metering, there are numerous sources of error, which are capable of compounding. Temperature sensors are accurate to within plus or minus some number, or fraction, of degrees. In a thermal energy meter, the actual temperatures of the flow are not very important to have accurately, but the difference in the two temperatures is very important to know accurately. In the case of the solar loop, temperature differences of only 10°F are typical. For this reason, matched pairs of temperature sensors are provided with each meter. This improves the accuracy of the temperature difference reading over using two random sensors of the same accuracy.

The flow meter for a thermal energy meter also needs to be very accurate. There are different types of flow meters that will work with free flowing fluids such as those used in a SDHW system. The flow meter for a thermal energy meter must have a digital output signal that can be sent to the calculator portion of the meter where the calculations are performed. The flow meter of the thermal energy meter used in this project is a positive displacement flow meter that uses a paddle wheel. As the paddle wheel turns, all fluid that passes through the meter is caught in between the legs of the paddle wheel. Since the volume of each of these regions is known and RPM of the wheel is easily measured the flow rate can be calculated by the meter. The temperature probes are

Figure 2.5 Temperature Probe Assembly

thermistors that sit in brass sleeves that are in the flow of the water. The researchers had much, unexpected, difficulty mounting the provided brass sleeve because the threading was different from those available in the US. An adapter was eventually found, but this unfortunately greatly increased the thermal mass of the temperature array and severely limited the depth of submersion of the tip of the temperature probe in water in the pipe. This large adapter may be seen in Figure 2.5. Both of these effects of the additional adapter made the temperature probe respond slower to temperature change. The performance of the probes in the proper setting was unable to be tested, but it is assumed the temperature time response would be improved. The affect this had on the accuracy of the data was limited because thermocouples were used to record the same temperatures independently. This issue is discussed fully in chapter 3.5.

The research done concerning the choice of the thermal meter for this project was actually completed by the Florida Solar Energy Center and Lakeland Electric. They researched to find a thermal meter that was affordable yet accurate enough for their SDHW metering project in Florida. Because the goals of this project are so similar to those of the Florida project it made sense to use this same meter. The meter of choice is the F2 Thermal Energy Calculator by The ABB Group. The meters used for this project cost about $500 a piece. ABB states that they have a maximum permissible error of 1.5% when there is a temperature difference of just 2 °C, the maximum permissible error decreases as the temperature difference increases

The meters have an LCD screen on the front of the calculator which is able to display, accumulated energy, accumulated volume, instantaneous energy flux, instantaneous flow rate, two temperature readings, the temperature difference, and several

other minor values (Figure 2.3). In the experimentation, only two values were collected by the datalogger from each thermal energy meter. This was because the meter was only able to digitally output two values, energy and flow volume. This output was in the form of switch closures. On the energy channel, one switch closure occurred for each tenth of a kWh, and on the flow channel, one switch closure occurred for each liter. The method required for this and how the closures were accounted for inside the datalogger is further discussed in the datalogger subchapter. Since only these two outputs were possible from the energy meters, additional thermocouples were used to monitor the temperatures of the water flows. A thermocouple was placed three inches downstream of three thermal energy meter temperature probes and upstream from the temperature probe in the hot water line supplying the house (Figure 2.2). The specifics of these thermocouples are given later in the thermocouple section, Chapter 2.2.3.

The two thermal energy meters measure the net energy added to the flows of water in the system, but an electric energy meter is needed to measure the electric energy supplied to the tank. An electric energy meter is much simpler, less expensive, and more accurate than a thermal energy meter. The meters work on the principle of electrical induction. The induction forces rotate a shaft in proportion to the electricity flow. The shaft then turns a series of gears that rotate a series of number wheels to display the accumulated energy. The experiment required a digital output so that it could be recorded by the datalogger. This output was provided by an optical eye device built into a normal electric meter. The eye 'watches' the indicator wheel turning and closes a switch each time 0.01 kWh has passed through the meter. The error of such an electric meter is very tiny. The heating load is a purely resistive load.

The cost of the meter in this experimental setup was substantially greater than what would be required for a non-experimental meter. GE manufactured the meter and Square D made the meter base (Figure 2.6). The meter used is this system cost about $100, but the same meter without the digital output would cost about $45. The cost to install such a meter would be about $75. The accuracy and reliability of watt-hour meters compared to thermal meters, particularly when the price is considered, is exceptional.

Figure 2.6 Electric Energy Meter

2.2.2 Datalogger

The datalogger in the monitoring system serves both to record measurements and to control the hot water load on the hot water system. The datalogger used is the CR10X from Campbell Scientific, Inc.(Figure 2.7). It is one of the most widely used low-cost dataloggers in the data acquisition field. The unit is very versatile. It can accept a very wide range of inputs, provide numerous types of outputs, and this all controlled with a user

input program running in the datalogger. It is this program that controls how all the inputs are handled and how all outputs are used. The program is entered by the user in up to three different program tables. Program Table 1 must contain the primary program to be executed by the datalogger. Program Table 2 is a table for an optional second program. Program table 3 is available for programming subroutines which may be called by instructions in Tables 1 or 2 or by a special interrupt. No interrupts were used in the data collection for this experiment. The program(s) in Tables 1 and 2 are each executed at a user-entered execution interval. That is to say that each program table runs once through at evenly timed intervals. The interval used by the researcher in this experiment was 2 seconds.

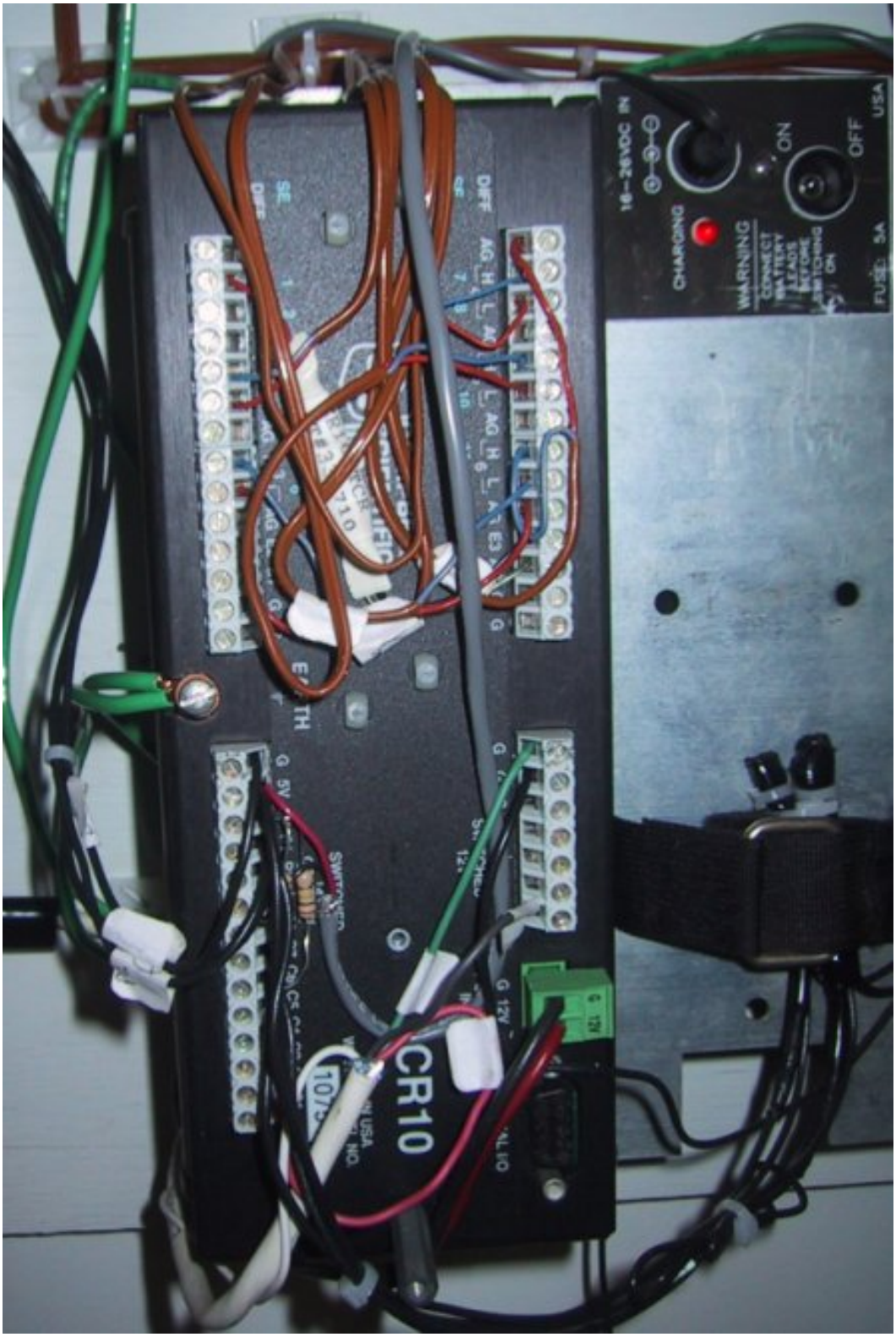

Figure 2.7 CR-10X Datalogger in Use

This interval means that every reading taken by the datalogger is collected every 2 seconds. This is too small of a time step to be practical for final storage, but it is needed to accurately measure the changes in the system. Data is stored to final storage on a different user-entered interval, 5 minutes in this case. So, every 5 minutes all of the 2-second data over the last 5 minutes are either averaged or integrated over the period and written to final non-volatile memory. The datalogger has an internal clock so that an accurate time can be recorded at each data point. This internal clock also makes it easy to impose a daily hot water draw profile on the system. This draw profile and its execution are discussed later in this subchapter.

This experimental setup required the datalogger to read two different types of inputs, switch-closure inputs from the thermal and electric energy meters, and voltage differentials from the thermocouples. These inputs must be connected to the proper type of input port. This was rather simple for the six thermocouples and the one reference thermistor because there were adequate input connection locations. However, serious difficulties occurred when all the needed switch-closure inputs where attempted to be wired to the CR10X. There were five total switch closure inputs (a type of pulse input) to be connected to the datalogger from the three energy meters. Each of the thermal energy meters are able to export only two outputs; volume and energy, although for each measurement it takes it 'knows' 4 different values; the two temperatures, the volume of flow, and the energy added. The electrical meter has only one value to output, energy, and it does so with switch closures as well. It did not cause any difficulty.

The difficulty arises because the output channels on the F2 thermal energy calculator share a common ground lead and because they are also input channels. Each

output channel has two contacts, one of which is a common reference contact. These two contacts are momentary internally connected to send a 'pulse output' to signify a unit of either energy or fluid volume passing the meter. When the output is connected to one of the CR10X pulse inputs the output channel is connected to the datalogger pulse input and the common reference contact from the F2 is connected to the datalogger ground. The CR10X pulls the input to 5V when the switch is open, and when the switch is closed, the pulse input is at ground. In this configuration, everything works perfectly, but the CR10X has only two of these channels dedicated as only pulse input channels. Yet four are needed for each of the two pulse input channels from each of the two thermal energy calculators.

The CR10X also has three multipurpose control ports, labeled C6, C7, and C8 that can be used as pulse input channels. However, they function slightly differently. Instead of the F2 output switch being connected between the input channel and ground the control ports require the switch to be connected between the input channel and 5V. This results in the common reference contact in the F2 calculator being raised to 5V. When the switch is open, the control port is pulled to ground by an internal 100K ohm resister. When the switch is closed, the control port is at 5V. The problem is the reference contact in the F2 is held around 5V, which causes the calculator to treat the two output channels as inputs instead, and the desired output functionality of the channels is lost.

Two small circuits utilizing switching transistors were designed and constructed to allow the F2 outputs to work with the control inputs in the CR10X. The circuits allow the common lead in the F2 to remain at ground, and the F2 output channels to be connected to 5V on the CR10X via the switching transistor and a small resistor. When either switch in the F2 is closed a small current flows through the switch side of the transistor, thus

connecting the control port on the CR10X to the output channel of the F2. This pulls the control port down to ground, 0V, while the switch is closed. Once it reopens the transistor breaks the connection between ground and the control port, but it is still connected to 5V through a large 100K ohm resistor, thus it returns to 5V. This circuitry results in the control ports being in the opposite state than they would be in if the F2 could be wired as the datalogger expected. With this taken into account, the CR10X counts the pulse when the switch opens.

Every one of these pulses is counted and the total for the last five minutes is recorded each five minute period. The datalogger counts each pulse regardless of the execution interval. All other functions of the datalogger occur just once per execution interval. The thermocouples are read every other second and averaged every five minutes. The output of the datalogger, the hot water draw imposed on the system, occurs less regularly. It is controlled by some simple logic in the datalogger program, which is executed every other second. The draw profile used is discussed in detail in chapter 2.2.4, but the basic logic is explained below.

The CR10X is able to supply 5V, but only tiny currents, to several output channels to provide controls to a system. The CR10X can also supply 12V, at a small current, but neither of these are enough power to operate the solenoid valve. An external relay driver circuit was built to allow the 12V output from the CR10X to operate a relay because the port itself has such a limited drive capability. The relay then completes the power current supplying 120 Volt AC power to the solenoid valve. When this valve receives power it opens and allows hot water from the top of the tank to flow out to a drain in the house. This hot water flow is recorded by the datalogger, just as is any other hot water used in the

house. A running total of the hot water usage is kept each hour. When the amount of hot water used in the house is less than specified by the draw profile for that hour the logic in the datalogger opens the valve at 50 minutes past the hour. As soon as the correct amount of hot water has been drawn from the tank, the voltage is removed from the output channel and the solenoid valve rapidly closes.

The datalogger is powered by a 12V battery pack attached to the back of the base the CR10X is mounted on. The battery is kept charged with a DC wall adapter plugged into 120V AC power.

2.2.3 Thermocouples

The system used six thermocouples and one thermistor to monitor the temperatures in the system. The location of these thermocouples and the one thermistor are shown in Figure 2.2. As mentioned before, some of these thermocouples were installed to measure the same temperatures measured and used by the thermal meters because there was no method available to send their temperatures to the datalogger. The unexpected benefit of this was that the fast temperature response of the thermocouples exposed the slow response of the thermal meter temperature sensors caused by the additional pipe adapter required. These temperatures were used with the flow readings from the thermal meter flow meter to calculate a second version of the thermal energy meter readings, referred to simply as the calculated energy meter readings. However, this calculated version of the thermal energy meter readings was often much more accurate than the actual meter readings because the

slow response of the temperature probes used by the thermal energy meter caused them to underestimate the beginning of most flows. This issue is discussed further in Chapter 4.

Figure 2.8 Pipe Thermocouple

The CR10X determines thermocouple temperatures by first reading the temperature of the reference junction with the thermistors so that it can adjust for the fact it is not at 0 °C. The CR10X calculates the voltage that a thermocouple of the type specified, type T for all six thermocouples, would output at the reference junction temperature if its reference junction were at 0 °C, and adds this voltage to the measured thermocouple voltage. The temperature of the measuring junction is then calculated from a polynomial approximation of the National Bureau of Standards thermocouple calibrations. [11]

The thermistor used is made by Campbell Scientific for the CR10 series datalogger. It is used to measure the temperature of the reference junction, which are the terminal strips of the CR10X. The accuracy of this measurement is a combination of the thermistor's interchangeability specification, the precision of the bridge resistors, and the polynomial error. In a "worst case" example, all errors add to yield a ±0.4°C error. It is emphasized that this is the worst case. Campbell Scientific's experience shows that the overall accuracy is typically better than ±0.2°C. If the terminal that the thermocouple is wired into is at a

different temperature than the CR10TCR thermistor, this difference in temperature becomes an error in the thermocouple temperature measurement.

With the CR10X in one of the enclosure options, this error will generally be less than 0.3°C [11]. The CR10X in this system is not in one of these enclosures, which are designed to protect it from the elements when placed outdoors. Instead, it is mounted inside in an air-conditioned environment out of the path of any sunlight and is fitted with a Campbell Scientific thermistor cover designed to keep the temperature of the thermistor and the terminal strip as similar as possible. It is therefore believed that this error of 0.3°C is still an appropriate maximum error value caused by temperature differences between the thermistor and the terminal. This is typically the second largest source of possible error.

The temperature reading from the thermistor served also as the only reading of the indoor ambient temperature. This is unfortunate because it was later shown that the temperature of the thermistor was about 3 °F higher than the ambient temperature in the room. A type-T thermocouple plugged into a handheld Omega digital thermocouple reader was used to measure the temperature of the thermistor, which agreed with the temperature indicated by the thermistor. The temperature of the air in the room near the SDHW system was also measured with the handheld reader. Six air temperatures were taken, all about 2 to 3 feet away from the tank, at heights ranging from one half of a foot to 5 feet above the ground. The average of these temperatures was 70.2 °F. Over the same time, three thermistor readings were recorded. In addition, thermocouple measurements of the temperature of the actual thermistor indicated the thermistor is accurate. The average of these six temperature readings from the thermistor was 73.2 °F, just under 3 degrees above the true ambient temperature. Further test points also indicated 3 degrees Fahrenheit was

the constant difference between the recorded thermistor temperatures (the temperature under the cover) and the ambient air. In the future, unless stated otherwise, when ambient temperatures are mentioned it is this corrected ambient temperature to which it is referring.

The largest source of error is typically in the thermocouple output itself. The limit of this error is defined by ANSI to be the greater of ± 1.0°C or 0.75% over the temperature range of 0°C to 350°C. However, the actual error can be much less than these limits in certain situations. Luckily, the measuring situations in this system tend to be those with quite tiny thermocouple errors. Due to the physical laws defining how thermocouples work, thermocouples can not have an offset error (assuming the wires are each homogeneous and no secondary junctions exist). This means that all thermocouple error is due to a deviation in slope. In light of this and the fact the error limits are defined for such a large temperature range, the fixed temperature limit of error (± 1.0°C) is greater than one would experience when considering temperatures in the environmental range. Therefore, the percentage error is probably more accurate than the fixed error. Likewise, because thermocouple calibration error is a slope error as well, accuracy can be increased when the reference junction temperature is close to the measurement temperature. [11]

For the same reason, differential temperature measurements, over a small temperature gradient, can be extremely accurate. In order to quantitatively evaluate thermocouple error when the reference junction is not fixed at 0°C, one needs limits of error for the Seebeck coefficient for various thermocouples. Lacking this information, a reasonable approach is to apply the percentage errors, with perhaps 0.25% added on, to the difference in temperature being measured by the thermocouple [11]. The readings taken in the experimentation were in the range 20°C to about 70°C, thus leading to possible

thermocouple errors of 0.2°C to 0.7°C when calculated using this method recommended by Campbell Scientific.

The other sources of error are much smaller. The largest of these is the accuracy of the thermocouple voltage measurement by the CR10X. This measurement accuracy is specified as 0.2% (0.1% 0 to 40°C) of the full scale range being used to make the measurement. All of the measurements taken in the experimentation used the ±2.5 mV range. In fact, the actual accuracy may be better than this as it involves a slope error. For the range of temperatures measured in the experimentation, this accounts for only a possible error of around 0.06°C. The other two sources of error are even smaller. They both involve converting between voltage and temperature. The CR10X uses approximated polynomials for computing temperatures from thermocouple voltages. Over the environmental temperatures encountered in a hot water system the limits of error due to these approximations is only ± 0.001°C. Similarly, approximated polynomials are used to convert reference temperatures as found by the thermistor into equivalent thermocouple output voltages. Again, in this experimental setting, these errors only amount to ±0.001°C.

The magnitude of errors described in the previous paragraphs illustrate largest sources of error in a thermocouple measurement taken in this experiment are likely to be due to the limits of error on the thermocouple wire and in the reference temperature determined with the built-in thermistor. The errors from approximated polynomials and voltage measurements are extremely small. To illustrate the believed maximum possible error in the thermocouple readings taken in this experiment, the error on a sample reading of 60°C, 140°F, is examined. It is important to note that this is a worst case scenario, where all errors are maximum and additive.

A temperature of 60°C, a typical reading for hot water in the system, is measured with a type T thermocouple, using the ±2.5 mV range. The nominal accuracy on this range in 2.5 μV (0.1% of 2.5 mV), which at 60°C changes the temperature by about 0.07°C. The reference temperature thermistor is 25°C, but is indicating 25.2°C, and the terminal that the thermocouple is connected to is 0.3°C cooler than the reference temperature thermistor. Using the percentage limit of error for the thermocouple, its reading is off by 0.35°C = (0.75% + 0.25%) * (60 – 25°C). If the fixed limit of error were used instead of the percentage error, the addition to the total error from the thermocouple itself would jump to 1.0°C. The total polynomial approximation error totals an additional 0.002°C. The sum of these errors is (0.07 + 0.2 + 0.3 + 0.35 =) 0.922 °C, or 0.76 °F.

This level of error could be a problem when comparing two temperatures only 10°F apart, it could lead to a worst-case temperature difference error of over 3.0°F. In the case of a energy meter, this would correspond to an error of 30%! Obviously, this is very unlikely, even for this small temperature difference. The error would typically be much lower. On the other hand, the temperature probes used by the F2 thermal energy meters measure a temperature difference very accurately. Accuracy verification produced by ABB provided error values of temperature differences measured with the provided matched pairs of temperature probes. They gave error values for eight different sets of temperature readings, which included a range of temperature values and temperature differences. The verification data show the highest percent error seen in a temperature difference reading between 60 and 63°C, similar to the temperature differences often seen in solar loop, was just 0.005%.

2.2.4 Draw Profile

The experiment required that a hot water draw profile be implemented to impose a hot water load on the SDHW system in order to have the experiment serve as a reasonable representation of a SDHW system in North Carolina. The difficulty came in designing (or choosing) a draw profile. Several published profiles were considered, as were combinations of these published profiles. The draw profiles chosen for the experimentation were the draw profile defined by the U.S. Department of Energy (DOE) Test Procedure for Water Heaters and a modification of it used by SRCC. The DOE test procedure is used to verify the Energy Factor and First Hour Rating of all water heater models sold in the United States. A standard hot water load is needed in this DOE testing for the same reason one is needed in the experiments performed in this paper.

Solar Rating Certification Corporation (SRCC) also needs a standard water draw profile for its standard SDHW system test procedure. SRCC is a non-profit organization that certifies and rates solar collectors and solar hot water systems. They have developed the only widely recognized national standard for certification of solar systems in the U.S. The hot water draw profile it uses is the same as the DOE test, except that it prescribes specified energy draws instead of the specified volume draws in the DOE test procedure (note that these two procedures are equivalent if the difference in inlet and outlet temperature is 42.8 degrees C). There are several other differences between the SRCC procedure and the DOE procedure as well. One primary difference is that the SRCC procedure is performed in a computer simulation rather than by an actual test. Because of

this, SRCC has added hourly solar radiation and outdoor ambient air temperature profiles, and specifies that the draw profile begin at 9:30 AM solar time.

Both of these hot water draw profiles consist of six even hourly draws that are started in the morning (9:30 AM solar time by SRCC ,DOE does not specify a time so 9:30 AM solar time is used as well). They both specify the environmental temperature (19.7 °C, 67.5 °F), auxiliary set temperature (57.2 °C, 135 °F: DOE gives a range of ±5 °F), water main temperature (14.4 °C, 58 °F), and draw rate {0.189 liters/second (l/s), 3.0 gallons/minute (gpm)}. In the experimental setup, accurately maintaining these temperatures is neither easy nor necessary. Because the goal of these experimentations is to understand and test the effectiveness of energy metering strategies, following this procedure to the letter has no particular benefit. The DOE/SRCC procedures were chosen so that the experimentation used a standard draw profile very familiar to people in the DHW and SDHW industry. The other draw profiles considered, ASHRAE and WATSIM, among others, where ultimately not implemented because they are not as fundamental to the industry as the DOE and SRCC procedures are.

Research performed by Knudsen [12] showed that the difference in net utilized solar energy in a SDHW system similar to the one tested decreased by slightly less than 10% when a very detailed realistic profile was imposed compared to when a very simple profile of 3 even daily draws was imposed. A similar drop in performance was seen in the TRNSYS simulations performed in Chapter 5. Nearly all of this loss of performance occurred because of mixing caused by the tapping of the hot water [12]. In a realistic load profile, more than 3 draws, or even 6 as in the case of the DOE test, occur most every day, thus causing the tank to experience more mixing each day. The flow rate of actual use

varies from less than 1 gpm in many hand faucet uses to about 1.5 – 2.5 gpm for showers to over 3 gpm for some clothes washers and bath fillings. No research was found that specifies the effect of hot water draw rate on the performance of a SDHW system, but it is suspected that the primary effect it would have is that higher draw rates would increase the level of mixing in the hot water tank, and thus hurt the performance of the SDHW system. It is believed that the magnitude of this effect is quite small when a realistic profile is compared to the specified draw profile.

As mentioned earlier, both the DOE and the SRCC draw profiles specify the indoor ambient temperature (19.7°C, 67.5°F), auxiliary set temperature (57.2°C, 135°F), and water main temperature (14.4°C, 58°F). In the experiment, the ambient temperature remained relatively constant, but somewhat higher than specified, at about 75°F. This difference will slightly affect the level of heat loss experience by the hot water tank, but has no particular influence on the findings of the experiment. The auxiliary set temperature, however, has significant influence on the performance of the system and possibly on the performance of the tested metering schemes. This issue is discussed fully in the next subchapter, chapter 2.2.5. The water mains temperature also has significant influence on the performance of the system. The water mains temperature in Raleigh during the summer months was significantly warmer than the specified temperature.

This difference in water mains temperatures has a great influence on the volume of the draws specified by the SRCC draw profile. This is because the SRCC profile specifies a certain amount of energy per draw instead of a certain volume as in the DOE test. The amount of energy to be drawn in each draw is defined using the water main temperature, the auxiliary set temperature, and the draw volume as defined by the DOE profile. When

either of these temperatures changes significantly, the volume of the SRCC-defined draw must also change significantly. During the summer in Raleigh, the water mains temperature is about 15 degrees F higher than the SRCC energy draw on which it was based. This had the effect of raising the average daily hot draw to nearly 105 gallons per day, compared to the 64.3 gallons specified by the DOE test procedures. The SRCC draw profile (energy draws) was implemented for approximately a month of the testing time. This test was used because, as mentioned before, this is the profile used by SRCC, which is the industry-accepted SDHW certification organization.

The actual use of domestic hot water varies greatly from household to household. It even varies from region to region and season to season. It is therefore obvious that one single draw profile cannot accurately model the hot water usage of every household. For this experiment, the exact draw profile is not of great importance. The important factors in the profile are that there are a number of draws spread throughout the day and that the magnitude of these draws is in the range of a typical household. There have been many studies on effects of hot water use profiles on SDHW systems, but that is not the focus of this paper. It is the author's belief that although the draw profiles used may not accurately represent actual hot water use, its less-than-perfect representation does not degrade the value of the data acquired by the experimentation, because the goal of the project was to understand the dynamics of the meters, and the DOE/SRCC profile provides adequate dynamics

2.2.5 Tank Auxiliary Temperature Settings

Like most SDHW systems, the one used in this experimentation had a backup heating system, electric resistance heating coils in this case. Two separate thermostats control power to the two coils in the hot water tank. Details of how they function are provided in chapter 2.1. Each of these thermostats has a user-determined temperature set point, the temperature to which the water is heated by the auxiliary heating system. Both the DOE and the SRCC test procedures define the tank auxiliary temperature to be 135°F ± 5°F. However, it is obvious that this setting of 135°F should not be used blindly. Water heaters in the U.S. come from the factory set from 120 to 140°F, depending on the manufacturer, and many organizations recommend setting the thermostats to 120°F.

The Department of Energy itself officially recommends to people to set there thermostats to 120°F [13]. They recommend this for two main reasons. First, there is a danger of burns and scalds with water above 120°F. This reason for the lower setting is of limited relevance in a SDHW system because the system will already have an anti-scald valve (tempering valve) since the water will be heated well above 120°F at times by the solar energy alone. The second reason that DOE recommends 120°F as the set point is to limit standby energy losses. In the case of SDHW systems, a significant portion of the year the solar energy cannot meet all the household needs and the temperature of the tank will ultimately be determined by the electric heating element set point. The higher the set point the higher the standby losses. A lower set point has an additional advantage for SDHW systems. In the case of a direct system, as tested, the water sent through the solar collector will often be of lower temperature when the tank has a lower set point. This means that the

water experiences less thermal losses as it passes through the collector, thus increasing its net gain of energy. The advantage of lower tank temperatures in a one tank indirect system is similar. Because the solar energy enters the tank via a heat exchanger, when the water in the tank is cooler the water delivered from the solar collector does not have to be as hot to effectively deliver its energy. This leads to lower water temperatures entering the collector and thus smaller losses. The annual simulations performed in this study predict that the experimental system would experience 23% greater annual losses with a set point of 135°F than if it has a set point of 120°F.

Hot water at 120°F is satisfactory for most household hot water needs. The one exception is that automatic dishwashers require water at 140 °F for optimum cleaning. Further, many dishwasher detergents are formulated to clean effectively at 140 °F and may not perform adequately at lower temperatures. However, most modern dish washers include a booster water heater which is able to heat the hot water it needs up to 140 °F. A booster water heater adds about $30 to price of a new machine. One can also be manually added to an existing automatic dishwater currently without one. The DOE does not recommend setting the DHW thermostat below 140°F if there is an automatic dishwasher without a booster heater served by the DHW system [13].

The DOE discussed many of these same topics in 1998 when it last amended its test procedure for water heaters [14]. In the published document, there were nine commenters involved in the discussion. These commenters were primarily from utilities from across the country. Three of nine commenters in the discussion believed the thermostat setting in the test procedure should be lowered to 120°F ± 5°F. The reasoning given all related to the fact that they believe this setting better represents both actual and recommended use. In

contrast, six commenters, individually or in support of another commenter's position, opposed lowering the thermostat setting from 135°F ± 5°F. Their reasons were: (1) a setting at 120°F could pose a potential health risk (e.g., legionella) to consumers, (2) a setting of 135°F is necessary to meet consumers' expected hot water needs, (3) a setting at 135°F reflects realistic household settings, and (4) changes to the thermostat setting will not alter the comparative ranking of water heaters but would result in a substantial cost to industry in retesting and relabeling. For these reasons, the DOE's final decision was that the revision of the thermostat setting from 135°F ± 5°F to 120°F ± 5°F was unwarranted at that time. The set point defined in the SRCC water draw is also at 135°F ± 5°F because it is only a slightly modified version of the DOE water draw. The potential health risk of a thermostat setting of 120°F is less of a threat in the case of SDHW because the water in the system is still occasionally heated to or above 135°F.

Set points of both 135°F and 120°F were used in the experimentation in order to expose the metering schemes to the likely range of set points seen in SDHW systems. During each experimental period the tempering value was set to the same temperature as the tank set point. This was accomplished by raising the temperature of the tank slightly above the set point, opening the hot water draw valve, and then adjusting the setting on the tempering valve until the hot water output was at the tank set point. The tempering valve works by mixing cold water with the hot water from the tank, and the temperature setting determines their ratios. This means that for a single tempering valve setting the actual temperature of the tempered water is a function of the temperature of both the cold and hot water. This means that on strong solar days with very low loads ,when the tank

temperature is quite high, the temperature of the tempered water can be somewhat higher than desired.

The first period of experimentation, when the water draws were equal energy draws rather than equal volume draws (SRCC profile), the higher setting of 135°F was used so that the volume of each draw would not deviate too much from the volume draw defined by DOE. Even with the set point set to 135°F, the volume of these draws were larger than the volume defined by DOE because the water main temperature was higher than defined by DOE. The second period of experimentation, which immediately followed the first, used the DOE draw profile, with the exception of the thermostat set point. It was set to 120°F to represent the large number of actual consumers who have their thermostats set to 120°F and to take advantage of the higher performance it affords SDHW systems. The draws during this period were of equal volume rather than of equal energy.

2.2.6 The Three Experimental Periods

The experiments performed were divided into three periods, each representing different operating conditions of the SDHW system. The details of the three different periods, and how each was chosen, are described in the preceding sub-chapters of chapter 2. The table below displays an overview of the setup of the three experimental periods.

Table 2.1: The Three Experimental Periods

	Summer - SRCC	**Summer - DOE**	**Winter - DOE**
Dates of Experiment	June 11th – July 12th 2003	July 14th – Aug.11th 2003	Dec. 7th -17th and Dec. 24 – Jan 11th 2004
Tank Set Temp & Tempering Valve	135 °F	120 °F	120 °F
Metered Draws of:	Energy	Volume	Volume
Average volume of daily draws (liters)	395	250	251
Average energy of daily draws (kWh)	12.8	7.4	10.7
Start Time of Draws	9:30 AM (±15min) Solar Time	9:30 AM (±15min) Solar Time	9:30 AM (±15min) Solar Time

2.2.7 Metering Schemes

The goal of this research was to develop and verify a metering scheme for SDHW systems, particularly for those in North Carolina. The general procedure used to do this started with developing the experimental monitoring and datalogging system previously described. Then the test procedures were designed to provide the most useful data possible. Using this experimental setup, some general metering schemes were developed. Some of the metering setup and schemes were based on what is working for Lakeland Electric in Florida. They use a Btu meter and an electric meter to determine the amount of sellable

solar energy delivered. The quantity they meter is actually solar gain minus tank losses. The goal of their metering project, as well as the goal of this investigation into SDHW metering, is to meter the amount of auxiliary (electric) energy offset due to the SDHW system. However, there is no way to do this directly. Instead, either the solar gain is measured directly, which is slightly higher than the amount of auxiliary energy offset, or, as Lakeland is doing, the solar gain minus the tank losses is calculated, which is lower than the amount of auxiliary energy offset by the SDHW system.

The data from the three experimental periods was used to evaluate the following metering schemes for accuracy. The accuracy referred to here is the ability of each scheme to measure the energy it is attempting to meter. Then, TRNSYS computer simulations of a validated system model were used to determine how well each of the two general schemes (single solar meter or hot water load thermal meter and an electric meter) represented the amount of auxiliary energy offset by the solar system. These schemes were developed for consideration based on the goals of accuracy, low cost, reliability, and robustness. It is believed that this group of metering schemes represents the full range of workable physical metering schemes. The schemes that include temperature estimations were designed in an attempt to lower the cost of the metering setup.

Solar-Loop Thermal Energy Meter

One thermal energy meter is installed on the solar loop of the system. The meter reads out the amount of solar energy delivered to the hot water tank. In order to

arrive at the amount of electric energy offset by the solar system some correlation must be made.

Hot Water Load Thermal Energy Meter and Electric Meter

One thermal energy meter is installed across the hot water heater, referred to as the hot water load thermal energy meter. A second meter, an electric watt-hour meter, is installed inline with the electric heating elements in the tank. The metered value is obtained by subtracting the electric energy used (electric meter) from the total useful energy delivered (thermal meter). This difference is the amount of solar energy delivered to the tank plus the thermal losses from the tank and the pipes between the tank and the thermal meter. This value could be used directly as a measure of solar energy utilized, as Lake Land Electric does, or if desired an estimated amount of lost energy could be subtracted to find the total amount of solar energy collected.

Electric Meter and the Load Cold Water Flow Meter with Temperature Estimates

This scheme is a modified version of the previous scheme. It replaces the expensive thermal energy meter with a flow meter and average monthly estimates of the temperature of the cold city water and the hot water used in the house. This

is considerable because both of these temperatures are relatively constant each month. The meter value is calculated monthly from the flow meter reading and the temperature estimates.

The Solar Loop Flow Meter and Temperature Difference Estimate

This is a modified version of the first scheme. A flow meter is installed in the solar-loop. The solar energy collected is calculated by using a monthly, or even constant, estimate of the solar-loop temperature difference.

Solar Loop Temperature Difference with Watt-Hour Meter to Determine Flow Rate

This scheme is purely academic at this time. Its implementation would require some custom electronics. The temperature difference of the solar-loop is measured with thermocouples, which can give very accurate results when measuring temperature differences. The flow rate through the solar-loop is determined by monitoring the power being delivered to the solar pump. For accurate flow rate values from this power, some calibrations must be performed on the system. An electronic 'calculator' similar to the one in the thermal meters would calculate the

solar thermal energy entering the tank. The largest potential advantage of this scheme is the cost savings from not requiring a physical flow meter.

Chapter THREE RESULTS

The detailed monitoring and data logging system resulted in very large amounts of data to analyze. The data were downloaded into a raw data file every week to avoid the incoming data from writing over itself due to limited capacity in the datalogger. Then, the data was sent to a spreadsheet file where it was conditioned and analyzed. The raw data paints a fairly accurate picture of all the goings-on in the SDHW system. Data points were recorded every 5 minutes. This is not fine enough to see exactly when draws start and stop or to know exactly when the electric heating elements came on or off, but it is fine enough to understand most of the dynamics of the system. To began the presentation of the results a 'walk-through' of one typical day's (July, 21st, day 202) data is presented with detailed commentary on the information reveled by the raw data.

3.1 One Day Walk-Through

Each day of data contained over 5000 data points. In order to see the image of the SDHW system's performance that day, each 5-minute set of data must be examined and understood in context with its neighboring sets of data. In this way, an understanding of the details of the dynamics of the SDHW system may be gained. The following is an example

of this most intuitive form of data analysis. This type of analysis was not done on all of the data, but it was initially performed on several days of data in order to gain a better understanding of the system. It was also performed on interesting bits of data as a tool to determine the functionality of the system or the meters at any given time. The reader will be lead through a qualitative analysis of one full day of raw data from the monitoring system. This serves to both demonstrate some of the information available from such analysis and to expose the reader to some of the internal dynamics of the system. The day was July 21st, the 10th day of the first monitoring period. The set point was 135 °F and the draw profile followed SRCC test procedure. Figures 3.1 to 3.4 at the end of the subchapter display much of the data mentioned in the walk through.

At midnight (local time), the system is in a dormant phase. There will not be any measurable flow through either of the flow meters for nearly 7 hours and the electric heating elements will not come on for over 9 hours. Until the sun comes up enough to cause the valve to open and fill the solar collector or someone turns on some hot water, the system just sits and waits. During this period, the tank is slowing losing some of the energy it has stored to the ambient environment. The data readily shows this slow, steady loss in the temperature readings from the thermocouple in the system, particularly those on the sides of the tank. The thermocouple monitoring the upper half of the tank read 129.3 °F at midnight and cooled to 126.3 °F by 7 AM. The lower half of the tank cooled from 127.3 °F to 122.5°F in the same time. It is obvious that much of this heat passes through the insulation covering the tank, but some of the heat is also lost through the pipes and other connections into the tank.

At this time, the thermocouples in the water in the cold supply and hot demand pipes read 10 and 15 °F, respectively, above the indoor ambient temperature. These temperatures fluctuate no more than about a degree apiece from midnight until just after 7 AM when some water was run through them. The only source for this heat is the hot water in the tank. It likely traveled both through the walls of the metal pipes and with convective currents of water in the pipes. In order for the temperature to stay so constant, a steady, but small, flow of heat must have been exiting the tank through the pipes. This heat then left the pipes through their insulation.

The temperatures of the solar supply and demand pipes fluctuated a similar amount, but always stayed within about ½ °F of the ambient temperature. These pipes were insulated very similarly to the load water paper pipes, so this showed that practically no energy made it from the hot water tank to the thermocouples, approximately 5 feet away. This does not rule out the possibility that some energy was lost via the solar pipes. In order for this to occur the energy would have to make it out into the room air before making it to the thermocouples. At the time this data was recorded the solar loop pipes contained a significant amount of exposed metal, possibly serving as a thermal short circuit between the ambient air and the warm water in the solar pipes..

Then, sometime between 7:00 and 7:05 AM, a small amount of hot water was drawn out of the tank. There was enough flow for the water meter in the cold water line to indicate 1 liter of flow, although, the actual flow could have been anywhere from a small fraction of 1 liter up to nearly 2 liters. More information is revealed by examining the temperatures recorded by the thermocouples in the pipes. These temperatures are recorded in two ways. In the first method, which was referred to earlier, readings are taken every 2

seconds and averaged over the entire 5 minutes. The second method only records the temperature if a flow pulse was registered during that 2-second period. This works very well on larger draws, but in the case of this tiny draw the results leave something to desire. The data shows that at the time of the draw the water in the cold pipe was 87.1 °F and the temperature in the hot pipe was 86.6 °F. This would mean that the water flow through the hot water outlet pipe was cooler than the water that had been sitting there and just the opposite in the cold pipe. But, the average temperatures of the water in the cold water supply pipe over the entire 5 minutes dipped just over 1 °F. The hot pipe temperature dipped too, but only by 0.2 °F. This suggests that the draw was quite small, unable to produce much change in the temperature of the pipe, but enough to make measurable changes, suggesting some flow did occur. Similar events occurred several other days at nearly the same time. The cause of these occasional tiny draws was not determined.

Nothing happened, other than the continued slow loss of heat, until sometime between 9:00 and 9:05 AM. Again, one liter of cold water was recorded as it flowed into the hot water tank. This appears to be a smaller amount of flow than occurred at 7 AM because the drop in the average temperature of the cold pipe did not occur. Then between 9:10 and 9:15 AM nine litters of cold water flowed into the tank to make up for the nine liters that filled the solar collector at the same time. This happened when the thermostat in the solar controls was heated enough to operate the slide valve and allow the pressured water in the tank to fill and pressurize the solar collector. This same event occurred between 9:00 and 9:30 most every morning during the summer experiments. Evidence this is what occurred comes from the temperature readings. While the flow was occurring the temperature in the hot water pipe did not change, but the temperature in the cold water pipe

dropped over 10 degrees F. Also, the flow meter in the solar supply line to the collector recorded 6 liters of flow. (The full 9 liters are not recorded by the solar flow meter because some of the water flows up the return line when the collector is initially being filled.) Further, the temperatures of these flows were 102.8 °F on the way to the collector and 104.6 °F on the return trip. The average temperatures of the water in these pipes over the entire 5 minute period was identical to this, suggesting the flow started close to 9:10 and continued the entire 5 minutes.

This event caused quite a lot of change to occur. The average temperature for that 5 minute block of time of the bottom half of the tank dropped nearly 7 °F. This in turn caused the lower thermostat to trip, sending power to the lower heating element. This occurred at about 9:12:15 AM. This can be deduced by the amount of electric energy that passed through the meter during that period because the power is always 4500 Watts. In total, the heating element was on for about 11 minutes and 40 seconds before the thermostat reached its set point, removing power from the element.

From 9:15 until a little before 9:45 the solar loop pump was running, pumping about 1 liter per minute through the solar loop. This was not a very profitable time for the system. During this time, the returning water was hotter than the supply water during only half of the time blocks. This poor performance was due to both low irradiation (the pump would have pumped at higher flow rate with more irradiation) and the capacitance of the collector which took some of the heat from the water to warm itself. During this entire time the water at the bottom of the tank, as seen by the temperature of the water sent to the solar collector, was steadily rising in temperature as it was heated by the rest of the water in the tank and the electric heating element. The thermocouple placed about a third of the

way up the outside of the tank showed that at this level the water temperature recovered within a couple of minutes from the cold makeup water.

After this period of solar pump operation, the pump turned off for over 5 minutes, came back on for a few minutes and then turned off again for about 40 minutes. During this solar idle period, a liter of flow was recorded on the house side. This time the hot water temperature peaked as expected. The temperature of the flow was 131 °F and the average temperature of the water for that 5 minute block increased to 127 °F, suggesting that the flow occurred very early in the time period. Before the solar pump started back up, the temperatures of the solar loop pipes dropped about 15 °F each. When the PV panel did again receive enough sunlight to pump the water that had been sitting in the collector had gotten quite hot. The water that came back during the first 5 minutes averaged 138.3 °F. The pump would not be off again for an entire 5 minute block until 5:45 PM when it shut down for the day. Although, there were a couple of periods with only 1 liter of recorded flow during which it is believed flow stopped for some of the period. It was about 15 minutes into this long block of solar activity that the system recorded its first pulse ($1/10^{th}$ of a kWh) of solar energy.

At 10:50 AM (local time, about 9:30 solar time) the first planned hot water draw began. It is known that the draw occurred at a constant flow rate, so by knowing the flow volume the length of the draw can be concluded. In this case, the draw lasted approximately 8 minutes and 15 seconds, the valve closed as programmed when the meter said that 2 kWh of thermal energy had flowed out of the system. A little over 2 minutes into the draw, the lower heating element came on. This time it would stay on for over 26 and one half minutes, supplying just over 2 kWh of energy to the hot water tank.

This first draw pulled over 16 gallons (61 liters) of hot water, at about 127°F, from the tank, so during this same time 16 gallons of cool makeup water rushed into the bottom of the tank. This water was sucked up into the solar loop while it was coming in, resulting in large energy gains (temperature difference) for the solar collector for about 10 minutes. At the end of this period much of the heat of the collector had been removed by this cooler water. So, over the next 30 minutes or so, the water recently heated by the heating element gained almost no energy while in the collector because its energy was needed to reheat the collector.

During the period between hot water draws the temperatures of the water in the hot and cold pipes across the water heater showed some heat loss. At the end of the draw, the water in the hot pipe was over 125 °F and the water in the cold supply pipe was about 78 °F. Over about the next 20 minutes the water in the hot pipe gave up some of its energy to the surroundings to bring its temperature down to just over 100 °F. At the same time, the cool water in the supply pipe drew out energy from both the hot water line and the hot water tank, raising its temperature by about 10 °F.

This hour-long cycle repeated for the next 5 hours with only slight variation on this day. On other days of more intermittent sunlight, there were greater variations, primarily because more electric energy was needed after the draw and the tank temperatures were slightly lower because there was little solar energy added. As the day progressed, the maximum temperature in the tank increased, but by only about 3 °F above its temperature before the first draw. The water returning from the solar collector experienced a peak temperature in the mid-afternoon, of about 3 °F higher than the morning or late-afternoon high temperatures. The water delivered to the house as useful hot water ranged in

temperature from 125.7 °F during the second half of the first draw up to 129.9 °F in the second to last draw. It is important to remember that these hot water temperature readings are taken after the tempering valve. Comparison to the top of the tank temperature reveals that the tempering valve lowered the water by over 5 °F.

After the last draw the solar pump ran for about another hour and 45 minutes, but little solar energy was collected the last 30 minutes. However, it did collect energy, according to the temperature readings, in all but the last liter of water flow. At least on this day, the control logic was right on, collecting about as much solar energy as possible for the conditions. Over an hour passed after this final liter of water ran through the solar collector before the wax thermostat cooled enough to open the spool valve. This event was shown in the data when the solar water meter registered 5 liters of water, yet the water in the supply line was 10 °F warmer than the normally hotter return line. Examination of the average temperature in the lines reveals that some water drained from each pipe, but that the water in the supply line was hotter. It is known that it took 9 liters to fill the collector, so, there must have been about 4 liters drain out the return pipe, which did not get recorded because that pipe was not equipped with a water meter.

This draining took place at about 7:50 in the evening. After this time there was no more flow recorded by either of the water meters the rest of the day. The water at the temperature sensors in all 4 pipes connected to the hot water heater were all still at elevated levels. The water in these pipes continued to drop in temperature as they cooled. The water temperatures in the solar pipes came to steady-state sometime around 10 PM, at temperatures very near the ambient temperature. The water temperatures in the house pipes came to steady-state about 11:00 PM at about 10 and 15 °F above ambient

temperature. The system was in this state of steady-state at midnight when the daily cycle began again. All but one of the seven recorded temperatures are within one half of one degree Fahrenheit from their value 24 hours earlier. The seventh, the temperature reading of the bottom one third of the hot water tank, is only 1.2 °F lower than its value at the start of the day. This level of consistency was not atypical. However, larger differences in consecutive midnight temperatures were seen in days of drastically different levels of insolation.

This day was typical for the first experimentation period. The energy meters reported that 9.9 kWh of electric energy was delivered to the hot water tank, 12.1 kWh of thermal energy was delivered in the form of useful hot water, and 5.2 kWh of solar thermal energy was collected. This was a typical solar day; the average solar energy collection per day for this period was 4.29 kWh.

The researcher's understanding of the dynamics of the system clearly increased with this type of soft analysis of the raw data. The gain in understanding was invaluable for accurately performing the hard analysis of the data and the analysis of the considered metering schemes. The figures below present much of the data discussed above in way that is easy to understand. Figure 3.1 is of the volume of flow data from both of the flow meters. Each data point represents the number of liters of water flow that passed through each flow meter in the last five minutes. Figure 3.2 shows the temperature readings from the seven thermocouples monitoring the system. Each data point represents the time-average of the reading over the previous five minutes. The graph immediately following (Figure 3.3) is a close up of the above graph from 11:00 AM until 2:00 PM. This was included to make the crowded lines more easily visible. The final graph (Figure 3.4) is this

section contains the energy data from the thermal energy meters. Each data point represents the number of kilo-Watt-hours of thermal energy (electrical in the case of the electric meter) that passed through each meter over the previous five minutes.

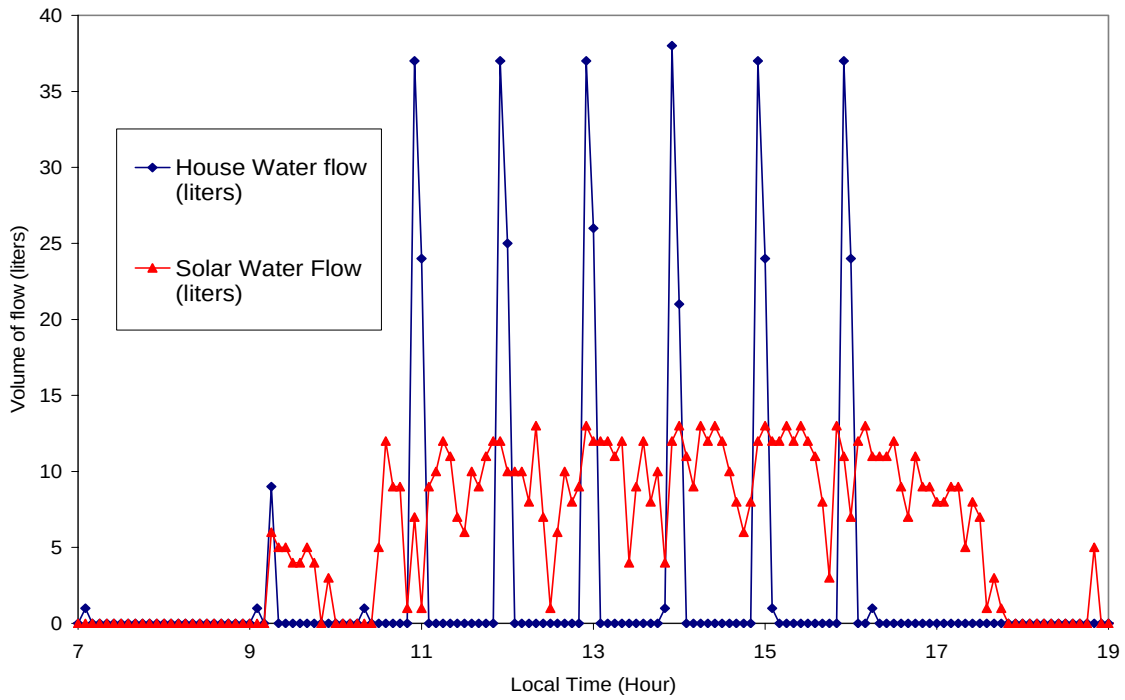

Figure 3.1 Flow Volume through Both Flow Meters, Day 202

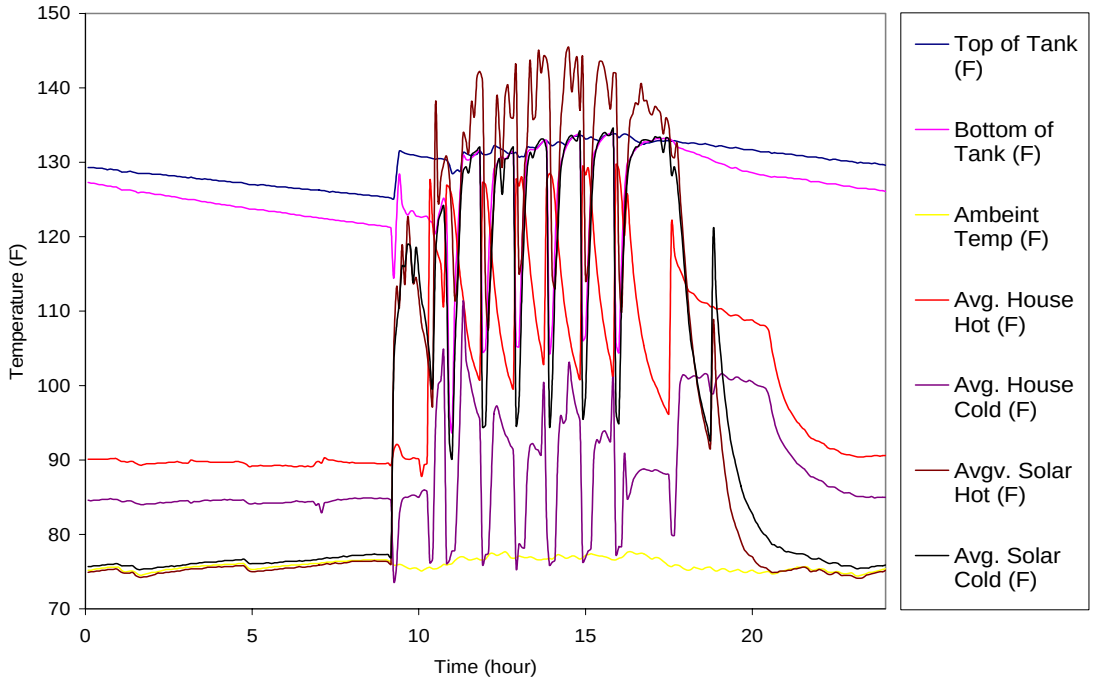

Figure 3.2 All Thermocouple Temperatures, Day 202

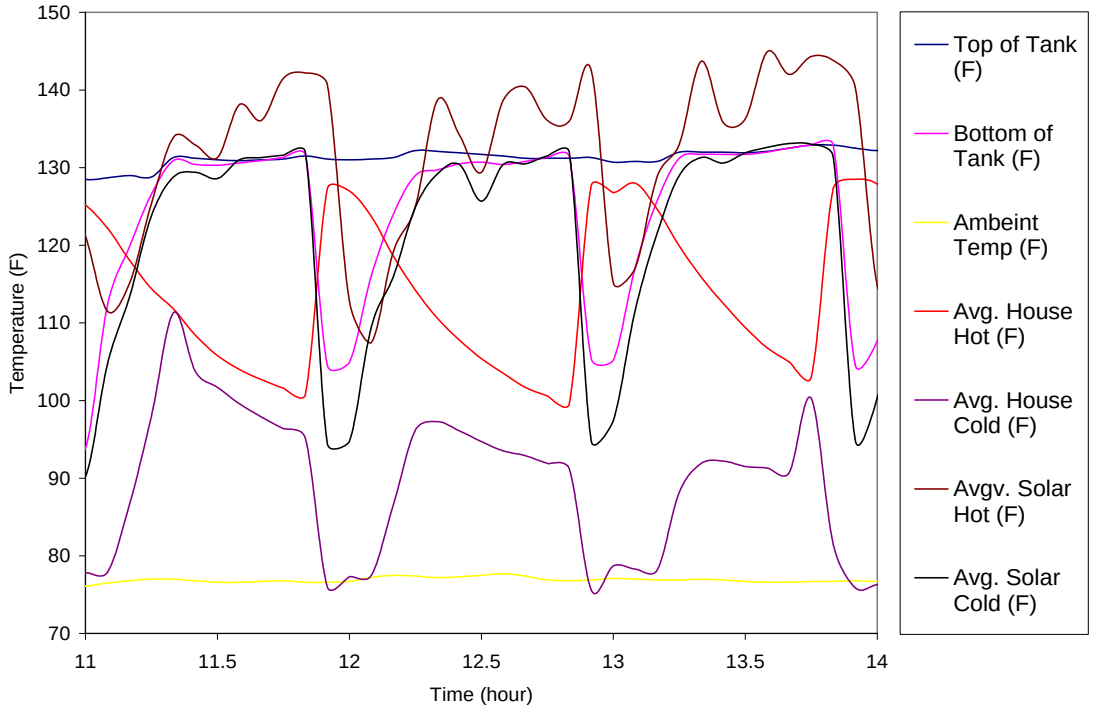

Figure 3.3 All Thermocouple Temperatures, Day 202 from 11AM to 2PM

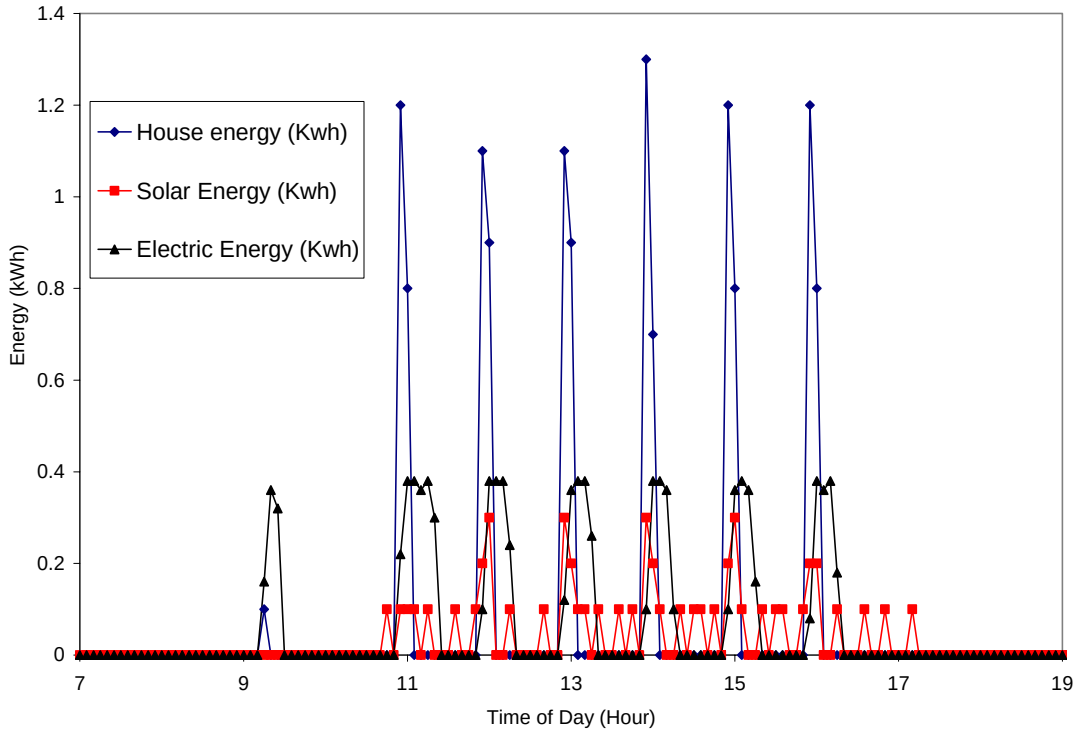

Figure 3.4 5-minute Energy Data from the Three Energy Meters, Day 202

3.2 Losses and the System Energy Balance

It is known that the tank, and at times the pipes as well, lost energy to the surroundings. Unfortunately, without a much larger budget it was not possible to measure these losses explicitly, but in order to understand the system fully and to account for all of the energy involved, the losses must be calculated in some manner. This was accomplished by solving the daily tank energy balance for the system losses. This equation is as follows:

$$\begin{aligned} Losses \;=\; & \\ Solar\;\; Energy \;+ Electric\;\; Energy \;- & \\ House\;\; Energy \;- \Delta\; Internal\;\; Energy & \end{aligned} \tag{3.1}$$

The change in internal energy was calculated in a spreadsheet using the temperatures from the two thermocouples attached to the hot water tank. The calculation took advantage of a water properties add-in. The specific internal energy of water at the given temperature and pressure was easily calculated. The density of the water was also calculated based on the assumption the entire tank was at the average of the two measured tank temperatures. The equation is as follows:

$$U = u \cdot \rho \cdot V \tag{3.2}$$

This energy balance was performed on the energy totals from an entire day. The value for the change in internal energy used in the equation was the difference in the total internal energy of the water in the tank from midnight to midnight because at midnight the system is in near-equilibrium and the state of the system at this time is nearly constant from day to day.

The graph below (Figure 3.5) gives a glimpse at the thermal losses experienced by the tank (including the pipes inside of the meters). Days of large solar energy collection tend to mean higher average tank temperatures, which means more heat loss from the water in the tank, and more losses via the solar pipes. This effect is apparent from the graph of the daily meter totals from the first monitoring period. The level of daily losses as calculated from the energy balance (using the energy values calculated using the thermocouple temperatures) ranged from under 1.75 kWh to 3.3 kWh.

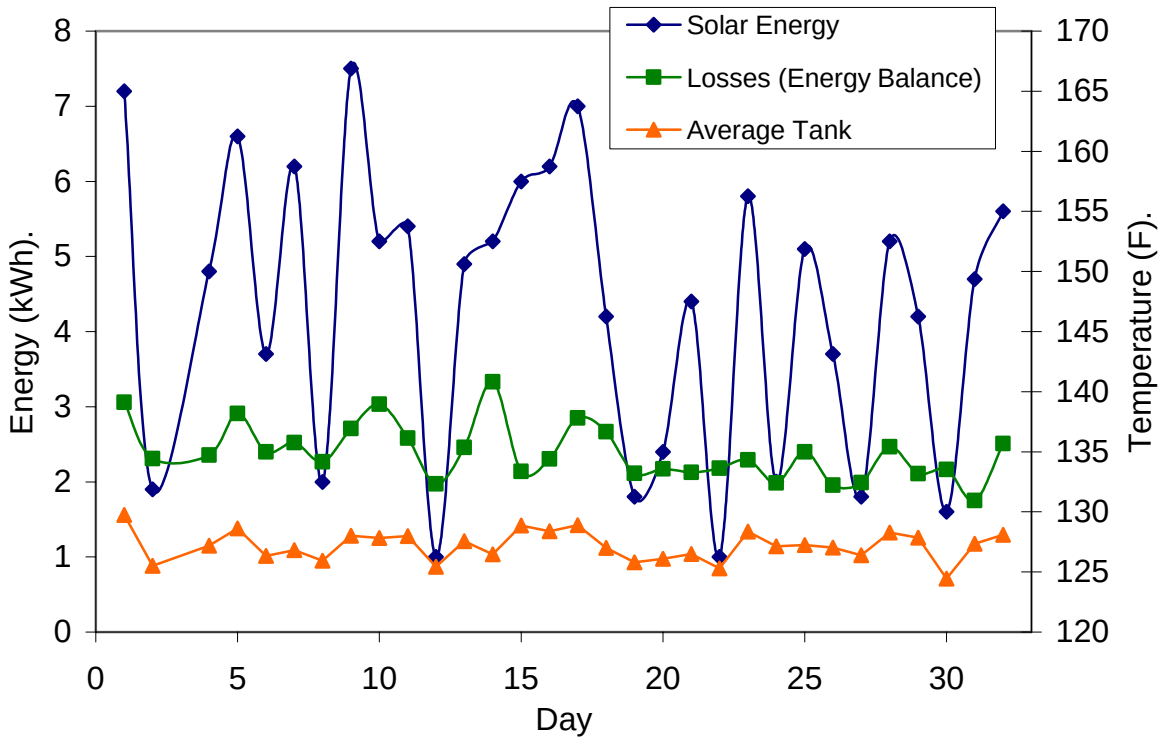

Figure 3.5 Daily Solar Energy, Losses and Average Tank Temperature in Period 1

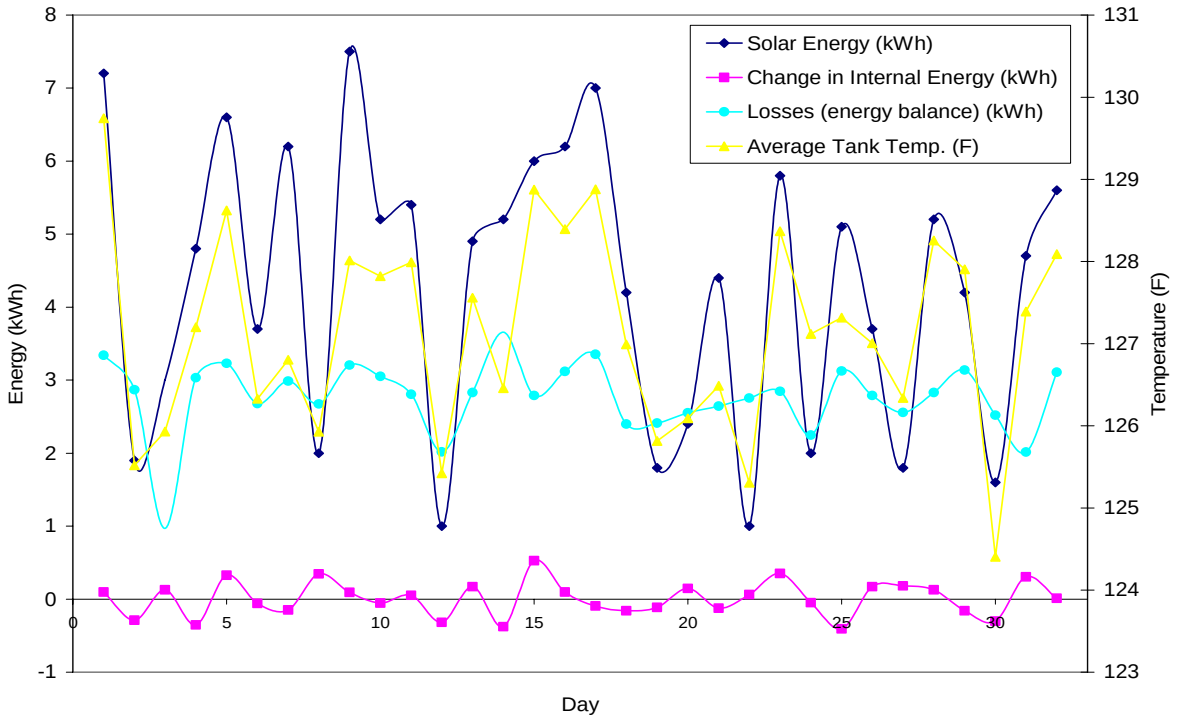

Figure 3.5 Solar Gain's Affects on Tank Temperature and Losses

The lowest calculated loss of any day occurred on Day 3 with a total of -0.13 kWh of losses. This data is known to be in error and was not shown in the above graph (notice there are no data points on Day 3). The error was caused by a malfunction with the spool valve that is discussed extensively in the presentation of the results from the first monitoring period.

Another location where significant losses occurred was in the pipes between the energy meter close to the tank and the solar collector on the roof. The round trip between these points is over 100 feet long and includes passage through walls, floors, and the attic. Most of this piping is well insulated, but some hard to reach sections were left uninsulated. The outcome of this long trip was that significant levels of useful energy were lost on this journey. No temperature readings were taken at the collector, so it is hard to know exactly, but it is believed that up to 4 kWh of energy were lost from theses pipes on very sunny days. These losses effectively cut the maximum efficiency of the collector from about 0.7 to 0.5. It appeared that on some days of intermittent sunlight more energy was lost from these pipes than was collected by the solar energy system.

These pipe losses are not a part of the tank energy balance because they occurred outside of the solar thermal meter. Therefore, these losses are not explicitly mentioned in the results presented in chapters 3.3 – 3.5, but they are considering in the TRNSYS computer model of the system. The daily losses from the tank, as calculated from an energy balance using the calculated thermal energy meter readings, are presented in the following presentation of results. Because the thermal losses experienced by the system were not able to be explicitly measured, they served as the pivotal remaining piece needed to complete

the energy balance. The other energies in the system energy balance were all explicitly measured. In addition, these energies were all large compared to the amount of daily losses experienced by the system.

When the losses are calculated from an energy balance, small percentage errors in the daily energy measurements could lead to large percentage errors with the remainder of the energy balance, the thermal losses. Thus, the total amount of thermal losses, as calculated from a system energy balance, is a valuable indicator of accuracy of the measurements of the other energy flows. However, this is not able to serve as an indicator for each meter reading independently, only for the conglomeration of all of the meter readings. Although, a heat transfer model may be constructed to estimate the system losses and thus allow for further analysis on the system energy balance. This was done in Chapter 4.

3.3 Summer – SRCC (First Monitoring Period)

The first period of monitoring produced the results seen below in both a chart and a graph summarizing the mass of recorded data into daily totals of the metered variables. This data alone provides a lot of information on the performance of the SDHW system, but very little information on the performance (both accuracy and relationship to offset electric energy) of the metering system. Verification of the accuracy of the metering system is provided later in the chapter 3.6. The first graph, figure 3.6, shows the daily totals of the three energy meters monitoring the system.

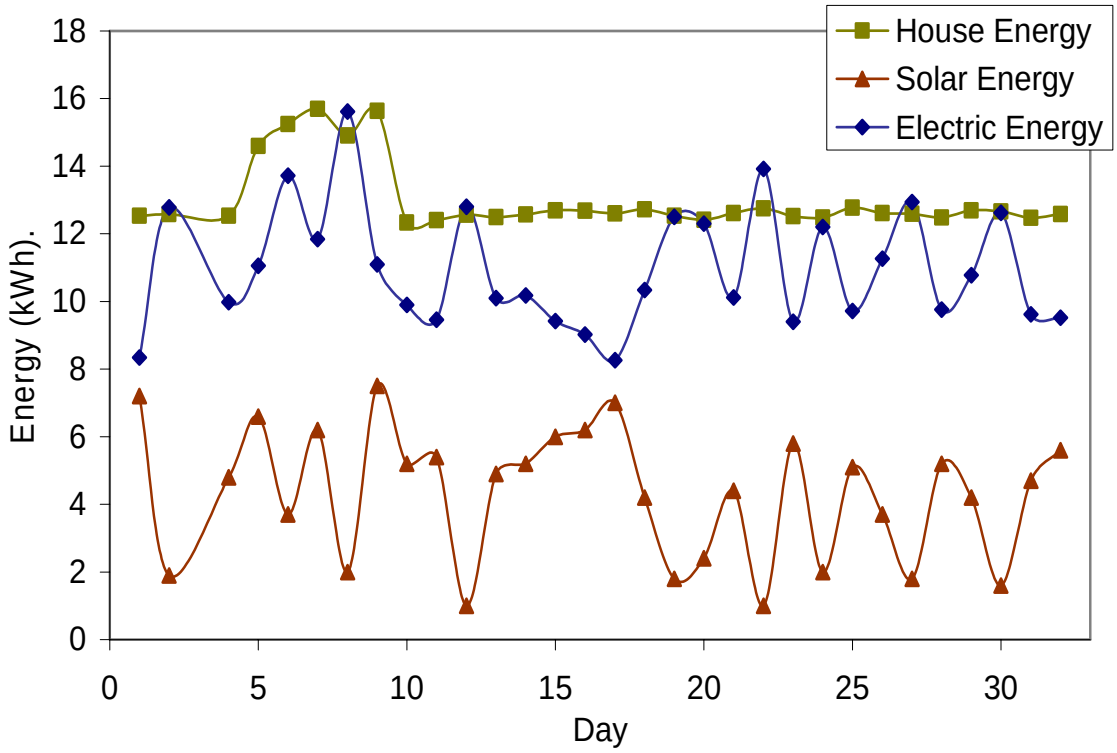

Figure 3.6 Daily Metered Energies in Period 1

The hot water draw profile used during this month of testing followed the basic criteria of the SRCC test. This test requires that each draw contain a set amount of useful energy (called House Energy). Table 3.1 below, and Figure 3.6 above, show that several days in the beginning of the period used much more energy than specified by the SRCC test. Two problems caused this wandering from the defined draw profile. The problem that occurred on Day 3 was a malfunction of the spool valve. At the end of the day when the spool valve moved into position to drain the collector it malfunctioned and became stuck in a position that allowed the pressurized hot water in the tank to pass to the drain used to drain the collector. It stayed in this position for about 40 minutes before it self-corrected the problem and fully closed. The temperature of the water incorrectly drained

was not recorded because it did not pass by a thermocouple. It is known that the water came from the bottom of the hot water tank. The temperature of the bottom of the tank was about 125 °F when the draining started and dipped down as low as 88 °F toward the end of the event. However, these measurements are from higher up on the tank than where the water was actually drawn from, so even this does not really give an accurate temperature of the water lost. As this hot water ran down the drain, it took valuable thermal energy with it.

This lost energy was not correctly recorded by any of the meters; therefore, this day of data was not used in compiling data on system performance. Some debris in the system, perhaps solder from the new meter installations, wedged in the valve causing it to stick in an improper position. This problem occurred several other times during the experiments, most notably about 2 months later during the second monitoring period when the tank erroneously drained for over 12 hours! It malfunctioned again on Day 14 of this period, although this time for a much shorter period, only 3 liters of hot water were drained. This caused an error of no more than 0.06 kWh, and was thus considered a minor error that did not devalue Day 14's data. However, this error is the reason Day 3 in Table 3.1 is grayed-out. It is not included in the average and total values given at the bottom of the table.

The increased house energy use of days 5 through 9 was caused by a programming error in the datalogger program The error occurred during some program updating to improve the utility of the recorded data. A mistake was made in the placement of a decimal, which caused the draws to continue past the specified 2 kWh. The draws only stopped at the end of the hour because of a programmed safety stop to turn off any over-running draw. This did not cause any errors in the monitoring system, it simply caused the

draws to run longer than desired. After the last draw on day 9, the mistake was found and corrected.

Table 3.1 below provides the most important measured and calculated daily values for this first period. The fourth column, entitled 'House Energy (calculated)' refers to the energy calculated to pass through the house-use meter when the volume data from the flow meter was used in conjunction with the thermocouple temperatures rather than calculated in the thermal meter using the temperature probe temperature difference. The eighth column, 'Change in Internal Energy this Day', refers to the change in internal energy in the tank from midnight to midnight as calculated from the average of the two tank thermocouples.

Table 3.1 Period 1 Daily Data Totals

Day	House Water Flow (liters)	House Energy (kWh)	House energy (calculated) (kWh)	Solar Water Flow (liters)	Solar Energy (kWh)	Solar Energy (calculated) (kWh)	Electric Energy (kWh)	Change in Internal Energy this Day (kWh)	Measured Losses (energy balance) (kWh)	Solar Fraction
1	0	0.0	0.0	0	0	0.0	0.0	0.00	0.00	0.00
2	353	12.1	12.4	1007	7.2	7.2	8.3	0.10	3.06	0.46
3	375	12.1	12.4	348	1.9	1.7	12.8	-0.29	2.31	0.13
4	494	14.4	15.1	513	3	2.6	12.5	0.13	-0.13	0.19
5	369	12.1	12.4	673	4.8	4.4	10.0	-0.35	2.36	0.32
6	429	14.1	14.5	934	6.6	6.7	11.1	0.33	2.91	0.37
7	465	14.8	15.1	565	3.7	3.7	13.7	-0.06	2.40	0.21
8	478	15.2	15.6	894	6.2	6.1	11.8	-0.15	2.52	0.34
9	469	14.6	14.7	377	2	1.7	15.6	0.35	2.27	0.11
10	461	15.3	15.6	1063	7.5	7.3	11.1	0.09	2.71	0.40
11	382	12.1	12.2	858	5.2	5.3	9.9	-0.05	3.03	0.34
12	385	12.0	12.3	938	5.4	5.5	9.5	0.05	2.58	0.36
13	387	12.1	12.1	216	1	1.0	12.8	-0.32	1.97	0.07
14	376	12.0	12.4	859	4.9	4.9	10.1	0.17	2.46	0.33
15	387	12.1	12.4	829	5.2	5.2	10.2	-0.38	3.33	0.34
16	366	12.1	12.6	885	6	5.9	9.4	0.53	2.14	0.39
17	371	12.0	12.6	891	6.2	6.0	9.0	0.10	2.30	0.41
18	389	12.0	12.5	1065	7	7.0	8.3	-0.09	2.85	0.46
19	396	12.3	12.1	638	4.2	4.3	10.3	-0.16	2.67	0.29
20	387	12.0	12.2	291	1.8	1.7	12.5	-0.11	2.11	0.13
21	388	12.0	12.3	407	2.4	2.3	12.3	0.15	2.17	0.16
22	382	12.0	12.4	681	4.4	4.3	10.1	-0.12	2.13	0.30
23	402	12.1	12.5	268	1	0.8	13.9	0.06	2.18	0.07
24	376	12.0	12.4	870	5.8	5.7	9.4	0.35	2.29	0.38
25	393	12.0	12.2	394	2	1.9	12.2	-0.05	1.99	0.14
26	401	12.1	12.7	813	5.1	5.0	9.7	-0.41	2.40	0.34
27	388	12.0	12.6	627	3.7	3.5	11.3	0.17	1.95	0.25
28	390	12.0	12.4	348	1.8	1.6	12.9	0.18	1.99	0.12
29	374	12.0	12.3	748	5.2	5.2	9.8	0.13	2.47	0.35
30	385	12.0	12.6	683	4.2	3.8	10.8	-0.16	2.11	0.28
31	384	12.0	12.3	280	1.6	1.5	12.6	-0.30	2.16	0.11
32	371	12.0	12.2	680	4.7	4.6	9.6	0.31	1.75	0.33
AVG	386.39	12.18	12.51	654.68	4.19	4.09	10.67	0.02	2.23	0.27
TOTAL	11978	377.5	387.86	20295	129.8	126.7	330.8	0.50	69.12	

The two graphs below show the temperatures experienced by the SDHW system over the monitoring period. The first graph displays the temperatures of the actual water flows, i.e. these are the daily mass-weighted averages of temperatures recorded every two seconds while a flow was occurring. All of the temperatures in the second graph are time-

averaged temperatures taken every two seconds throughout the day. The data from Day 3 has not been included in either of these graphs because it was flawed. Any flawed or incomplete data during the other two monitoring periods were treated the same. That day of data was included but grayed-out in the data table and then omitted from any graphs. Notice in the graph that the day numbers from the table correspond to the same day's data in the graph, but that any grayed-out days do not contain any data points.

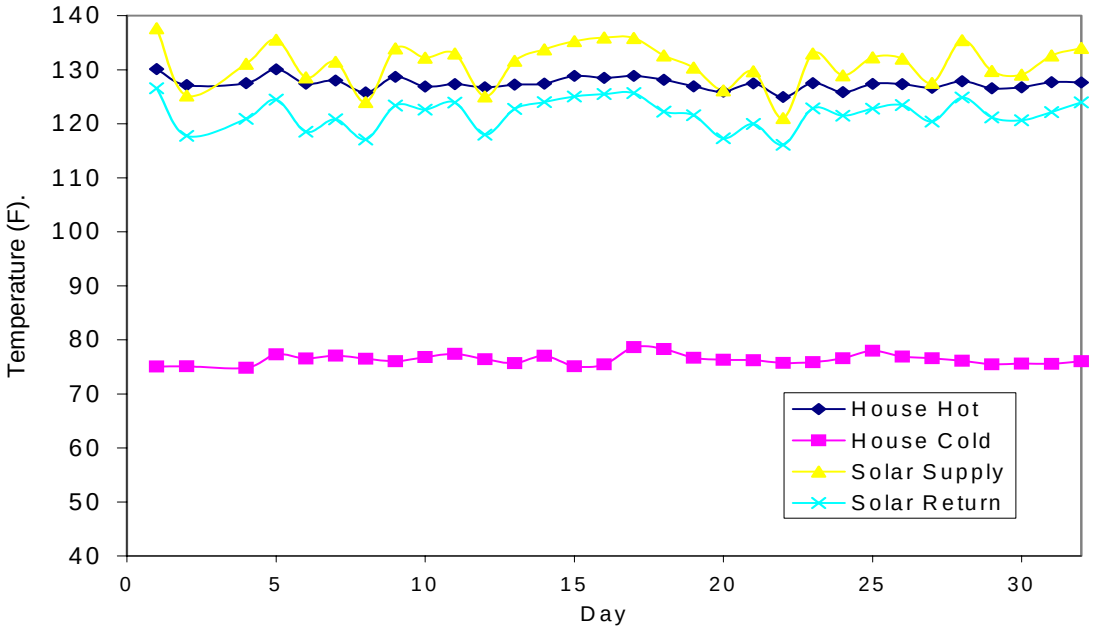

Figure 3.7 24-Hour Average Temperatures in Period 1

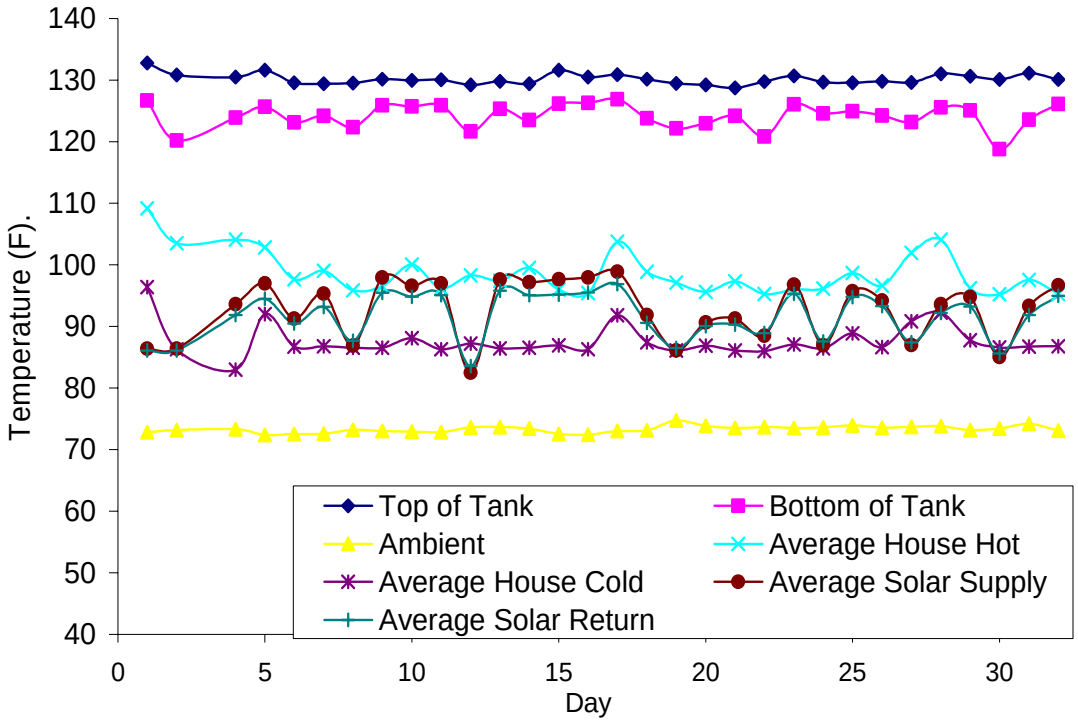

Figure 3.8 Temperatures of Water Flow During Period 1

3.4 Summer – DOE (Second Monitoring Period)

The second monitoring period was separated by just one day from the first monitoring period. The dates were July 14th to August 11th, 2003. The experiment for this period prescribed a different hot water draw profile and set the tank thermostats to a lower set point than the first month-long experiment. The draw profile used this period was that of the DOE. Recall that this profile demands draw of a specified volume, rather than a specified energy content. In addition, the set point was moved down to 120 °F from 135 °F. These two system changes, as well slightly sunnier weather caused the results to differ

from those of the first period. Again, the raw data was condensed into daily values for easier viewing and comprehension and may be seen here in Table 3.2.

Table 3.2 Period 2 Daily Data Totals

Day	House Water Flow (liters)	House Energy (kWh)	House energy (calculated) (kWh)	Solar Water Flow (liters)	Solar Energy (kWh)	Solar Energy (calculated) (kWh)	Electric Energy (kWh)	Change in Internal Energy this Day (kWh)	Measured Losses (energy balance) (kWh)	Solar Fraction
1	267	6.8	7.1	448	3.3	3.4	6.00	0.17	2.38	0.36
2	131	3.4	3.7	546	3.4	3.4	1.90	0.35	1.33	0.64
3	249	6.4	6.8	517	2.7	2.5	5.82	-0.14	1.87	0.30
4	249	6.6	7.1	719	4.7	4.6	4.30	-0.31	2.22	0.52
5	249	6.4	6.8	634	4.4	4.3	4.34	0.06	1.87	0.50
6	1363	12	14.6	693	3.8	3.9	8.70	-1.92	0.08	0.31
7	4952	26.2	17.8	1138	6.1	5.3	21.78	1.00	8.42	0.20
8	252	6.5	7.1	839	6.5	6.4	2.82	0.04	2.09	0.69
9	250	6.5	6.9	612	4	4.1	4.60	-0.34	2.17	0.47
10	250	6.7	7.3	878	6.7	6.9	3.28	0.47	2.38	0.68
11	251	6.8	7.4	911	6.9	6.7	2.80	-0.11	2.30	0.71
12	253	6.5	7.2	1094	7.7	7.7	2.04	0.25	2.37	0.79
13	252	6.5	7.1	1066	8.3	8.3	1.36	0.04	2.52	0.86
14	252	6.2	6.9	1038	8.3	8.3	1.12	0.11	2.48	0.88
15	257	6.6	7.3	1046	7.9	7.9	1.84	-0.08	2.50	0.81
16	251	6.8	7.3	977	7.9	7.8	1.98	-0.02	2.46	0.80
17	249	6.6	7.2	1035	7.9	7.9	2.04	0.12	2.67	0.80
18	249	6	6.5	264	1.6	1.8	5.86	-0.94	2.11	0.23
19	240	6.2	6.8	768	6	6.1	3.54	0.90	2.07	0.63
20	251	6.3	6.8	919	6.9	6.9	1.78	-0.36	2.32	0.80
21	257	6.1	6.9	940	6.5	6.7	2.90	0.35	2.38	0.70
22	244	6.2	6.7	452	3.5	3.5	4.24	-0.90	2.07	0.46
23	252	6.5	7.3	1027	8	8.1	2.00	0.71	2.12	0.80
24	240	6.2	6.8	194	1.3	1.4	6.08	-0.74	1.57	0.18
25	249	6.7	7.4	822	6.3	6.0	4.24	0.94	1.99	0.59
26	248	6.5	7.1	262	1.2	1.1	6.42	-0.74	1.36	0.15
27	252	7	7.4	617	4.2	4.2	5.02	0.28	1.69	0.45
28	243	6.5	7.1	401	2.5	2.6	6.00	0.00	1.57	0.30
29	369	11.8	11.4	1125	7.4	7.3	1.52	-4.91	2.53	0.83
AVG	294.0	6.78	7.40	761.6	5.49	5.5	3.60	2.13	0.92	0.75
TOTAL	7351	169.6	185.0	19040	137.3	137.5	89.90	53.54	0.00	

There are several differences immediately evident when compared to the previous period. The daily load, or house, energy is only about half of the daily load of the first experimentation period and the volume of useful hot water was 250 liters/day compared to nearly 400 liters/day during the first period. The average daily solar gain was nearly 25% larger and the system required only one third as much electric energy. These differences caused the solar fraction to be much higher as well. In addition, the daily change in internal energy seems to fluctuate noticeably more than it did during the first period. This is due to both the smaller draws and the lower set point, allowing the average tank temperature to climb significantly higher than the set point temperature on strong solar days.

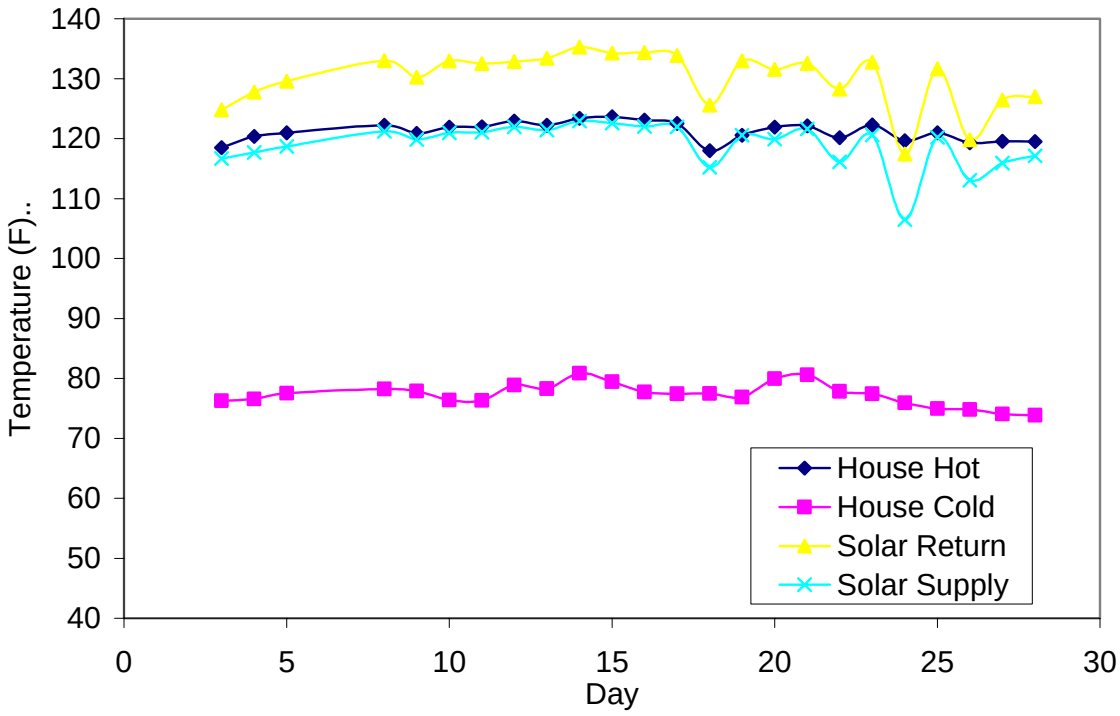

Figure 3.8 Daily Water Flow Temperatures for Period 2

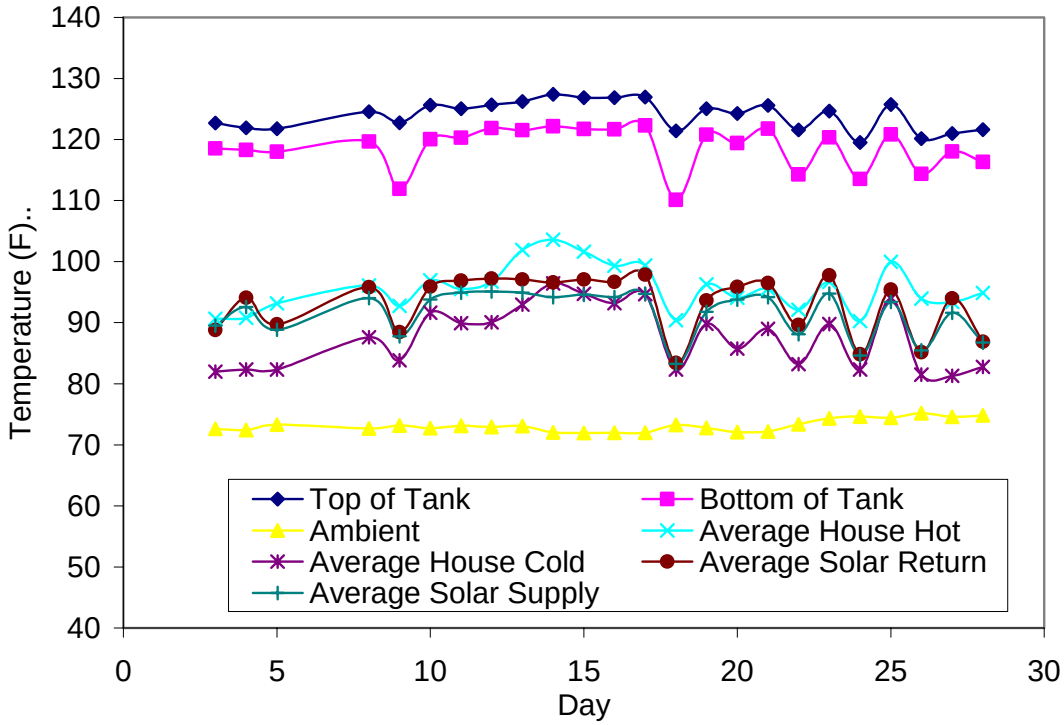

Figure 3.9 24-Hour Average Temperatures for Period 3

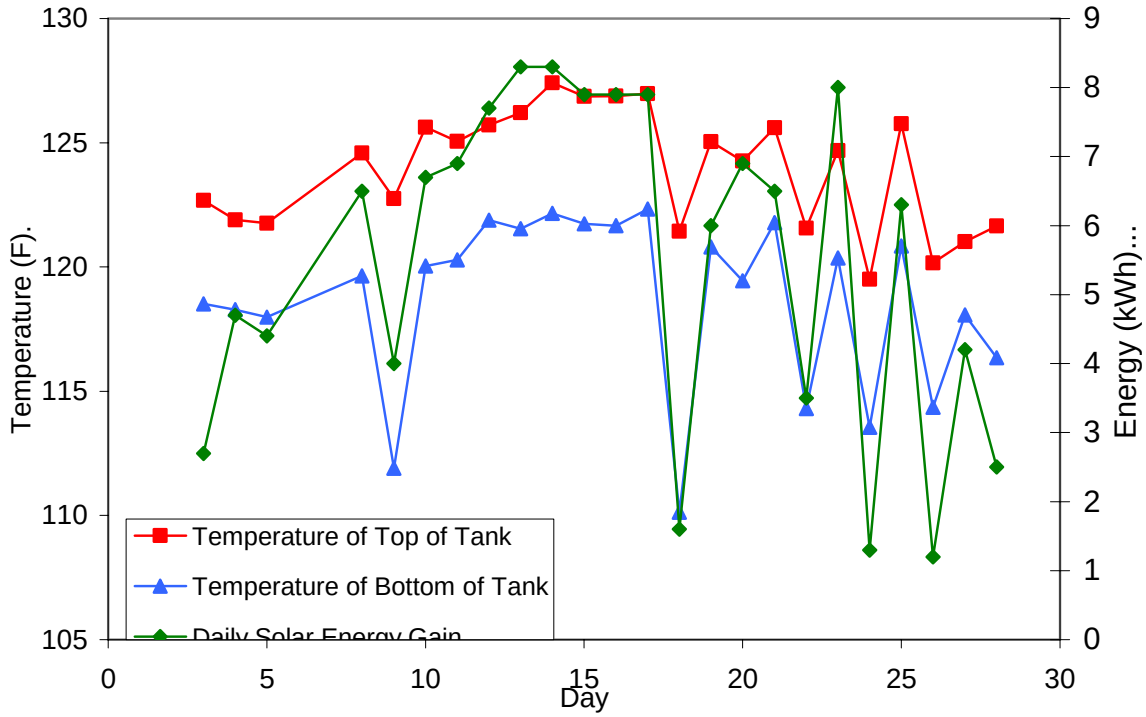

Figure 3.10 Daily Tank Temperatures Compared to Solar Gain

The results of this experimental period differed from prior results primarily because of the rather large differences in hot water draw volume and the difference in set point temperature of the hot water tank. Both of these factors played a role in the great volatility of the tank. The results of this volatility are seen in the greater variance of the daily change in internal energy of the tank. The smaller draws meant less energy use each day, this therefore allowed the solar gain to be great enough to significantly raise the temperature of the tank on very sunny days. The lower set point increased the difference in tank temperature between sunny and overcast days. This also caused a slightly greater range of thermal losses from the tank.

A more important effect of the lower set point was the increased efficiency of the solar collector. The hotter the water in the collector the more energy it loses to the environment both on the round trip and while in the collector itself. On average over the entire monitoring period (excluding grayed-out days), the water that flowed to the solar collector was only 2.8 °F cooler than the water from the first period. (118.9 versus 121.7) The returning water during this period averaged 129.9 °F, compared to 130.9 °F during the first period; only 1 °F cooler.

Study of the detailed data revealed that the equilibrium temperature of the water in the house pipes after a long period of no flow (i.e. overnight) is 4 to 5 °F cooler in the hot water line and 2 to 4 °F cooler in the cold water line than during the first monitoring period. This clearly shows that less heat was lost through these pipes when the system reached steady-state than when the tank set point was 135 °F. It is also obvious that the higher tank temperatures in the first period caused greater heat loss through the sides of the

tank. However, the greater solar gain during this period increased the losses from the solar pipes, thus the total difference in daily heat loss was not large.

3.5 Winter – DOE (Third Monitoring Period)

The final monitoring period occurred some time later, December 7th to December 17th and December 24th to January 11th. The break in data occurred when the data was not downloaded for an extended period over the winter holidays. The two days grayed-out are both partial days of data on either side of the break. This period was chosen to help determine the functionality of the meters during the winter when less sunlight is typically available. The system parameters were not changed from the second monitoring period, so both thermostats were both still set to 120 °F and the draw profile used was the DOE profile. Again, this meant that each draw contained a specified volume, 40 liters.

The weather during this period was obviously different than the other two periods, which were during the summer. The average daily solar collection was about 72% of the value for the first monitoring period and 55% of that of the second period. Many days during this period collected over 5 kWh of solar energy, however, there were six days that collected 0.2 kWh or less, and four more that collected no more than 2 kWh. Unfortunately, not only was less energy collected, but more was needed to provide equal amounts of useable hot water. This is because the cold input water entered the tank at a much lower temperature than during the summer. The average temperature of the measured cold-water inlet during this period was just over 51 °F, compared to over 75 °F

during the summer. These lower input temperatures also caused poor results from the thermal meter, and to a lesser extent the calculated thermal meter.

In order to gain greater understanding of the losses experienced by the uninsulated solar-loop and house-side pipes, all uninsulated metal was heavily insulated with ¾" thick rubatex insulation. This extra insulation clearly resulted in less thermal loss from the pipes, particularly in the solar-loop, where most of the exposed metal was and which often contained moving hot water for 6 to 8 hours a day. The effect this insulation had can be seen in the Table 3.3 below, and details of the difference it made and the information revealed are discussed in chapter 4.5.

Table 3.3 Period 3 Daily Data Totals

Day	House Water Flow (liters)	House Energy (kWh)	House energy (calculated) (kWh)	Solar Water Flow (liters)	Solar Energy (kWh)	Solar Energy (calculated) (kWh)	Electric Energy (kWh)	Change in Internal Energy this Day (kWh)	Measured Losses (energy balance) (kWh)	Solar Fraction
1	258	8.9	10.6	1168	5.3	4.9	6.16	-3.26	4.15	0.46
2	269	9.9	10.8	1009	4.8	4.5	7.20	-0.24	1.43	0.40
3	257	9.2	10.8	753	3.6	3.2	8.48	0.04	1.14	0.30
3	251	9.5	10.9	0	0	0.0	11.32	-0.15	0.58	0.00
4	262	9.2	10.7	995	5	4.8	6.80	0.18	0.96	0.42
5	259	9.2	10.6	924	4.6	4.4	7.48	0.25	1.19	0.38
6	249	8.9	10.8	204	0.9	0.6	10.48	-0.29	0.77	0.08
7	240	9.1	10.7	0	0	0.0	11.22	-0.02	0.55	0.00
8	258	9.8	11.1	999	4.9	4.4	7.32	-0.05	1.02	0.40
9	254	9.3	11.1	269	0.8	0.7	11.20	0.02	0.94	0.07
10	247	9.5	10.8	51	0.1	0.1	11.00	0.19	0.46	0.01
11	254	9.6	10.9	666	3.3	3.1	8.38	-0.34	0.88	0.28
12	240	8.8	10.9	304	2	2.0	8.88	-0.49	0.76	0.18
13	249	8.8	10.9	1000	4.9	4.6	7.18	0.19	0.73	0.41
14	249	9	10.9	1027	4.8	4.5	7.38	0.02	1.06	0.39
15	249	8.8	11.0	1023	5.9	5.6	6.76	0.34	1.27	0.47
16	249	9.1	10.9	1027	5.9	5.7	6.40	-0.01	1.32	0.48
17	249	9.1	10.8	923	5.4	5.3	6.46	-0.35	1.38	0.46
18	255	9.2	11.1	820	5.1	4.9	6.66	-0.07	0.89	0.43
19	249	9.2	10.7	1006	5.5	5.2	6.92	0.33	1.22	0.44
20	249	8.8	10.8	910	5.6	5.4	6.46	-0.02	1.27	0.46
21	245	9.1	11.0	156	1	1.1	10.00	-0.51	0.60	0.09
22	249	8.6	10.8	837	5.5	5.3	6.74	0.60	0.85	0.45
23	240	8.6	10.7	11	0	0.0	10.56	-0.51	0.74	0.00
24	250	9.1	10.7	170	1.1	0.9	10.46	0.34	0.51	0.10
25	248	8.8	10.3	822	4.7	4.4	6.34	-0.12	0.84	0.43
26	256	9.3	10.8	893	4.6	4.4	7.28	-0.09	1.30	0.39
27	260	9.5	11.2	128	0.2	0.0	11.52	0.23	1.05	0.02
28	241	9	11.0	0	0	0.0	11.20	-0.38	0.58	0.00
29	249	9.3	11.5	695	1.9	0.7	10.76	0.18	0.25	0.15
30	249	9.2	11.2	981	4.9	4.5	7.90	0.15	1.21	0.38
31	249	9.6	11.3	868	5	4.6	7.54	0.43	0.63	0.40
32	0	0	0.0	0	0	0.0	0.00	0.00	0.00	0.00
AVG.	251.21	9.19	10.89	626.4	3.28	3.05	8.56	0.00	0.93	0.27
TOTAL	7285	266.5	315.9	18167	95.1	88.5	248.22	0.12	26.9	

The solar input was clearly less than during the prior monitoring period, which took place in the late summer, but many days during this period still collected as much as the average day in the prior period. However, the energy balance during this period a drastically lower level of system losses. This large drop was due to three factors: less incident solar energy, extra pipe insulation, and meter errors due to much colder makeup water. The first factor is rather obvious and had been mentioned previously. The extra insulation made a significant difference in the level of system thermal loss. It is estimated that it reduced the system losses by an average of 0.3 kWh per day. The third factor is the most complex and least understood.

It was known that the cold makeup water caused the actual thermal house meter to under-meter, which clearly occurred this period. It would appear that this effect would also have occurred in the actual solar thermal meter, but in actuality, the actual meter read an average of 0.23 kWh per day higher than the calculated solar thermal reading. This minor anomaly is not yet understood.

A close examination of the energy balance loss measurements revealed that there was an error in the calculated energy meter readings. On each no-solar-flow day, the losses are around 0.5 kWh per day. This is 0.4 to 0.5 kWh per day lower than the losses known to occur in the system. The losses on the other, high solar, days were also about 0.4 to 0.5 kWh lower than expected. This would indicate that the calculated house meter over-metered the house hot water usage by about 0.4 or 0.5 kWh per day. However, the opposite was predicted, because the thermocouples also experience some temperature delay, therefore causing them to slightly under-meter. The energy difference seen could be accounted for by 3 °F of combined error between the two thermocouples. Because this

error was not seen in the earlier periods, and because the cold-water temperature is the only drastically different parameter, the cold water thermocouple is suspected. However, the true cause of the under-metering by the calculated house meter is not known.

Once these metering errors were corrected, the energy balance-derived losses were still significantly lower than the prior period. The average daily difference was 2.13 kWh minus 1.40 kWh. The difference in daily loss figures is very close to the amount of loss reduction the heat transfer analysis predicted would occur from the added insulation. It is therefore believed that the added insulation caused this remaining drop in losses (the drop in solar gain also played a minor and more easily assessed role). Further, this agreement is strong evidence for the accuracy of the high levels of loss attributed to the uninsulated pipes in the prior periods.

Note in the temperature graphs below that some data points and the connecting lines are missing in the solar data. This is because the 3 solar days that had zero solar flow obviously never experience a solar flow temperature to measure and record, therefore these data points were not included in the graph.

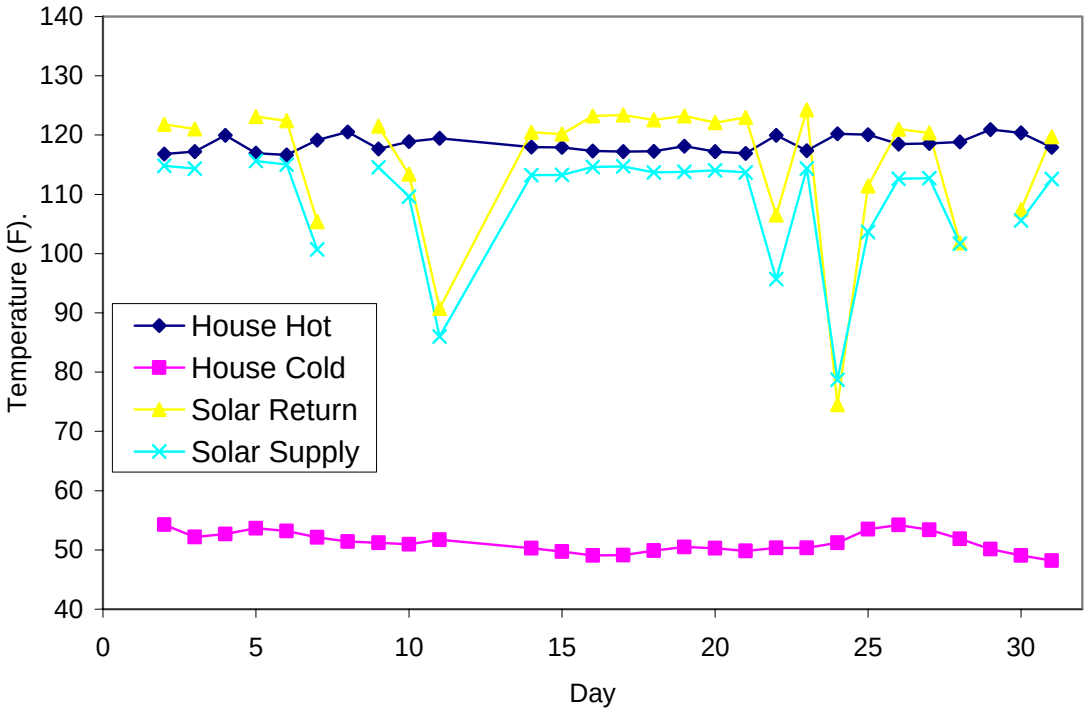

Figure 3.11 Average Temperature of Water Flows in Period 3

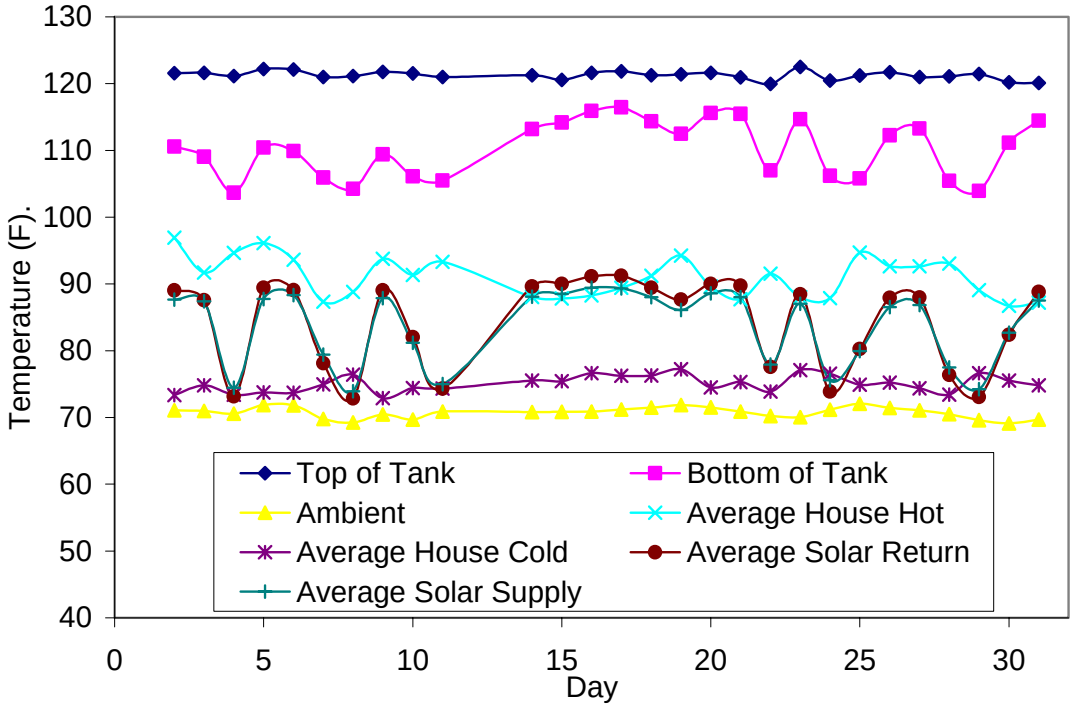

Figure 3.12 24-Hour Average Temperatures for Period 3

3.6 Verification of Results

In order for the presented results to have meaning, the collected data from which they were produced must be known to be correct beyond a reasonable doubt. This was accomplished by verifying the accuracy of each of the measurement instruments. A collection of means were used to accomplish this. The verification process started before any data was recorded. Accuracy testing was performed on the thermal meters by the manufacturer before they were shipped. Each meter underwent accuracy tests on the temperature difference reading of their matched pair of temperature sensors and on their energy metering. The largest percent error produced by either of the matched pairs of temperature sensors (measuring temperature difference) was only 0.119%. This was using temperatures of 40 and 140 ° C (104 and 284 °F). The maximum percent error of any of the energy metering tests on the two meters used was 0.63%, this occurred with inlet and outlet temperatures of 58 and 60 °C. (136.4 and 140 °F). These accuracy verification tests have led the researcher to trust the accuracy of the thermal meters when in a steady-state situation as in these manufacturer tests. Errors caused by transient effects are not ruled out by these test results.

In order to test the accuracy of the redundant thermocouples, the temperature readings from the thermocouples were used along with the flow pulse data from the thermal energy meter's flow meter to calculate the amount of thermal energy passing the meter. This secondary thermal energy metering value was calculated in a spreadsheet using the collected data. The specific heat of the water in question was calculated using a water property add-in using the average temperature of the two pipes. These calculations

of the amount of energy used were performed for each 5-minute period of data. The fact that these calculations are all performed in a spreadsheet means that modifications could be made to particular values.

This ability was taken advantage of to correct the miscalculations caused when the solar collector fills and other times when cold makeup activates the flow meter, but not when hot water flows out the hot water pipe. Making these adjustments made only a small difference on most days, 0.1 to 0.2 kWh, never more than 0.2 kWh on any day in the first two monitoring periods. However, during the third period, that difference ranged from zero kWh to about 1.0 kWh per day. The largest of these errors occurred on days when the collector filled one or more times shortly after a draw. The winter weather meant this occurred more often. In this situation the thermal meter 'sees' a great temperature difference and believes a large amount of energy has passed. In actuality the flow should not be measured, however its temperature should be considered when calculating the energy lost when the collector drains down. The calculated house energy meter readings presented in Chapter 3 do not include these corrections, however the daily house-use energy values used to calculate the thermal losses did include these corrections.

If the temperature difference between the meter temperature sensors was always the same as the temperature difference between the thermocouples then the two energy-use readings would have been equal. However, they were not always equal. During the first period, the calculated value was 2.7% greater than the reading from the thermal meter on average over the period. This curious gap continued to grow as the experiments continued and became disturbing. It was 9% during the second period and 19% during the third. The temperature of the cold city water coming into the tank was about 76 °F during the first two

periods and 51°F during the third. This suggests that the difference in the energy-use values was caused by discrepancies in the measurement of the temperature of the cold water. Close examination of the 5-minute data did indeed reveal this to be the case, but this was not understood until after the next experiment.

Numerous shorter experiments (up to one week) were performed between the second and third monitoring periods. Some of these results offered further insight into the discrepancy between energy-use values. The first such experiment monitored the system with both the solar system and the draw profile turned off. This meant that very little hot water was used each day and that the electric heating elements kept the tank temperature near the set point (120 °F). Over the 5-day period, the thermal energy meter reported that 0.7 kWh were used. Yet, the thermocouple/ flow meter calculations reported that over twice that amount had been used, 1.55 kWh. This energy was contained in 54 liters of flow, which were drawn in volumes of 1 to 5 liters. These draws occurred from 0 to 12 times in a day and were caused by primarily by people in the Solar House washing their hands. This large difference in readings occurred because the temperature probes from the energy meter are not able to respond as fast as the thermocouples to the rapid temperature rise that occurs when hot water begins to flow. Figure 3.13 shows the difference in the temperature probe and thermocouple pipe assemblies.

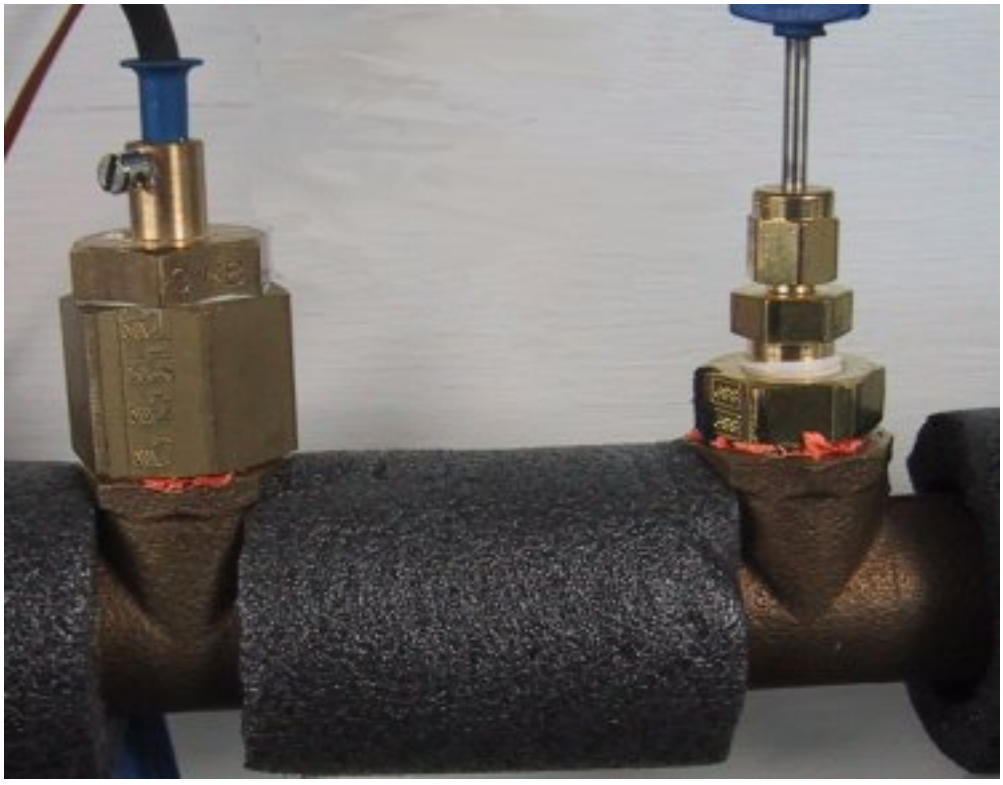

Figure 3.13 Size of Temperature Probe and Thermocouple Assemblies

Once this reaction time problem was understood, the role of the cold-water temperature on the energy reading discrepancy was also understood. The 5-minute data revealed that the water in the cold pipe just before a planned draw was nearly always significantly warmer than the cold water makeup water for the draw. Obviously, the colder the makeup water the greater the temperature difference between the temperature of the stationary water in the pipe before the flow and the temperature of the water in the flow, and thus the greater the error in the thermal energy meter's reading. The 5-minute data shows just that, greater error between the two energy readings when the temperature difference before and during the flow is larger. The slow response of the temperature probes also, of course, caused error in the temperature reading of the hot pipe water

temperature. This error made the meter underestimate the energy in the early part of practically every hot water draw.

The next period of experimentation was to produce the efficiency curve for the solar collector. This required that the tank begin the solar day at a cool temperature (in this case defined as below 80 °F). To achieve this, the tank was drained early each morning. This meant a very large and long draw occurred each day that gave some insight into the accuracy of the house-use energy meter. These draws lasted about 30 minutes and contained nearly 60 gallons. On average, the thermal energy meter recorded 5.63 kWh each day and the thermocouple/flow meter calculation recorded 5.26 kWh; 0.37 kWh less than the meter.

An examination of the 5-minute data clearly revealed again the difference in energy readings occurred because of the temperature probes' inability to quickly respond to temperature change. As expected, the thermal meter underestimated the energy flow in the first 5-minute period by an average of 0.17 kWh (values ranged from 0.11 to 0.24 kWh) over the seven days. After the first 5-minute period, on all seven days, the calculated energy reading and the meter reading agree (within ± 0.1 kWh, the size of the thermal meter pulses) until the hot water temperature began to drop severely. This period of tight energy flow agreement lasted for the bulk of the draw, usually over 20 minutes. Thus showing it took approximately 5 minutes of 2 gpm flow for the temperature probes to read the correct temperature. When the hot water temperature dropped (as measured by the thermocouple) quickly as the end of the original hot 50 gallons left the tank, the meter reading was always significantly greater than the calculated meter reading. This was clearly because the temperature probes were not able to respond quickly to the change in

temperature. Often the energy total for a 5-minute period was as much as four or five times higher than that measured with the thermocouples. The largest absolute difference was 0.56 kWh (0.7 Vs. 0.14 kWh).

A second important conclusion on the system accuracy was drawn from this same period of data. The large draw that occurred each day removed a large amount of energy from the tank, thus significantly dropping the tank's total internal energy. This provided an excellent opportunity to test the accuracy of this calculated value. The results were very consistent, as seen in the graph below. (Figure 3.14) Over the period of the draw plus the next five to fifteen minutes, depending on how long it took for the tank temperature readings to become stationary, the calculated change in internal energy is nearly identical to the energy reading from the thermal energy meter, but consistently about 0.5 kWh above the calculated thermal energy meter. Because of the known errors in the energy reading of the thermal energy meter, it is believed that the calculated change in internal energy was not 100% accurate. If the house energy meter value calculated with the use of the thermocouples was perfectly accurate then the calculated change in internal energy was consistently about 10% too high.

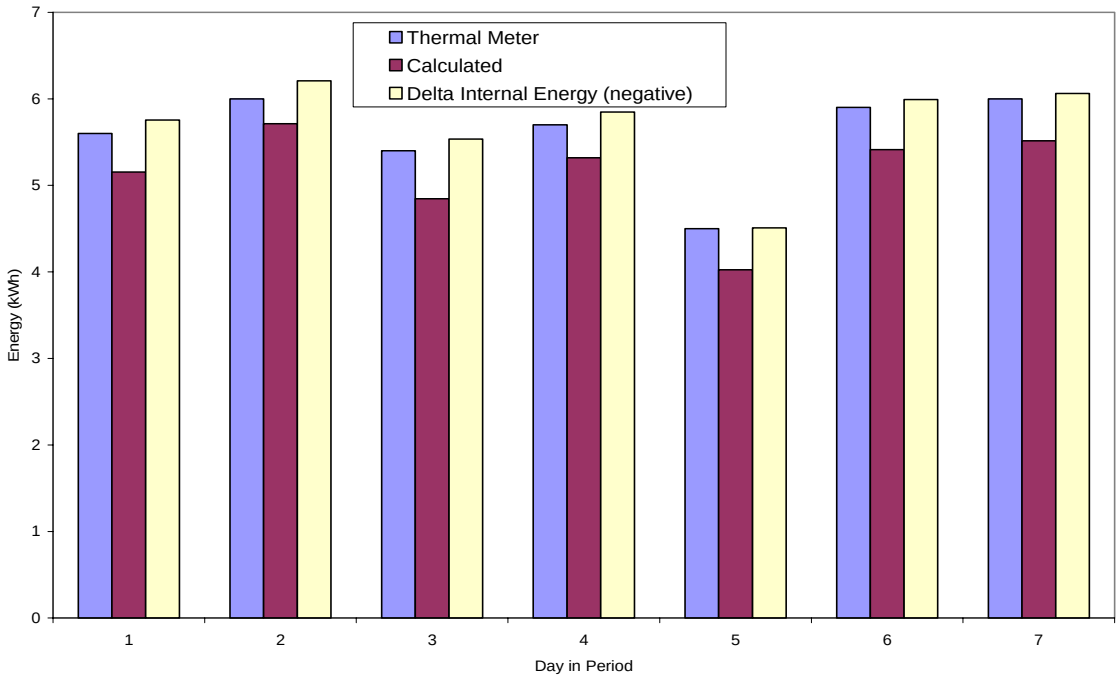

Figure 3.14 Comparison of Delta Internal Energy Calculation and Energy Meters

It seemed likely that the calculated change in internal energy is off by this much because of inaccuracy in estimating the average tank temperature from just two temperature readings. The tank is stratified which makes this task difficult. However, the data from this experiment was also analyzed using a top and a bottom weighted tank average temperature. Even using either the top or the bottom reading as the tank temperature the energy difference was only able to be brought down to 0.17 kWh per day. This is a 3.5% difference. It is believed that the majority of this error is in the tank average temperature measurement. This is because the other possible sources of error: the flow meter reading and the water flow temperature readings appear much less likely to be in error. This is because the flow meter has been shown to be more accurate than 3.5% and the measurement of the water flows are much more straightforward than the measurement of the average tank temperature. Also, no other instances of error have been found in any

of these devices, so it has been assumed that the majority of the error came from the most likely source.

It was possible to further study the dynamics and accuracy of the change in internal energy calculation by studying events in the 5-minute data when a known amount of electrical energy was added to the tank, raising its internal energy a known amount, while no other non-loss energy flows were occurring. This situation highlights the difficulty in accurately measuring the average tank temperature (particularly in non-steady state) with just two thermocouples on the side of the tank. Such a test is very difficult because after the energy has been added by the heating element it is a long time before the tank temperature readings are again stable. During this time the tank is also losing heat to the environment. It is not known how long it takes for the system to again be fully mixed, and even then the temperature distribution is not known.

In these quick tests on the data, the change in internal energy calculated was significantly more than the amount of electric energy added to the system. The best results were received when the second internal energy calculation was made on data over an hour after the heat addition. Even then the delta internal energy was often up to 50% greater than the electric energy added, if a much shorter time was used the delta internal energy was often nearly double the actual electric energy added! The accuracy of the electric meter has been thoroughly tested, so the only possible reason for this disagreement is an error in the estimates of the average tank temperature. Finally, it was concluded that a 10% error in agreement on the test described in the previous paragraph was adequate to prove the technique as acceptable, especially when the small size of the daily changes in internal energy experienced most days is considered. It is also important to remember that the two

internal energies compared to determine the daily delta internal energy are calculated at midnight, at time when there has not been any energy flows other than losses for over fives hours.

As mentioned earlier, it was necessary to rule out inaccuracies in the flow meters. The flow meters are integral to the two thermal meters, as well as to their calculated counterparts. The accuracy of the flow meters was tested using the captured volume method. First, the house flow meter had three 40-liter draws taken, each separated by 3 to 4 minutes. The water from all three draws was captured in a single large plastic container. The draw was taken as three separate draws to both best represent the actual use of the meter during the monitoring periods and to increase the volume of water involved in the test in order to improve the reliability of the test. The actual volume of the draw was measured with an accuracy of an estimated plus or minus one percent. The measured volume was 32.18 gallons, or 121.84 liters. The last draw before the test was an automatic 40 liter draw, thus it was stopped just as a volume pulse was produced by the flow meter. Therefore, the first pulse received during the test did in fact represent one entire liter of water. Similarly, the third draw in this experiment was stopped just as the 120^{th} pulse was received. Thus, the energy meter recorded 120.0 liters of water flow during the same period 121.84 (± 1.2) liters of water actually flowed. This means the flow meter of the house-side energy meter has an error of approximately 0.5 to 2.5%. This is a small amount of error; therefore, this flow meter is considered adequately accurate. If the flow meter experienced an error of 2.5% (it read less than the actual flow), this would account for approximately one quarter of the difference between the daily average calculated meter

reading and the daily average delta internal energy in the multi-day experiment presented earlier in the chapter.

A very similar test was completed to verify the accuracy of the flow meter in the solar loop. The setup required for this test was somewhat more complicated however. The test was performed during the day when there was enough sunlight out to open the spool value to the operate position, but at the same time the power to the solar pump was unplugged. The water was moved through the loop using the system water pressure in the tank. The flow rate was adjusted to 0.6 gallons per minute (indicated by the rotameter), using the ball value at the bottom of the supply line, for the first two runs and 0.4 gpm for the third run. The water was captured at the end of the loop by opening the strainer and allowing the water to flow into a large plastic bucket. After the collector was full of water and the flow reached a steady rate a fresh bucket was placed under the outlet and the time since the last meter flow pulse was recorded. In this way, partial pulses were able to be accounted for. The beginning and end of each test was planned so that one-half of a pulse worth of water, 0.5 liters, was captured both before and after the recorded pulses. Approximately five gallons of water (18.93 liters) were captured while the datalogger recorded the flow pulses produced by the flow meter. The actual volume of each test flow was accurately measured by hand. The data from the three runs are shown below. The percent error for the three tests ranged from 0.5% to 4.0 %, with a total volume percent error of 1.9%. After this test, it was understood that the solar loop flow meter was very accurate, and that henceforth it was considered as 100% correct in order to have a convenient standard for comparison.

Table 3.4 Solar Flow Meter Accuracy Test Results

Test Run #:	Volume Record by Flow Meter (liters)	Actual Captured Volume (liters)	Percent Error
1	19.0	18.9	0.5 %
2	21.0	20.2	4.0 %
3	20.0	19.8	1.0 %
Total	60.0	58.9	1.9 %

An accuracy problem was discovered involving the house-use thermal energy meter. This problem affected both the temperature probes and the thermocouples. On days in which the system did not receive adequate radiation to open the spool valve and fill the collector before the first draw serious inaccuracies arose when it did fill the collector. As the cold water rushed by the house-use flow meter the calculator began taking temperature readings and calculating the energy passing through the meter. However, there was not actually any useful hot water going to the house, instead warm water was being sent up into the collector, but because the first draw had already occurred the temperature probe in the hot pipe read an elevated temperature. Thus, the meter reported energy leaving system that did not leave. This problem was substantially worse in the winter when the cold water was so much colder than the indoor ambient temperature and the collector filled later in the day. This meant significant inaccuracies occurred even when the water in the hot pipe had cooled to its steady state temperature. The worst case was an abnormal day in the winter test period when the collector filled and drained three separate times, resulting in over-metering of nearly one kWh of energy. It was simple to account for these events in the energy meter calculation based on the thermocouple temperatures. The volume sent to the collector was manually removed from the house-use energy calculation.

The electric energy meter was also experimentally verified, although they are well known to be extremely accurate and reliable. The circuit has a 100% resistive load, so the power factor is one. The amperage was measured with a professional quality clamp-on ammeter and the voltage measured with a high quality multimeter. These readings were taken during a 5-minute period of heating by a resistive heating element. During this time, the amperage fluctuated between 18.6 and 18.7 amps (18.65 amps was used in the calculation below) and the voltage stayed constant at 243.0 volts. This results in a calculated delivered power of approximately 4532 Watts, just over the rated power of the heating element (4500 Watts). When this power is multiplied by 5 minutes, the product is $0.377\overline{6}$ kWh. During this 5-minute period, the electric meter recorded 0.38 kWh. However, the meter increments in 0.02 kWh. A quick look over the 5-minute revels that every time the electric meter is on for an entire 5 minute block it usually records 0.38 kWh, but every so often it records 0.36 kWh. An average of 120 of this periods found the average energy period to be $0.37\overline{6}$ kWh. This is a percent difference of just 0.27%. This tiny error could easily be accounted for by use of 18.65 amps, because the reading fluctuated the actual value could be marginally higher or lower. Clearly the meter is extremely accurate.

The temperature difference between the two flows on the solar loop (from 5 to 12 °F) is much smaller than the temperature difference (45 to 66 °F) between the two flows that determine the energy used by the house. This small temperature difference means that any errors in the individual temperature readings of the thermocouples have a much larger effect on the calculated thermal energy flow. However, the data did not suggest that this was a problem. The actual and the calculated solar thermal energy meter values tended to match quite well, considering the known time response issue. The largest daily difference

in magnitude experienced on any day during the three monitoring periods was 0.48 kWh (10.3% difference). On average over each of the three periods, these two values differed by 2.5%, 0%, and 7.3% respectively. The daily values did not vary very much from this average, suggesting there was not much random error, or imprecision, in the thermocouple readings.

Although the accuracy of the measurement instruments has been verified, complexities of the SDHW system and its metering still left analysis to be done in order to fully understand the functioning of the system and the metering of it. The majority of the required analysis was centered around the system losses, which were the unmeasured energy flows so important to accurately completing the system energy balance.

Chapter FOUR SYSTEM LOSS ANALYSIS

The raw and processed data presented in chapter 3 provided a good idea of how both the SDHW system and the monitoring system performed, but there was a need to know more. The need to closely study the system losses was not fully realized until the data from the first period was processed. At that point the larger than initially expected tank losses were discovered, and their incredible importance to the system analysis was further understood This prompted the running of several experiments and the detailed heat transfer analysis provided in Chapter 5. First, three experiments were performed to determine the losses from the tank and the pipes inside of the energy meters (the energy not accounted for by the energy meters and the change in internal energy). In each of these experiments, the solar energy system and the draw profile were disabled, leaving only the electric heating elements to add energy to the system and only losses to the environment (and occasional small draws in two cases) to remove energy. The first of these experimental periods was mentioned earlier in the discussion of the temperature probe response time.

4.1 Short Experimental Periods

The first of these periods, five days in late September of 2003 (day 262 to 266), left the hot water line to the house operable, thus allowing hot water to be used in the house; resulting in occasional small draws. During this period, 0 to 24 liters of hot water were used each day, these small draws caused large differences between the energy-use reading of the meter and the calculated energy-use reading based on the thermocouple temperatures. Over this period, the electric heating elements supplied 1.25 kWh on average per day. The house thermal energy meter recorded 0.14 kWh of hot water use and the calculated thermal energy meter reported 0.31 kWh of hot water use per day. The average change in internal energy per day was just 0.01 kWh. This meant an energy balance returned two different values of losses depending on which energy-use value was used. With the use of the thermal energy meter value, the energy balance shows that 1.10 kWh of losses occurred each day, while an energy balance using the calculated thermal energy meter value showed that an average loss of 0.93 kWh occurred each day (Table 4.1).

The next similar experimental period occurred 28 days later in late October (day 294 to day 301). Again, the hot water line was left operational. This time the electric energy supplied an average of 1.28 kWh each day. The energy meter recorded an average daily use of 0.21 kWh and the thermocouple calculation reported an average daily use of 0.40 kWh. This resulted in energy balances showing 1.03 kWh and 0.83 kWh of loss respectively. The best results came from the next experimental period when the hot water line was closed, so that the only energy input was the electric energy and the only energy

losses were the losses to the environment. The set point was 120 °F and the average tank temperature was a little under 115 °F. In this period, the average energy input was 0.864 kWh each day, and the daily losses calculated from an energy balance were 0.867 kWh. Because of the highly accurate nature of the electric energy meter, it is believed that this is an accurate level measure of the losses of the system under these conditions. The fact that the calculated losses from this period match well with the calculated losses from the two prior experimental periods where many small draws occurred suggests the calculated house energy meter is very accurate for small flows. This is noteworthy because even a small time response problem would expose itself under the condition of many short and separated draws.

Table 4.1 Experimental Daily Steady State Tank Losses

	Tank Average Temperature (°F)	Daily Losses Calculated from an Energy Balance using the Calculated Meter Readings (kWh)
Experiment 1	115	0.93
Experiment 2	115	0.83
Experiment 3	115	0.87
Average	115	0.877

All three of these experiments occurred with the tank set point at 120 °F, so the system would experience greater losses with the set point at 135 °F. The average tank loss from these periods (Table 4.1) is considered the 'foundation' of the losses experienced by the system. With almost not load, and no solar flow, the tank was in a quasi-steady state. The losses were greater with the solar system running. This was because the average tank temperature was higher and also because the solar pipes were at a much higher temperature than when the system was not operating (~15 °F higher on average over an entire day, up to

60 °F higher during operation). The exact losses under dynamic conditions are explored in the next chapter. Losses were also greater when there was a significant amount of hot water use spread out during the day. This was because the pipe supplying the hot water spends more time at an elevated temperature (~6 °F higher on average over an entire day). However, this last effect is quite minor.

Other short experimental periods also gave some insight into the accuracy of the meters and the actual system losses. The first such experiment lasted just four days. During this period, the solar energy system was disabled and the DOE draw profile was executed. The cold city water during this period was quite cool (60 °F) and caused the two energy-use meter readings to differ by 0.88 kWh (over an 11% difference) on average per day. The energy balance loss calculation revealed respective losses of 1.75 and 0.87 kWh. The daily losses as calculated using the calculated energy meter value is nearly identical to the daily losses found in the prior experiment. Both of these periods involved the same set point and ambient temperatures, so therefore very similar daily losses were expected. This close agreement of calculated losses suggests the energy-use readings from the thermocouple-based energy calculation were accurate and that there was very little increase in system losses due to the execution of the draw profile. The calculated losses using the actual house energy meter reading showed again that there was a significant amount of error in this thermal energy reading.

4.2 Loss Calculations from Heat Transfer Analysis

The data from the experimentations provided a good idea of the levels of heat loss from the system; however, a fundamental heat transfer analysis provided a basis for comparison. It also helped determine the relative size of the losses from each loss region. The "tank" lost energy to the surrounds from two regions, the tank and both the house and solar pipes near the tank. Losses did occur in the pipes farther away from the tank, but these energies were already accounted for by the thermal meters. This energy lost from the house pipes away from the tank does not differ between SDHW and DHW systems. So, although important to the homeowner, these losses were not considered in this study. Similarly, the solar loop between the meter and the solar collector experiences significant losses to their surroundings. These losses are modeled using the pipe loss calculations developed for the near-tank pipes.

4.3 Tank Heat Loss Heat Transfer Analysis

The majority of the losses occurred in the tank. It is the center of the system and will thus be analyzed first. The tank itself may be divided into three surfaces: the top, bottom, and sides, to facilitate loss calculations. These heat loss paths are all in parallel. Any heat flowing through one of these pathways must overcome both the effective

conduction and convection resistances to heat transfer. The losses from the tank alone are defined as:

$$q_{Tank,loss} = q_{sides,loss} + q_{top,loss} + q_{bottom,loss} \tag{4.1}$$

The equations for the heat loss rate through the sides and the top are very similar. Both include series resistances of a conductive resistance through the insulation (the sides include an extra insulating blanket as well) and a convective resistance from the outside of the tank to the ambient air. The differences are due to geometry.

$$q_{sides,loss} = \frac{T_{Avg.Tank} - T_{\infty}}{\frac{\ln\left(r_{Tank,OD} / r_{Tank,ID}\right)}{2 \cdot \pi \cdot l \cdot k_{Tank,insu}} + \frac{\ln\left(r_{wrap,OD} / r_{wrap,ID}\right)}{2 \cdot \pi \cdot l \cdot k_{wrap,insu}} + \frac{1}{2 \cdot \pi \cdot r_{wrap,OD} \cdot l \cdot (h_{air} + h_{rad})}} \tag{4.2}$$

$$q_{sides,top} = \frac{T_{Avg.Tank} - T_{\infty}}{\frac{t_{insu}}{\pi \cdot r_{wrap,OD}^{\ 2} \cdot K_{insu}} + \frac{1}{\pi \cdot r_{wrap,OD}^{\ 2} \cdot (h_{air} + h_{rad})}} \tag{4.3}$$

The equations above do not include the heat transfer resistance between the water in the tank and the inner tank wall, the conduction through the actual metal tank, or any contact resistances between any layers. This is because the resistances of these are so low compared to the conduction through the insulation and the free convection to air that they are neglected.

Table 4.2 Basic Hot Water Tank Parameters

	$Radius_{ID}$ (ft)	$Radius_{OD}$ (ft)	Length (ft)	Thickness of insulation (in)	K of insulation (Btu/hr·ft·F)	h_{air} (Btu/(hr·ft^2·F)
Tank Sides	0.6667	0.7917	4.58	1.5	0.0143*	See wrap
Wrap	0.7917	0.8750	4.58	1.0	0.0350	0.305**
Top	n/a	0.7917	n/a	1.5	0.0143*	0.416**
Bottom	n/a	0.7917	n/a	0.75	0.0143*	n/a

*A higher value (0.02) was used to account for thermal short circuits. The results with this higher value also agree much closer with experimentally determined loss amounts, and these are the results presented in this chapter. See chapter 4.4 for more details.
** Correlation calculations for the tank at 115 °F

The dimensions in the table above are as defined by the manufacturer. The k-values of the wrap came from Incoperia and DeWitt [15]. The heat transfer coefficient, h was calculated using various methods, the values presented are from empirical correlations and are a function of the estimated temperature difference between the surface and the ambient air, based on the tank average temperature. The values presented are for the tank when the thermostats were set to 120 °F, and the tank average temperature was about 115 °F.

The free convection coefficient h_{air} for the wrap was calculated based on the "thick cylinder" limit. Thus, when the boundary layer thickness δ_T is much smaller than the cylinder diameter D, the curvature of the lateral surface does not play a role, and the Nusselt number can be calculated with the vertical wall formulas. This condition is known to be satisfied when

$$\frac{D}{L} \geq \frac{35}{Gr_L^{1/4}} \tag{4.4}$$

The calculation of the Grashof number,

$$Gr_L = \frac{g \cdot \beta \cdot (T_s - T_\infty) \cdot L^3}{\nu^2} \tag{4.5}$$

required both the ambient temperature and the surface temperature [16]. Nine surface temperature readings were taken spread evenly over the sides of the tank when the average tank temperature was 110 °F. These were made using a type T thermocouple and an Omega digital handheld thermocouple reader. These readings indicated that the surface of the insulating wrap around the tank was only about 2 °F above the ambient temperature. This tank temperature represents the lowest end of the range of average tank temperatures experienced by such a system, and therefore will be the situation most at risk of not meeting the thick cylinder condition. When the temperature difference between the wrap surface and the air is 2 °F, the values of the inequality shown above are: 0.289 > 0.238, thus the condition was met at all times during the monitoring periods.

The calculation of h first requires calculating the Rayleigh number. The Rayleigh number,

$$Ra_L = Gr_L \cdot \Pr \tag{4.6}$$

is based on the characteristic length L of the geometry. In the case of the sides of the tank, this is the length, or vertical height of the tank. Next, the average Nusselt number was calculated from the correlation developed by Churchill and Chu [16] that may be applied over the entire range of Ra_L. This correlation is for a constant heat flux situation and is of the form

$$\overline{Nu}_L = \left\{ 0.825 + \frac{0.387 \cdot Ra_L^{1/6}}{[1 + (0.492/\Pr)^{9/16}]^{8/27}} \right\}^2 \tag{4.7}$$

This average Nusselt number was then used to calculate an average heat transfer coefficient h. The actual calculations were performed in a spreadsheet on every five minute set of data, utilizing some data lookup features. The calculated value for the average heat transfer

coefficient for the sides of the tank was 0.329 (BTU/hr·ft^2·°F), or 1.87 (W/m^2·K) for the case of a temperature difference of 3 °F.

Table 4.3 Calculation of Average Convection Heat Transfer Coefficient for the Sides of the Tank

Average Tank Temp (°F)	Temperature difference (°F)	Gr_L	Ra_L	Average Nu_L	Average h_{sides} (W/m^2·K)	Average h_{sides} (Btu/h·ft^2·F)
110	2	4.69E+08	3.31E+08	87.55	1.649	0.291
115	2.33	5.47E+08	3.87E+08	91.99	1.721	0.304
120	2.66	6.26E+08	4.43E+08	95.43	1.785	0.315
125	3	7.05E+08	4.99E+08	99.16	1.875	0.330
130	3.33	7.83E+08	5.55E+08	104.31	1.924	0.339
135	3.66	8.61E+08	6.11E+08	104.85	1.974	0.348
140	4	9.38E+08	6.63E+08	108.19	2.046	0.361

The heat transfer coefficient for the top of the tank was found using an average Nusselt number correlation developed by McAdams. Incoperia and DeWitt [15] note that improved accuracy may be obtained by altering the form of the characteristic length on which the correlations are based. In particular with the characteristic length defined as

$$L \equiv \frac{Area_{surface}}{Perimeter} \tag{4.8}$$

The recommended correlation for the average Nusselt number for an upper surface of a heated plate is

$$\overline{Nu}_L = 0.15 Ra_L^{1/3} \qquad \text{for} \qquad \left(10^7 \le Ra_L \le 10^9\right) \tag{4.9}$$

Again, the temperature of the surface of the top of the tank was measured in numerous places and at a range of different average tank temperatures, the results are

shown in Table 4.4. This was used to calculate the Grashof, Rayleigh, and average Nusselt numbers as was done for the sides of the tank

Table 4.4 Calculation of Average Convection Heat Transfer Coefficient for the Top of the Tank

Average Tank Temp (°F)	Estimated Temperature Difference (°F)	Ra_L	Average Nu_L	Average h_{top} ($W/m^2 \cdot C$)	Average h_{top} ($Btu/hr \cdot ft^2 \cdot F$)
115	5.0	1.57E+07	35.57	2.36	0.416
120	5.7	1.79E+07	37.14	2.47	0.435
125	6.5	2.05E+07	38.79	2.58	0.454
130	7.2	2.27E+07	40.12	2.67	0.470
135	7.9	2.49E+07	41.37	2.75	0.484
140	8.6	2.71E+07	42.54	2.83	0.498

An effective heat transfer coefficient of radiation heat loss, h_{rad}, was calculated for both the sides and top of the tank. The calculation of this coefficient made it a simple matter to include the radiation losses in the tank loss calculations. The coefficient was calculated as shown in equation 4.10.

$$h_{rad} = \varepsilon \cdot \sigma \cdot \left(T_s^2 + T_{air}^2\right) \cdot \left(T_s + T_{air}\right) \tag{4.10}$$

where Ts is the temperature of the surface in Kelvin. The exact temperature of the surface is of little importance because no temperature difference is used. Instead, h_{rad} is used to calculate the thermal resistance (eqns. 4.2 and 4.3) of the sides and top of the tank, so only the overall temperature difference is needed. The outer coating of the insulation blanket is made of some type of plastic, so an emissivity of 0.8 was used in the calculations. [17] This emissivity was used for the top surface calculations as well. The top is partially covered with the edges of the wrap, but most of the rest of the surface is a coated metal. The emissivity of this material is difficult to know without actual testing. In lieu of this testing,

because the exact value had a very small effect on the total tank losses, 0.8 was used for the top emissivity as well.

Table 4.5 Calculation of Effective Radiation Heat Transfer Coefficient

Average Tank Temp (°F)	Sides h_{rad} ($W/m^2 \cdot C$)	Sides h_{rad} ($Btu/hr \cdot ft^2 \cdot F$)	Top h_{rad} ($W/m^2 \cdot C$)	Top h_{rad} ($Btu/hr \cdot ft^2 \cdot F$)
115	4.70	0.827	4.73	0.834
120	4.70	0.828	4.74	0.835
125	4.71	0.829	4.75	0.837
130	4.71	0.830	4.76	0.839
135	4.72	0.830	4.77	0.840
140	4.72	0.831	4.78	0.842

The average tank temperature and the ambient temperature remained fairly constant during each monitoring period, so a different set of values of h was used for each of the three monitoring periods (one for the sides and one for the top). This was necessary because surface temperatures were not recorded throughout the experiment, and attempting to estimate them for each 5-minute time step would be no more accurate and much more trouble than using an average value over the entire period.

However, when all of the calculations were made, the daily calculated losses were clearly less than those indicated in the experiments. Although, it was uncovered in literature that it is the norm for hot water heaters to lose twice (or up to 5 times [18]) what would be expected from their nominal R-Values [19, 20]. To account for this, the k value of the tank insulation was increased, representing insulation degradation and thermal shortcuts in the tank. A k was chosen so that the calculated surface temperatures closely matched what had been measured. Once there was a calculated heat flux, q, for each loss

pathway (tank sides, tank top, tank bottom) it was possible to calculate the surface temperature. The surface temperature of the bottom was assumed to be in excellent contact with the floor and is therefore known, so there was no calculation to be performed for the tank bottom. In the case of the tank sides and top, it was possible to calculate the surface temperature from equation 4.11. The tank insulation k value that produced calculated surface temperatures that matched the measured surface temperatures was 0.020 Btu/hr·ft·F. At this k value, the total tank loss agreed well with experimental values. Although it is somewhat difficult to find a true average surface temperature by taking individual handheld readings, the error is believed to be within one degree Fahrenheit

$$T_s = T_{Tank} - q \cdot \left(R_{insu} + R_{wrap} \right) \tag{4.11}$$

Table 4.6 Results of Tank Sides and Top Calculations during the Three Monitoring Periods

		Average Tank Temperature (°F)	Estimated Temperature Difference (°F)	Average h_{air} (Btu/h·ft^2·F)	h_{rad} (Btu/h·ft^2·F)	Average Daily Calculated Losses (kWh)
Summer – SRCC	Side	129	3.3	0.350	0.829	0.93
	Top		7.1	0.465	0.838	0.11
Summer – DOE	Side	121	2.7	0.320	0.827	0.83
	Top		5.8	0.442	0.835	0.11
Winter – DOE	Side	117	2.5	0.310	0.827	0.78
	top		5.3	0.425	0.833	0.11

The heat transfer circuit for the bottom of the tank does not include a convection resistance because it is obviously not exposed to free air. The heat transfer circuit for the bottom of the tank includes two parallel conduction resistances, which are modeled as a

single conductive resistance. One is the tank insulation and one is the metal support ring holding the weight of the tank away from the floor. The support ring is metal and has a wall thickness of just 0.005 ft. In fact, the support ring does not thermally connect the tank and the base pad. If this was not the case, the metal ring would conduct away over twice the energy lost by the rest of the tank! There is a thin, 0.125 inch disc that creates a thermal break between the support ring and the base pad. This was modeled, as it is in WATSIM (a computer modeling program for hot water heaters developed by DOE), by calculating the ring conductivity based on the assumption the ring is 50% steel and 50% foam insulation [21]. This results in a composite conductivity close to that of the insulation and therefore in very little heat transfer through the support ring. The end of the circuit is the ambient temperature, representing the floor on which the tank sits as a constant temperature heat sink. The final equations is

$$q_{bottom,loss} = \frac{T_{Avg.Tank} - T_{\infty}}{\frac{t_{insulation}}{\pi \cdot r_{Tamk}{}^{2} \cdot k_{insulation}}} + \frac{T_{Avg.Tank} - T_{\infty}}{\frac{h_{ring}}{\left(\pi \cdot r_{Tank}{}^{2} - \left(\pi \cdot \left(r_{Tank} - \frac{t_{ring,wall}}{2}\right)\right)^{2}\right) \cdot K_{ring}}} \quad (4.12)$$

The required dimensions and other parameters are given below in Table 4.7.

Table 4.7 Tank Bottom Losses Parameters

	Vertical Height (in)	Cross section area (ft^2)	K (Btu/hr·ft·F)
Bottom insulation	0.75	1.375	0.0275
Support Ring (as modeled, including insulating disc)	0.75	0.0209	0.02832

Table 4.8 Calculated Tank Losses Compared to Tank Loss Experimental Results

	Average Tank Temperature (°F)	Daily Total Losses (k = 0.0143 Btu/hr·ft·F) (kWh)	Daily Total Losses (k = 0.020 Btu/hr·ft·F) (kWh)	Daily Side Losses (kWh)	Daily Top Losses (kWh)	Daily Bottom Losses (kWh)
Summer - SRCC	129	0.87	1.21	0.93	0.11	0.16
Summer - DOE	121	0.79	1.09	0.83	0.11	0.15
Winter - DOE	117	0.73	0.98	0.78	0.11	0.13
Experiment - electric only	115	0.877		n/a	n/a	n/a

The test case mentioned in Table 4.8 above is the case described in chapter 4.1 in which the only energy input was the electric heating elements, and the only energy leaving the system was losses. Because of the accuracy of the electric meter, it was possible to use the results of this test to establish a very meaningful experimental loss standard (at a given average tank temperature and ambient temperature). The Table 4.6 above shows that the measured loss was greater than experimental period. This was because energy balance derived losses showed that the tank did in fact experience greater losses when it was actively experiencing both load and solar flows than it did in the steady-state test case.

This test data was also used to establish an experimental effective R-value for the tank. This was found to be 7.4 (Hr·ft·°F/Btu). The effective R-value of the tank should not change much as the tank average temperature and the ambient temperature change. For this reason, this value may be used as a standard for comparison. It is possible to calculate an effective tank R-value based on analytically derived losses. This is more difficult to do with energy balance-derived losses because the tank loss component of the total losses can

only be extracted from the "tank and pipe" total losses by estimating size of the other loss components. The methods used to estimate, or calculate, these other loss components are the subject of the next chapter.

4.4 Feed-Through Losses Heat Transfer Analysis

The other main loss pathway for energy to escape the tank is through all the devices that 'feed through' the tank. The major feed-throughs are the two sets of water pipes attached to the tank, the pipes on the 'house side' and those in the solar loop. These two pairs of pipes are used in very different ways. The house pipes carry water for relatively short periods of time, only up to 9 minutes at a time in the experimental monitoring periods. One of the pipes carries cold water while the other carries hot water. In contrast, the solar pipes tend to carry water for a very long period, and both, not just one of these pipes, carry heated water. There are other important differences in the two pairs of pipe. The house pipes both enter the tank at the top, thus natural convection tends to cause hot water to migrate up and out of the tank, into these pipes. The solar-pipes attach horizontally at the bottom of the tank and do not experience much heat transfer from these steady-state convective water flows. The final important difference is the solar control system in the solar pipes. The odd shapes and functionality of the devices means there is typically more uninsulated metal exposed to the air. The large amount of uninsulated metal meant large amounts of thermal losses. Burch, Wood, Huggins, and Thornton's [19] calculations indicate that these uninsulated elements increase heat loss from 50 to 200%.

In 1993 (the system tank was manufactured not many years later), SRCC was assuming that these and other factors halve the effective R-value of the total piping system [19].

Existing heat traps in the system were removed prior to this experimentation because they were found to be severely corroded and inoperable. To avoid future problems with corrosion during the experimentation, new heat traps were not installed. "Based on efficiency data provided by the water heater industry, heat traps prevent a loss of approximately 540 Btu/day (0.16 kWh) from a 50-gallon electric water heater" [21]. This is approximately the amount of energy calculated later in the chapter to have been lost each day by the house pipes. This is a small value when compared to the amount of energy metered by the thermal energy meter, but it is a significant portion of the system losses. Perhaps more important, if the losses from these sections of pipe are calculated accurately this information may be used to determine the accuracy of the physical energy meters. Therefore, these pipe losses are important when an accurate image of the system energy flows is desired.

The thermal meters should meter all of the energy that passes through them in the flowing water. However, they do not meter any energy lost by the pipes between the tank and the meter. Nor are they able to meter any energy conducted past them along the metal pipe or in tiny water convection currents. This motion of this soon-to-be-lost energy down the pipes is not explicitly included in the loss calculations, but its effect is included. All the energy carried down the pipes away from the tank increases the temperature in the pipe, as read by the thermocouple, thus this portion of the loss pathway is measurable, albeit slightly crudely (a singe thermocouple for each pipe). The rest of the loss pathway for this energy (as well as for the energy that is lost before the meter) is conduction through any

insulation and finally convection to the ambient air. Neither of which are readily measured. Thus, these thermal resistances are estimated through heat transfer analysis.

There was only one temperature reading recorded for each pipe during each time step. Therefore, this is the only variable that is available to represent the temperature profile of the water along each pipe. Obviously, there is not one single temperature state for any of the pipes and rapid changes in temperature may occur when a flow begins. In the case of the house pipes, this is further complicated by the interplay of the hot and cold water that occurs in the tempering valve. The house pipes are often in a transient state, only reaching quasi-steady-state overnight. The solar-pipes tend to spend more of the time in one of two states (both quasi-steady-state): sustained full solar flow or sustained no solar flow. Thus, at least in the case of the solar pipes, the one temperature reading for each pipe may often be capable of accurately representing the current heat loss scenario. For the sake of simplicity, the two temperature readings of the water in the house pipes will be assumed to represent uniform water temperatures in these pipes and therefore be used to calculate the heat loss. At times, these temperatures will under-represent the heat loss and over-represent it at other times.

Once the interior water temperature were established for the pipe sections near the tank, the loss calculations for the pipes looked very similar to those of the tank. Again, the losses were modeled using an effective resistance model. Also again, the convective resistance between the water in the pipe and the pipe itself, the conduction resistance through the pipe, and the contact resistance between the pipe and the insulation are all neglected. However, the calculations are more complicated than those of the tank because each pipe contains sections of both horizontal and vertical pipe and because the vertical

pipe sections are long and thin enough not to meet the simplifying “thick cylinder” limit. Beyond these complexities, not all of the piping was insulated, nor was all of it in neat simple geometric shapes.

The effective resistance circuit for any of the pipes is shown below in Figure 4.1. Most of the pipe surfaces were covered in insulation; these pipe sections are represented by the middle line of the circuit. Other sections of pipe and devices/hardware inline with the pipe were not insulated. These sections had two parallel loss pathways, represented by the top and bottom lines of the circuit (with only one resistance a piece). Because these sections of pipe were uninsulated, they reached high temperatures at times, which meant both significant radiation and natural convection losses occurred.

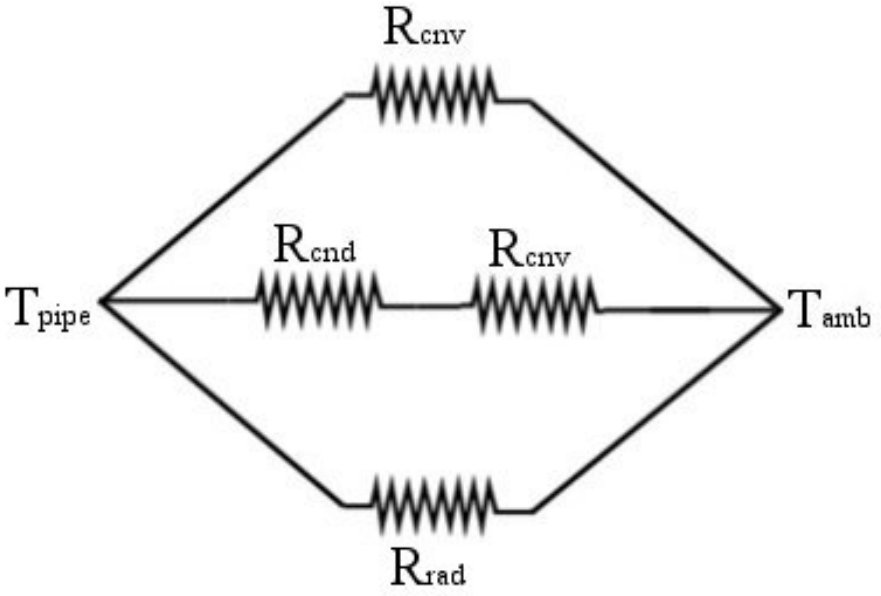

Figure 4.1 Diagram of the Thermal Circuit Describing Pipe Losses

The losses through the insulated portions of the pipes were calculated very similarly to the losses from the sides of the tank. The equation was as follows

$$q_{pipes,insulated} = \frac{T_{pipe,water} - T_{\infty}}{\frac{\ln\left(r_{insu,OD} / r_{insu,ID}\right)}{2 \cdot \pi \cdot l \cdot k_{insu}} + \frac{1}{2 \cdot \pi \cdot r_{insu,OD} \cdot l \cdot \bar{h}_{air}}} \tag{4.13}$$

$$q_{pipes,uninsulated} = q_{pipes,uninsulated,cnv} + q_{pipes,uninsulated,rad} \tag{4.14}$$

where,

$$q_{pipes,uninsulated,cnv} = \frac{T_{pipe,water} - T_{\infty}}{\frac{\ln\left(r_{insulation,OD} / r_{insulation,ID}\right)}{2 \cdot \pi \cdot l \cdot k_{insulation}} + \frac{1}{2 \cdot \pi \cdot r_{insulation,OD} \cdot l \cdot \bar{h}_{air}}} \tag{4.15}$$

and

$$q_{pipes,uninsulated,rad} = (T_{surface}{}^4 - T_{surroundings}{}^4) \cdot A_{surface} \cdot \sigma \tag{4.16}$$

The only variable in the equations above that required significant calculation was the average heat transfer coefficient h, and it required great work to calculate it for each of the over 25,000 data sets in the three monitoring periods. A number of factors complicated the task. The pipes contained many horizontal and vertical sections of various lengths. Some sections were fully insulated, others were uninsulated. Surrounding objects, including other pipes, affected the airflow across the pipes. Finally, the equations required the surface temperature of each section of insulation during each 5 minute period, which was obviously not measured.

The average heat transfer coefficient for all of these sections of pipe was calculated from a Nusselt number correlation. The correlation used was proposed by Lienhard [16],

$$\overline{Nu}_l \cong 0.52 Ra_l^{1/4} \tag{4.17}$$

in which

$$\overline{Nu}_l = \left(\bar{h} \cdot l\right)/k \quad \text{and} \quad Ra_l = \left(g \cdot \beta \cdot \Delta T \cdot l^3\right)/\left(\alpha \cdot \nu\right) \tag{4.18}$$

and $\bar{h}$ is the heat transfer coefficient averaged over the entire surface of the body. The correlation is a simple form that works for natural convection heat transfer from bodies of various shapes, including irregular shapes. Lienhard's characteristic length l, on which both Nu_l and Ra_l are based, is the distance traveled by the boundary layer fluid while in contact with the body. In the case of a horizontal cylinder, for example, $l = \pi D/2$. In the case of a vertical cylinder, l = height * 2. According to Sparro and Ansari [16], the error from Equation (4.17) was on the order of 30 percent at $Ra_l \sim 10^4$, and less than 8 percent when Ra_l exceeded 10^6. The data here met the first case approximately 5% of the time and the second case the rest of the time.

This correlation was used to calculate the average heat transfer coefficient for all of the house and solar pipes near the tank. Once the heat transfer coefficient was known for a particular section of pipe it was a rather simple step to then calculate the estimated heat loss from that section. The diagram below shows how the piping systems were broken down into small sections for more accurate heat loss estimate calculations.

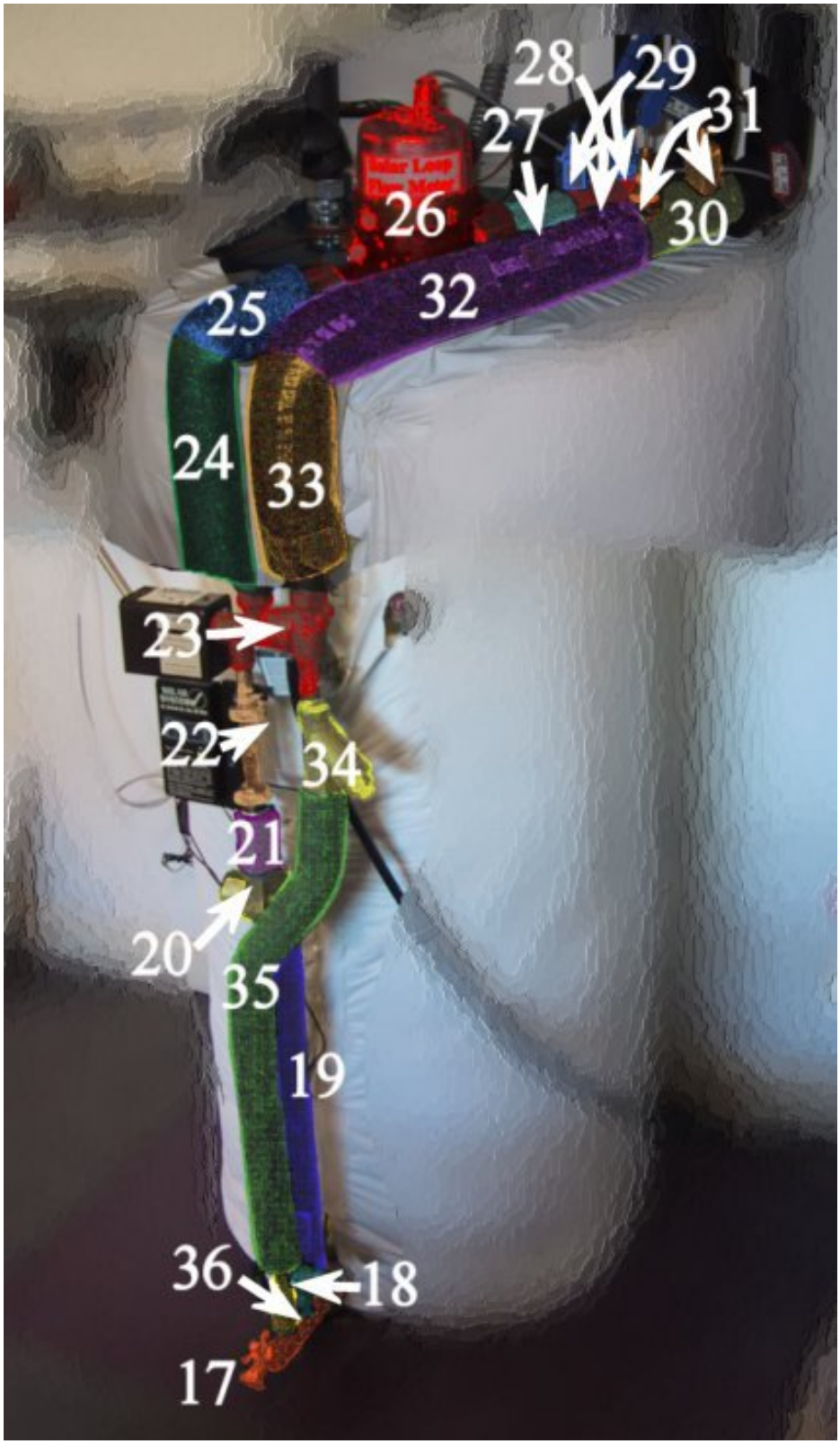

Figure 4.2 House Pipe Sections for Heat Transfer Analysis

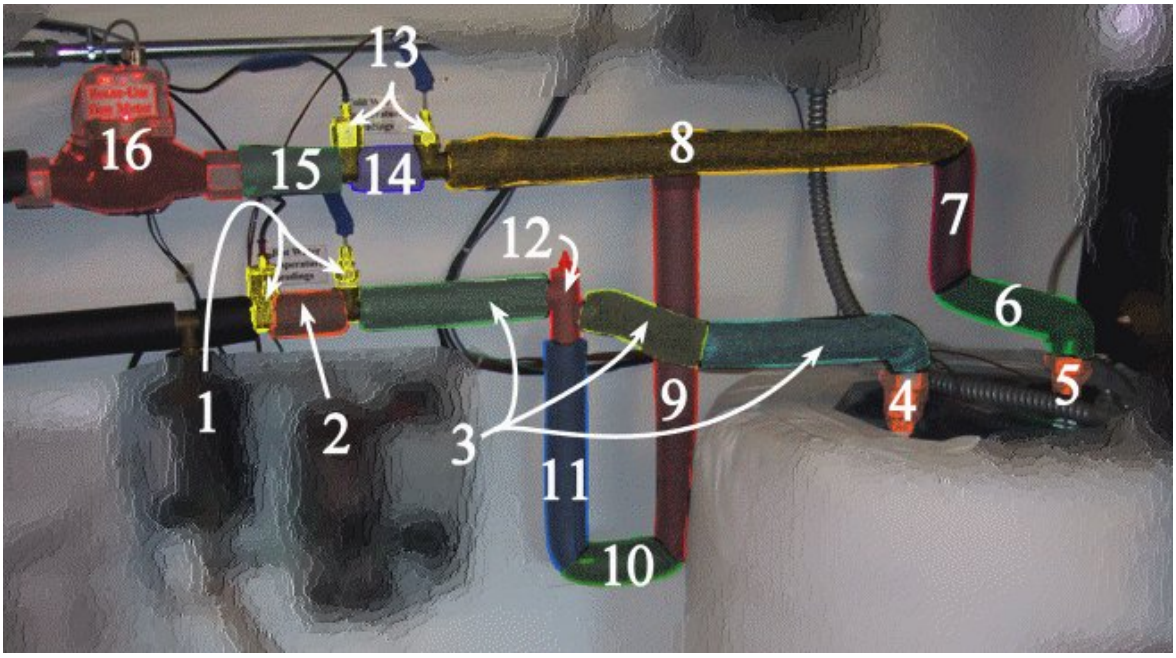

Figure 4.3 Solar Pipe Sections for Heat Transfer Analysis

The characteristics of each section were entered into the same spreadsheet containing all of the 5-minute data for a monitoring period. The spreadsheet was programmed to then use the section parameters along with the recorded pipe temperature that period to lookup the estimated surface. In the case of an uninsulated metal section this was simply the recorded pipe temperature. In the case of an insulated section the estimated surface temperature was looked up in Table 4.9. Which was derived with the help of the experimental results also shown in the table.

Table 4.9 Measured and Estimated Pipe Insulation Surface Temperatures

HOUSE AND SOLAR PIPES		
House Water (°F)	Measured Surface (°F)	Estimated Surface (°F)
30	-	70.5
35	-	71
40	-	71.5
45	-	72
50	73	72.5
55	-	73
60	-	73.5
65	-	74
70	-	74.5
75	-	75
80	75	75.5
85	-	76
90	72	76.5
95	-	77
100	-	77.5
105	-	78
110	-	78.5
115	79, 80	79
120	79.5	79.5
125	-	80
130	-	80.5
135	82	81
140	-	81.5
145	82	82
150	82.5	82.5
155	-	83
160	-	83.5
165	-	84
170	-	84.5
175	-	85

After the surface temperature was known, the spreadsheet was then used it in conjunction with the characteristic length of the pipe section to lookup the average heat transfer coefficient. This was looked up in a table created by first calculating Ra_l for each possible combination of delta T (surface temperature – ambient temperature) and

characteristic length. Delta T in this table ran from 0 to 75 °F by single degrees and the characteristic length range ran from 0.082 to 2.133 feet and contained the characteristic lengths of each section of pipe. Nu_l was then simple to calculate from Ra_l for each point in the table. Then from this point, it was again simple to calculate the next step, the average h, for each point in this table. It was this value of $\bar{h}$ that was returned by the lookup function in the primary worksheet. Then equation 4.2 was used to calculate the estimated heat loss rate through that section of pipe during that 5-minute period. The heat loss rate was then multiplied by 5 minutes and the units were converted to give the total estimated kWh of energy lost during the 5-minute period.

All of these small of periods of loss were totaled each day and grouped together in the categories seen below. The uninsulated values do not include the radiation losses in order to be able to compare the convective losses of each category. The values in the table below are the daily averages of the estimated losses over each monitoring period.

Table 4.10 Breakdown of Total Pipe Loss Calculation Results

	Daily Total Losses (no Drain) (kWh)	Hot House Insulated Losses (kWh)	Cold House Insulated Losses (kWh)	Hot House Uninsulated Losses (kWh)	Cold House Uninsulated Losses (kWh)	Solar Supply Insulated Losses (kWh)	Solar Return Insulated Losses (kWh)	Solar Supply Uninsulated Losses (kWh)	Solar Return Uninsulated Losses (kWh)
Summer – SRCC	1.78	0.12	0.05	0.19	0.19	0.04	0.03	0.21	0.37
Summer – DOE	1.67	0.11	0.05	0.18	0.18	0.04	004	0.20	0.36
Winter – DOE	1.16	0.07	0.03	0.10	0.10	0.03	0.03	0.03	0.11

As mentioned at the beginning of the chapter, radiation losses from the uninsulated sections were calculated. This calculation assumed both bodies (pipe section and the surroundings) acted as blackbodies. Although neither are true blackbodies, the assumption

greatly simplified the problem and was close enough to give a reasonable result. Rough metal, as much of the exposed metal is, can have quite a high emissivity, but polished metal usually has a very low emissivity. A second needed assumption was that the outer surfaces were at the same temperature as the temperature of the water in the pipe. Both of these assumptions are non-conservative, causing the estimated radiation losses to be higher than actually occurred, in effect bounding the radiation losses. The radiation loss rate was calculated as follows

$$q_{rad} = (T_{surface}{}^4 - T_{surroundings}{}^4) \cdot A_{surface} \cdot \sigma \qquad (4.19)$$

where, σ is the Stefan-Boltzmann constant, 5.670 X 10^{-8} W/m^2·K^4. These radiation losses were not negligible, but they were small compared to other losses.

Table 4.11 Breakdown of Pipe Radiation Loss Calculation Results

	Daily Total Pipe Losses (kWh)	House Hot Pipe Radiation Losses (kWh)	House Cold Pipe Radiation Losses (kWh)	Solar Supply Radiation Losses (kWh)	Solar Return Radiation Losses (kWh)
Summer – SRCC	0.68	0.04	0.04	0.07	0.09
Summer – DOE	0.66	0.03	0.03	0.07	0.08
Winter – DOE	0.20	0	0	0	0

In order to understand the pipe losses further, as well as an attempt to minimize losses, all of the exposed metal inside of the two thermal meters was insulated with 3/4 inch thick quality foam rubber pipe insulation (Figures 4.4 and 4.5). This was done on October 10th, 2003, so it was therefore in place during the third monitoring period. The equations in the spreadsheet were set up in a manner that little more was required than

changing the k of the insulation on the newly insulated pipe sections from zero (served to indicate no insulation, not a k of zero) to the k of the new insulation. This then meant that all of the pipe losses were calculated by equation 4.2 and that no radiation losses were considered.

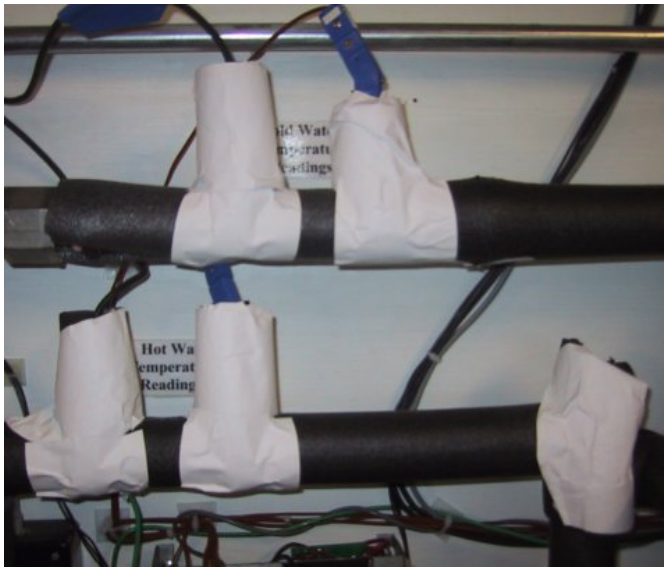

Figure 4.4 Most of the Additional Insulation Applied to House Pipe Sections

Figure 4.5 Additional Insulation Applied to the SDHW System Controls

The final loss pathway to be considered was draining of the solar collector when adequate insolation is no long available. This loss is different from the aforementioned losses because it is at least partially metered by one of the energy meters. Well, the statement that it is partially metered is probably an overstatement, but the solar flow meter values (in context with the rest of the data) do revel when the drain occurred. The solar flow meter recorded five liters of flow each time the collector drained, and because the water flowed down both the supply and the return lines the two temperature sensors experienced very similar temperatures. Thus, the meter recorded a negligible amount of energy when the solar collector drained. An examination of the data shortly before the drain occurred revealed the approximate temperature of the last water sent to the collector before power to the solar pump was removed. The amount of energy lost down the drain was calculated with the assumption that the energy lost was the energy needed to heat nine

liters of water (the amount required to fill the collector and the solar pipes) from the monthly average city cold water temperature to the temperature at which the drained water was sent to the collector. The equation to calculate this energy is as follows

$$Q_{draindown,loss} = \left(T_{last,solar} - T_{city,water}\right) \cdot Cp_{water} \cdot m_{drain} \quad (4.20)$$

where $T_{last,solar}$ is the temperature of the last water sent to the collector, and $T_{city,water}$ is the average city cold water temperature that period.

4.5 Solar Pipe Losses between Meter and Collector

The collector efficiency curve produced by SRCC for solar collectors is based on the fluid flows entering and leaving the collector, but in actual use the fluid must flow to and from the hot water tank. In the case of the solar house the collector is mounted on the roof approximately 25 feet above the solar loop connection to the hot water tank. This results in about 121 feet of piping between the two points. The piping in the actual solar collector is only 8 feet long. Therefore, the water travels over ten times as far in its commute to and from the collection site as it does in the collection site. However, because the water passes through the collector in numerous parallel pipes it travels through the collector at a slower rate than during its commute. Although steps were taken to well insulate most of the piping between the collector and the tank, significant losses still occurred when the solar loop was operating.

The calculation of these losses were not as straightforward as the other pipe losses for two primary reasons. The temperatures of the inlet and outlet flows at the base of the collector, or any other fluid temperature above the meter, were not known. The second reason was the ambient temperatures of areas the piping passed through differed. In addition, these ambient temperatures were not monitored either. However, unlike the case of the fluid temperatures at the collector, the ambient temperatures could be reasonably estimated. Most of the piping was in areas at more or less the ambient temperature of the interior of the house, which was measured by the monitoring system. The rest of the piping was in the attic that obviously experiences a more dynamic temperature. For modeling purposes it was assumed that the ambient temperature in the attic was midway between that of the interior of the house and the outdoor ambient temperature. This is believed to be a reasonable, yet simple, assumption.

These losses were calculated using the same methods developed to estimate the losses from the piping near the hot water tank. In fact, the same spreadsheet was used to calculate the pipe losses above the solar thermal meter. However, less was known about the temperature of the water in the pipes and the ambient temperature than with the pipes near the tank. In addition, these pipes only contained water during certain periods of the day. It was assumed that losses only occurred while there was flow through the solar loop. This greatly simplified the calculations, but perhaps it would have been more accurate to calculate the losses for the entire time there was water in the solar loop pipes. This however would have been very impractical because there was no way of knowing the temperature of the water in the pipes during the periods of no flow. These losses are minor compared to the losses that occur during the much longer periods of flow. Moreover, the

draindown loss calculation captures the losses that occur between the last period of solar flow and the solar draining.

The temperature of the water in the supply line was simply assumed to be the temperature measured at the solar thermal meter. The same was true of the return line. These assumptions meant that the average supply line temperature was overestimated and that the average return line temperature was underestimated. It was assumed that these errors approximately canceled each other. The error introduced from the attic ambient temperature estimation was greater, but not believed to be problematic.

The loss calculations broke the piping down in to a few different regions of insulated and uninsulated pipe as was done in the near-pipe heat loss analysis. A summary of the results is given below. See the TRNSYS simulation chapter for the modeling of these losses.

Table 4.12 Breakdown of Average Daily Calculated Losses from Upper Solar Piping

	Return Insulated (kWh)	Return Uninsulated (kWh)	Supply Insulated (kWh)	Supply Uninsulated (kWh)	Total Losses (kWh)
Summer – SRCC	0.28	0.43	0.30	0.27	1.28
Summer – DOE	0.39	0.56	0.44	0.38	1.78
Winter – DOE	0.27	0.35	0.32	0.25	1.48

4.6 System Loss Overview

This chapter seeks to provide an overview of the losses experienced by the SDHW system. This is done in a number of ways. First, the measured and calculated losses are compared to other sources of information on SDHW and DHW system losses. Next the tank's energy factor is calculated, compared, and discussed. Finally, the various losses from the three monitoring periods are all presented and each used in the full tank energy balance. This analysis is used to demonstrate the tightness of the system monitoring system and the accuracy with which the system losses were calculated, by both the energy balance and the heat transfer analysis.

It is worth noting some of the loss standards used by the Department of Energy's hot water simulation program, WATSIM. The program's documentation gives several characteristics of what it calls the Baseline Electric Water Heater, which is a basic low cost electric water heater that just meets the DOE. Energy Factor requirement. This model contains no energy savings additions such as heat traps or extra insulation. The tank used in the experiment would be described as a baseline electric water heater with an additional insulation blanket. The documents report that about 30% of the losses are through pipes, drain, pressure release, etc; places besides the well insulated sides, top, and bottom (feed-throughs). It also reports the: Natural Convection UA for Feed-Through (no heat traps) as $0.185 \frac{Btu}{hr \cdot °F}$.

In the program, this single value is used in calculating natural convection losses through all objects that feed-through the tank. Standard lengths of the feed-throughs are included in this constant value, the only variables needed to determine the amount of heat

lost is the temperature difference between the water in the tank and the ambient temperature and the amount of time under consideration. This constant is only for the case of steady-state losses, and not losses that result from the addition of heat from hot water use or a solar energy system. The results of this simple calculation may be seen in Table 4.13.

Table 4.13 Daily Calculated Pipe Loss Compared to Other Estimates

	Average Daily Calculated House Pipe Losses (kWh)	Pipe losses calculated from WATSIM UA (steady-state) (kWh)	30% of Daily Calculated Tank Losses (kWh)	Standard Estimate based on Heat Traps Savings (kWh)
Summer – SRCC	0.21	0.078	0.64	0.16 +
Summer – DOE	0.20	0.065	0.59	0.16 +
Winter - DOE	0.10	0.059	0.44	0.16 +
Electric-Only Test Period	0.11	0.059	0.26	0.16 +

The table above shows that the losses estimated via heat transfer calculations for the three monitoring periods are much more than WATSIM predicts. This is as expected because the tank in the experimental system was not in a steady state. The percentage of the total losses that came from feed-through losses during the first two periods were much lower than the 30% quoted in WATSIM literature [21], but this is because it did not consider a SDHW system. The final column indicates that the WATSIM information states that heat traps save about 0.16 kWh of loss each day, so, tanks without heat traps would expectedly lose more than this through its piping. Notice the actual values fit nicely into this mix.

It is relevant to consider the Energy Factor of the tank, defined as the (energy delivered)/(energy in). In the United States, a 50-gallon tank is required to have a rated

Energy Factor of 0.864 or greater. The DOE test procedure described in chapter 2.2.4 is the test used to determine a tank's Energy Factor. More or less hot water use, or different patterns of use will change the Energy Factor of a given hot water tank. The larger the draws the greater the Energy Factor will tend to be. This can be seen in the data below. This data is presented as a basis for general comparison of the three different monitoring periods. The values presented are the average daily Energy Factors over the entire test period. They was calculated as follows,

$$Energy\ \ Factor = \frac{E_{house,use}}{E_{electric} + E_{solar}} \tag{4.21}$$

where $E_{house,use}$, and E_{solar} are the corrected calculated energy meter values. It would be expected that the Energy Factor of the hot water tank in a single tank SDHW system would be lower than that of the identical DHW system. This is because the solar system both adds a new avenue for losses and it tends to raise the average tank temperature, further increasing the losses. With this said, the daily average Energy Factors found during the monitoring periods appear as expected with the exception of the winter period Energy Factor. It is higher than expected because of the unexplained under-metering of the house-use energy meter during this period. It was also a little higher because it experienced lower losses due to the added pipe insulation.

Table 4.14 Average Daily Calculated Energy Factor

	Average Daily Energy Factor
Summer – SRCC	0.855
Summer – DOE	0.778
Winter - DOE	0.920

Tank heat loss data and analysis indicate that the expected thermal loss coefficient (UA) based upon R-value of the insulation underestimates tank losses by about a factor of two. As stated earlier, the reason for this is thermal short circuits and pipe thermosiphoning. The tables below present a range of R-Values calculated from the relevant loss value. All of the tank R-values calculated from energy balance derived-losses using the actual thermal meter readings demonstrate the error in the readings. This is particularly true in the case of the winter period when the losses were known to decrease, yet the R-Value from the actual meter readings fell even lower. The R-Value derived from the calculated meter readings rose erroneously high due to the slight under-metering that occurred.

Table 4.15 Comparison of Tank R-Values Derived with Various Methods

	R-Value calculated from actual meter readings	R-Value calculated from calculated meter readings	R-Value calculated from calculated losses
Summer – SRCC	3.14	4.08	4.24
Summer – DOE	3.28	4.22	4.96
Winter - DOE	2.66	7.00	5.82

Manufacturer R-value	9
Experimental Steady-State R-Value	7.4

All of these various loss quantities can be boiled down to an average daily loss for each monitoring period. Table 4.16 below displays a summary of the measured (energy balance) and calculated (heat transfer analysis) losses during each of the three monitoring periods. The first column is the average daily loss as determined by daily energy balances using the actual meter readings. These values are deceivingly constant. When compared to the other measured loss or the calculated loss column, it is clear that the loss values should not have remained so constant over the three periods. The second column is the average daily loss as determined by daily energy balances using the calculated thermal energy meter values that were corrected for false readings during the filling of the solar collector. The third through the seventh columns are the culmination of the work presented in this chapter.

Table 4.16 Summary of the Tank Losses with Total Fraction of Energy Accounted For

	'Measured' Losses from Energy Balance (kWh)		Calculated Losses from Heat Transfer Analysis (kWh)					Fraction of Total Energy Accounted for
				Calculated Loss Components				
	Actual Meters	Calculated Meters	Calculated loss, full	Tank	House pipes	Solar pipes	Drain down	
Summer – SRCC	2.83	2.39	2.24	1.21	0.21	0.47	0.35	0.99
Summer – DOE	2.64	2.13	2.03	1.09	021	0.45	0.29	0.99
Winter - DOE	2.67	0.93 / 1.40*	1.55	0.98	0.10	0.10	0.32	1.05 / 1.01*

*These values are with the cold water temperature corrected by 3°F

The tank loss calculations are rather simple and their results agree with experimental tests and the R-Value analysis presented above. They are therefore believed to be quite

accurate. The drain down loss is believed to be quite accurate because all three of the input variables are easily obtained. The mass of the drained water and the temperature of the cold makeup water are both well known, and the temperature to which the drained water was heated was easy to accurately estimate. The pipe losses are certainly more difficult to predict accurately, but it appeared that the equations used did a reasonable job. The pipe losses, particularly the uninsulated solar pipe losses, made up a large portion of the total losses of the system, perhaps unexpectedly so. Nevertheless, both the measured losses (energy balance) and the calculated losses agree quite well with each other during all three of these periods. Perhaps with the exception of the winter period where the calculated house thermal meter under-metered by about 0.4 kWh each day, but if this known metering error is manually corrected in the data the two groups of losses agree exceptionally well. Further, because of the author's faith in the relative accuracy of the calculated tank and drain down losses this agreement between the measured and calculated losses tends to verify the levels of pipe losses calculated

The final column of the Table 4.16 seeks to display the 'tightness' of the system monitoring and loss calculation. The fraction of energy accounted for is defined here as the total energy (a combination of known and calculated) to leave the tank divided by the total known energy to enter the tank in one day. The equation for each day is as follows:

$$Fraction\ of\ Total\ Enegy\ Accounted\ For = \frac{E_{House,use} + E_{Calculated,loss}}{E_{Electric} + E_{Solar} + \Delta IE} \qquad (4.22)$$

These values fluctuated from day to day, but over time the average was very near to one in all three periods. The value of this type of analysis is limited, but it does serve well as a way to quantify the agreement of the calculated losses with the measured energy values.

The calculation of these losses was not exact and required some assumptions and estimations. The calculated losses were then compared to 'measured' losses, but it must be remembered that these losses were not actually measured. The experimental loss values were derived by adding and subtracting larger measurements to arrive at one much smaller value representing the 'measured' system losses. Thus, small percent-errors in the large measured values would cause much larger percent-errors in the much smaller remaining piece of the energy balance, the losses. Considering all of these factors, it is believed that the agreement of the measured and calculated values is quite satisfactory.

Chapter FIVE TRNSYS MODEL

A computer model of the SDHW system studied was created in TRNSYS. TRNSYS is a transient systems simulation program with a modular structure. The model design and simulation execution were completed in the program IISiBat, a general graphical front-end program designed for use with any simulation program. TRNSYS allows a model of a thermal system to be built from a supplied library of components. Each component included in the model has a number of adjustable parameters, which are determined by the user. Each component also has a set of inputs and outputs. The inputs of each component may be either set to a constant number (the default), or connected to the output of a component. The user graphically links one component to another. Each link indicates a one-way information pipeline. The graphical link itself does not actually connect any variables, it merely provides the pathway on which to make those connections. The user must explicitly make all connections desired in the link. In ISSiBat this is done graphically after double clicking on the link. An example link dialog box is seen in Figure 5.1 below. In this box, connections are made by connecting an output of the component on the left to an input of the component on the right.

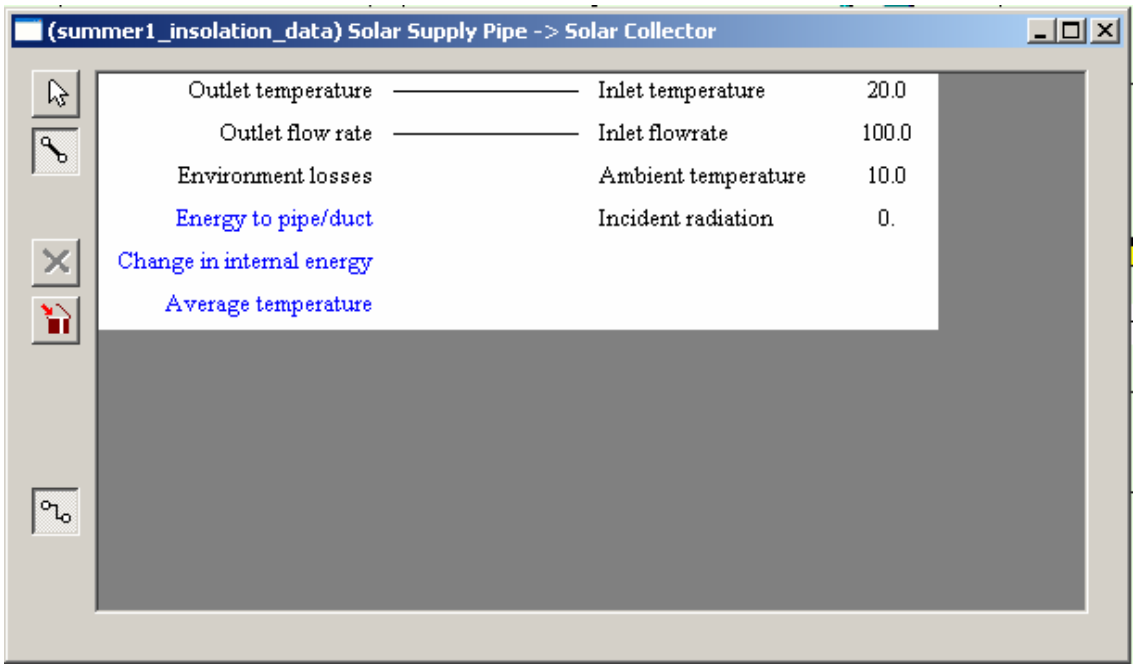

Figure 5.1 ISSiBat Link Dialog Box

After the physical model was fully defined (Figure 5.2), the simulation details had to be defined before it could be executed. The primary variables of the simulation are the simulation time step and the simulation start and stop times. The time step used for the simulations in this project was 0.2 minutes. Normally such a small time step would not be required, but in order to model the length of the hot water draws accurately in some of the simulations it was needed. The simulation start and stop times are based on the time of the available input data. In the case of a typical weather file, like TMY2 data, this time is one entire year. Therefore, the simulation may be defined to occur for any period in a year. In the case of actual data input, a start time of zero indicates the beginning of the input data available.

5.1 Validation Model

The model developed for the SDHW system in this study was validated by matching the output of the simulation using actual solar insolation data to the actual performance of the system over the first monitoring period. The attributes of the final validated model were very similar to the initial system attributes and are discussed in the following paragraphs.

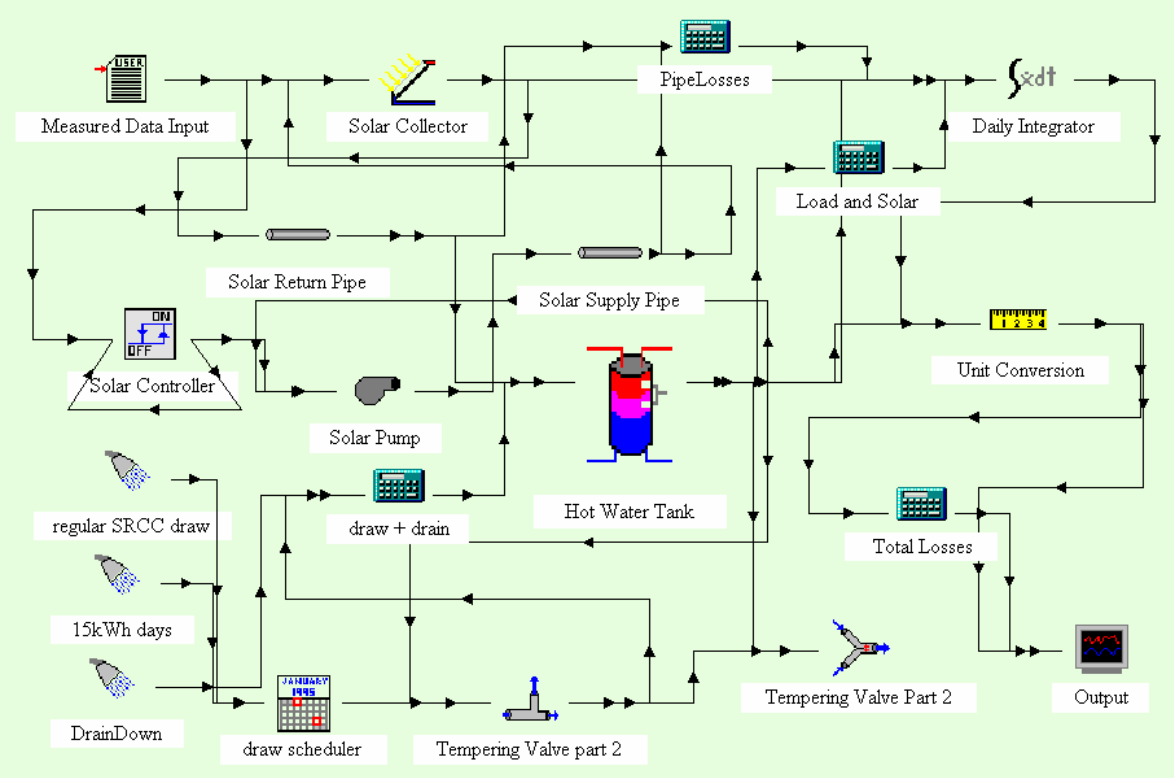

Figure 5.2 ISSiBat System Model of Period 1 using Actual Radiation Data

The center of the model is the hot water tank. This component contained two electric heating elements and two thermostats. Their positions, set points, and dead bands

were all included in the model. The model contained ten different temperature zones, or nodes, to account for stratification, both thermal and induced by cold water entry. The default number of nodes was just three, but this was found to be inadequate, and more than eleven nodes caused TRNSYS to crash often. The draw profile was defined by stating the exact start time, stop time, and flow rate of every draw in a water draw component. The makeup water was at a constant temperature of 76 °F throughout the simulation. In the simulation, the makeup water flow occurred automatically as water was drawn out of the tank. The solar collector component did not account for a drain down loss, so the drain down of the solar collector was modeled by simply adding a small draw at 6 P.M. The size of this draw was adjusted so that it contained 0.33 kWh of energy each day, the average amount of daily drain down loss over the entire period.

A simple on/off controller, based on the incident insolation on the roof surface, controlled the operation of the solar pump. The controller turned the solar pump on when the solar radiation reached an intensity of 1650 KJ/m^2*hr and off when the intensity fell below 1500 KJ/m^2*hr. These numbers were obtained by viewing the recorded insolation data beside the recorded solar flow data and then by making slight adjustments. The actual data revealed that the pump was both turned on and off over a range of insolation values. This is because the physical controller has both a capacitance and an integrating effect inherent in its nature. The controller model simply assumed a constant value for each of theses ranges. The upper band was chosen so that the pump came on each day in the period and the bottom of the range was chosen to have the best matching total daily solar flow volumes.. Therefore, although this control scheme is a little different from the thermostat

controller in the actual system, the results with it are quite good and the on and off insolation values both match quite close with what was experimentally seen.

The 'tank' losses (tank and pipe losses inside of the meters) were modeled in two parts. The losses from the actual tank, which were increased to include the losses from the house pipes as well, were accounted for by the hot water tank component. The value used for the tank heat loss coefficient was 0.2 BTU/ft^2·hr·F (effective R-Value of 5). Although this R-Value is slightly higher than the R-Values calculated in chapter 4.6, it produced tank (and house pipe) losses equal to what was measured and calculated (approximately 1.25 kWh per day). This anomaly is believed to be because of the tank surface area used in TRNSYS. The losses from the solar pipes between the meter and the tank were modeled with two TRNSYS pipe components, one for the supply pipe and one for the return. The length and internal diameter of each pipe were entered along with a single heat loss coefficient. Again, the external area used by TRNSYS was not indicated, so the loss coefficients were determined experimentally, based on the amount of daily solar pipe loss they allowed.

As the simulation model was being developed each system variable of the system was monitored closely to confirm agreement with the data. In a few cases slight adjustments were made to obtain a better agreement. For example, the set point of the thermostats were actually both set to 130 °F and not 135 °F. Notice in the actual data that the average tank temperature is only about 129 °F during this period and that the DOE, and therefore SRCC draw profile definitions defines the set point as 135 ± 5 °F. In addition, the data sheet of the tank thermostats states an uncertainty on the value of their dead bands. The timing of auxiliary heating in the validation simulations was closely monitored and the

tank thermostat dead bands were adjusted to achieve agreement with their physical counterparts.

The solar collector was modeled two different ways. The first, and simpler way, used an experimentally determined efficiency curve for the collector. The second used the collector efficiency curve given by SRCC for the collector and modeled the losses from the pipes between the collector and the thermal meter by the tank. Each method is described in further detail below.

5.1.1 Experimental Solar Collector Efficiency Curve

The data from which this curve was produced came from a five-day experimental period from September 28th to October 2nd, 2003. Each day the test was began with a cool tank of water in order to obtain a wide range of data. The electric backup power was disconnected and no hot water draws were allowed all day. The five days were all rather strong solar days and the system was fully monitored as it was during the monitoring periods. Also during this period, equipment from a different project at the NC Solar House collected 5-minute data of the incident solar radiation on the Solar House roof. The collector efficiency curve that was produced used most of the data collected, but a hand full of outliers were thrown out. A linear trendline was produced by the spreadsheet program and displayed on the graph along with its equation. (Figure 5.3)

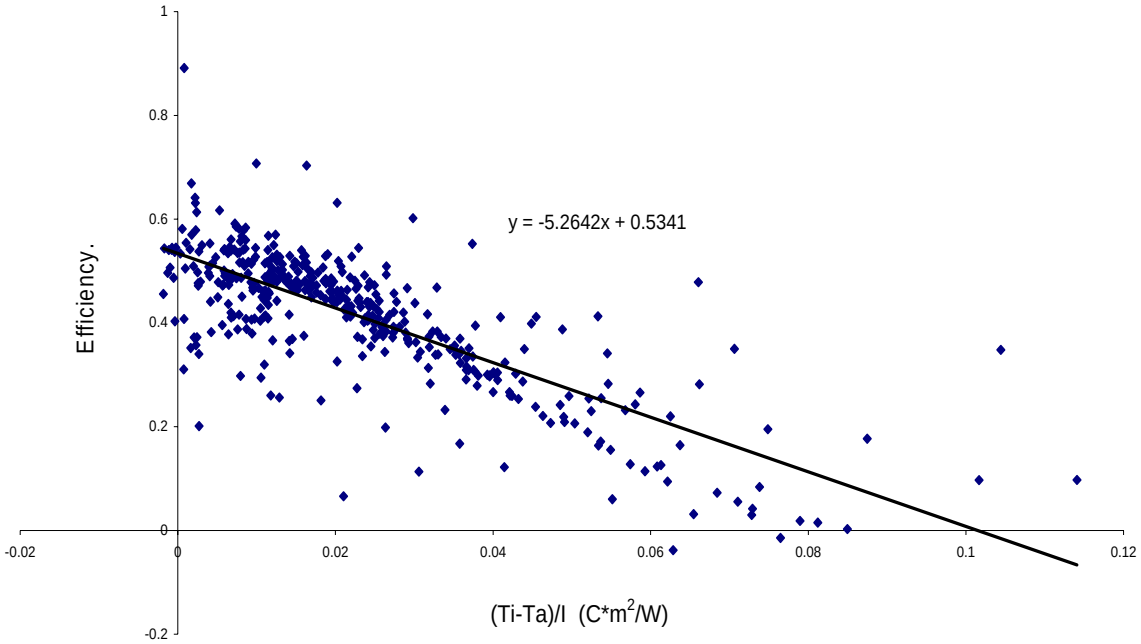

Figure 5.3 Experimental Collector Efficiency Curve

The collector efficiency equation produced from these data was significantly different from the one produced by SRCC's testing on the collector. SRCC's testing found a y-intercept of 0.706 and a slope of 4.9099 W/m^{2}K, as opposed to the y-intercept of 0.534 and a slope of 5.26 W/m^{2}K found by the author. However, the water temperature readings taken to produce the Figure 5.4 were taken at the thermal meter near the hot water tank instead of at the base of the solar collector. Thus, this experimental efficiency equation includes not only the losses for the collector, but also the losses of all the piping between the solar thermal energy meter and the solar collector

When the experimental efficiency curve was used as the efficiency curve of the collector in the simulation the results were good, in effect modeling both the collector and most of the solar piping in the collector component. However, to get near-exact matches in outputs, the maximum collector efficiency had to be lowered from 0.534 to 0.48. It is

believed this adjustment was needed because the curve was produced from data recorded when the set point of the tank was 120 °F. During the first monitoring period, when the tank set point was 135 °F, the water traveling through these pipes was about 15 °F hotter than when the curve was created. Thus, these pipes lost more energy than when the curves were produced and lowered the maximum 'collector' efficiency.

The outcome of this validation simulation is shown below (Figure 5.4). This graph displays the four energy flows over the entire first monitoring period. Each line represents the daily total of the named energy flow. The "Losses" variable included only the losses inside of the meters. Note the drain down loss was modeled as an additional draw at 6 PM each evening. Thus, the total daily load on the graph is 0.33 kWh above the true hot water load. In addition, to find the total losses for the tank each day this extra drain down loss must be added to the "Losses" variable.

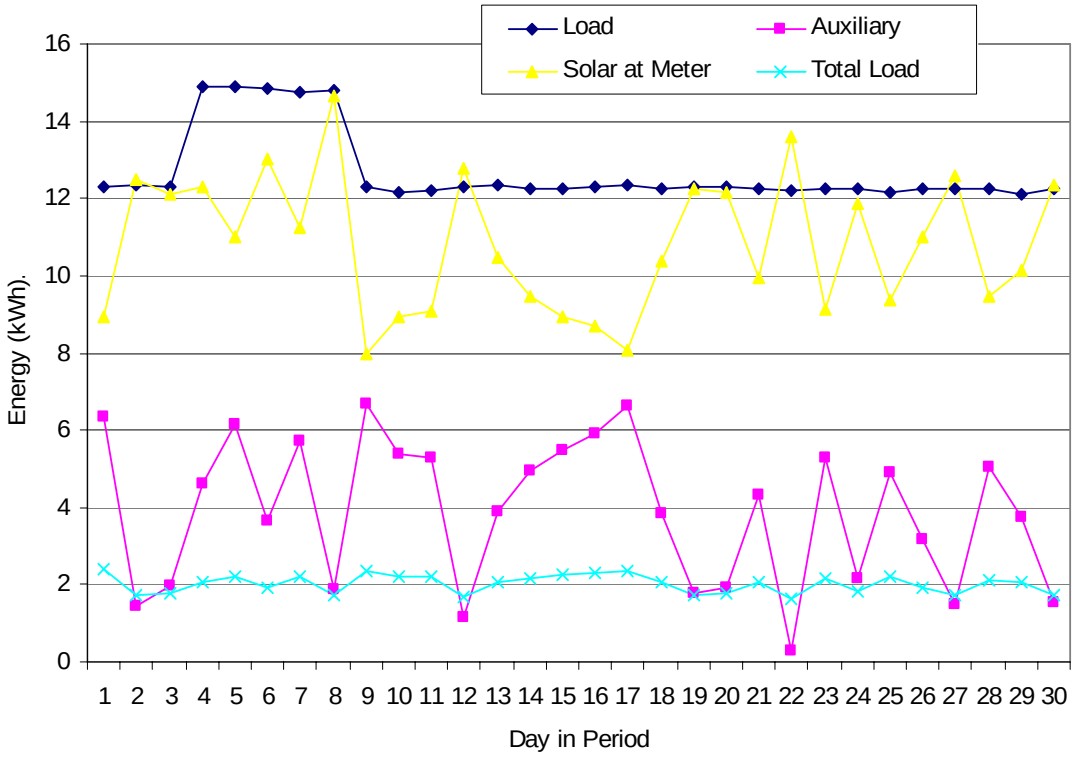

Figure 5.4 Results of Validation Simulation Using Experimental Collector Efficiency Curve

Notice the oddities in day 3. There was a malfunction of the spool valve when the system drained, causing extra water to be drained and false readings in the house energy meter. The "Total Losses" variable included in the graph represents the total losses from the tank and the nearby pipes as determined by an energy balance used the calculated meter values. A close inspection reveals a close match between the daily total levels of solar gain, auxiliary energy use, and system losses. Most of the differences that do exist tend to occur on poor solar days. This is because the model of the control system is not perfect and has difficulty is exactly matching the operation of the true system in marginal systems. In strong solar conditions, the model works exceptionally well.

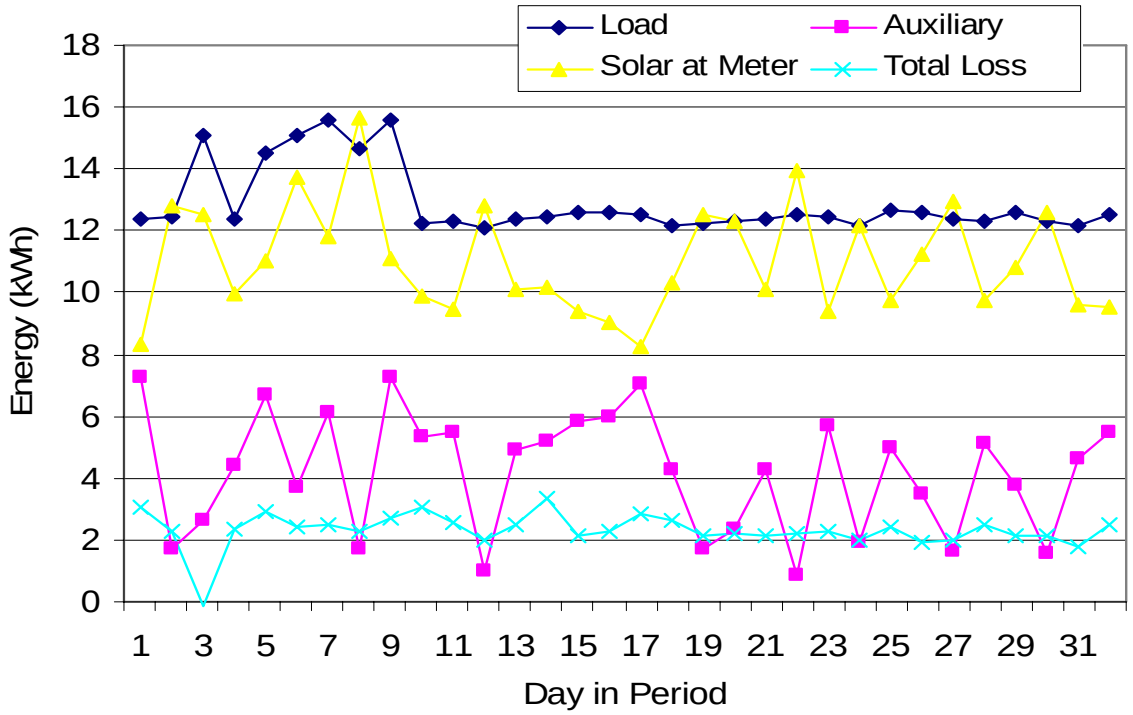

Figure 5.5 Daily Actual Data from Period 1

5.1.2 SRCC Collector Efficiency Curve with Pipe Losses

The second way to model the solar collector included the explicit modeling of the long pipes connecting it and the tank below. In this model, the solar collector efficiency provided by SRCC was used to define the solar collector component because there was no strong reason to suspect the collector performed any different than as expected. When the solar collector was modeled in this manner, it collected much more solar energy than was experienced in the monitoring periods. However, when the losses of the pipes between the collector and the tank were included, the amount of solar energy collected in the simulation was nearly identical to what was actually collected. In fact, the amount of pipe loss was

adjusted through the pipe heat loss coefficient until the daily energy values as measured at the meter matched the data. The amount of pipe loss required for the close matching of solar energy gains was very similar to the losses estimated by the heat transfer analysis. The losses from the set pipes in the simulation ranged from ~0 to 4.5 kWh per day, and the calculated loss estimates ranged from 0.6 to 4.0 kWh per day. Results of the simulation are seen below (Figure 5.6). Again, the "Losses" variable refers only to the losses from the tank and the pipes inside of the thermal meters. The "Solar at Meter" variable refers to the full solar collection at the solar collector minus the losses from the pipes from the collector to the thermal meter by the tank.

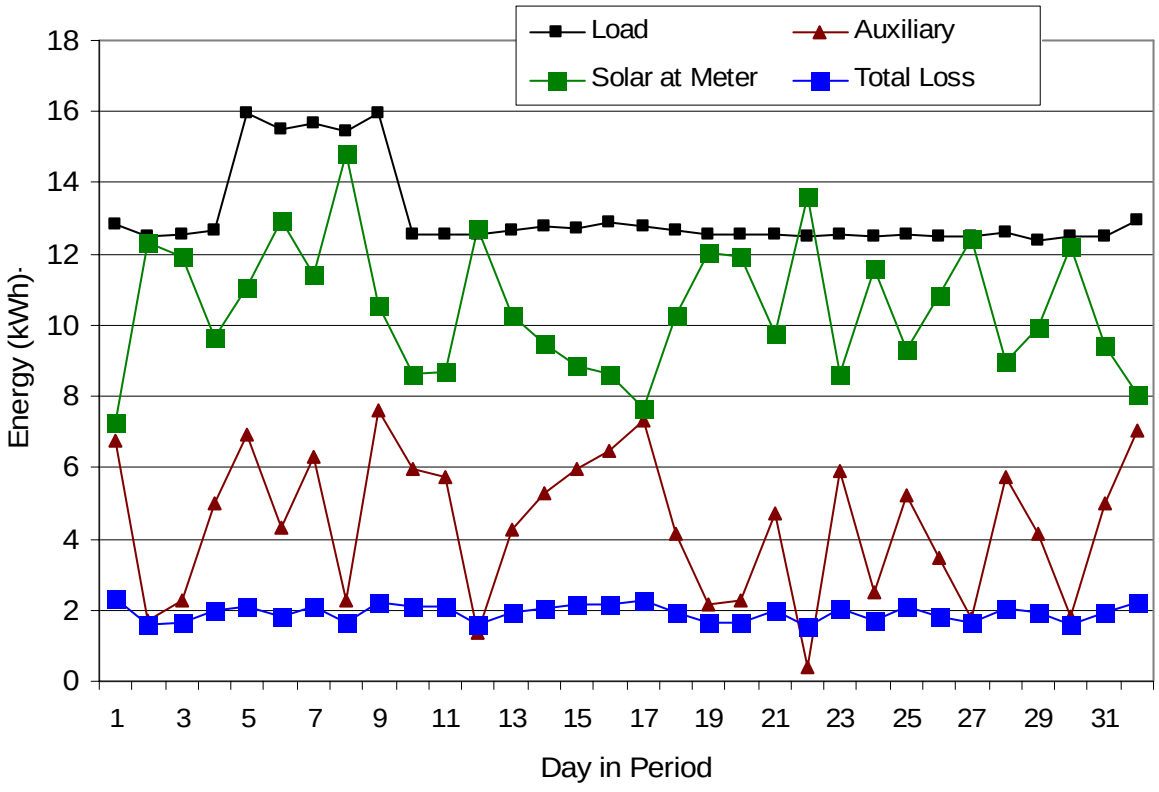

Figure 5.6 Results of Validation Simulation Including Solar Pipes

The results of this simulation also matched very well with the results from the experimental period. This fact gave validity to the pipe loss calculations developed earlier and suggested that the collector was functioning as expected. This indicated that a very large percentage of the collected solar energy was lost on the round trip up to the collector. Figure 5.8 clearly shows the losses experienced between the solar collector and the tank relative to the actual collected energy. The values are all from the simulation of the first period using the actual insolation data as an input. The "Solar_at_Collect" variable represents the energy collected by the solar collector. The "Solar_at_Meter" variable represents the energy collected by the solar collector minus the pipe losses between the collector and location of the solar thermal energy meter in the SDHW system studied. Finally, the "Solar_at_Tank" variable represents the energy gain experienced by the tank from the solar collector. Many days about 40% of the energy gained by the water while in the solar collector was lost between the collector and the relative thermal 'safety' of the hot water tank.

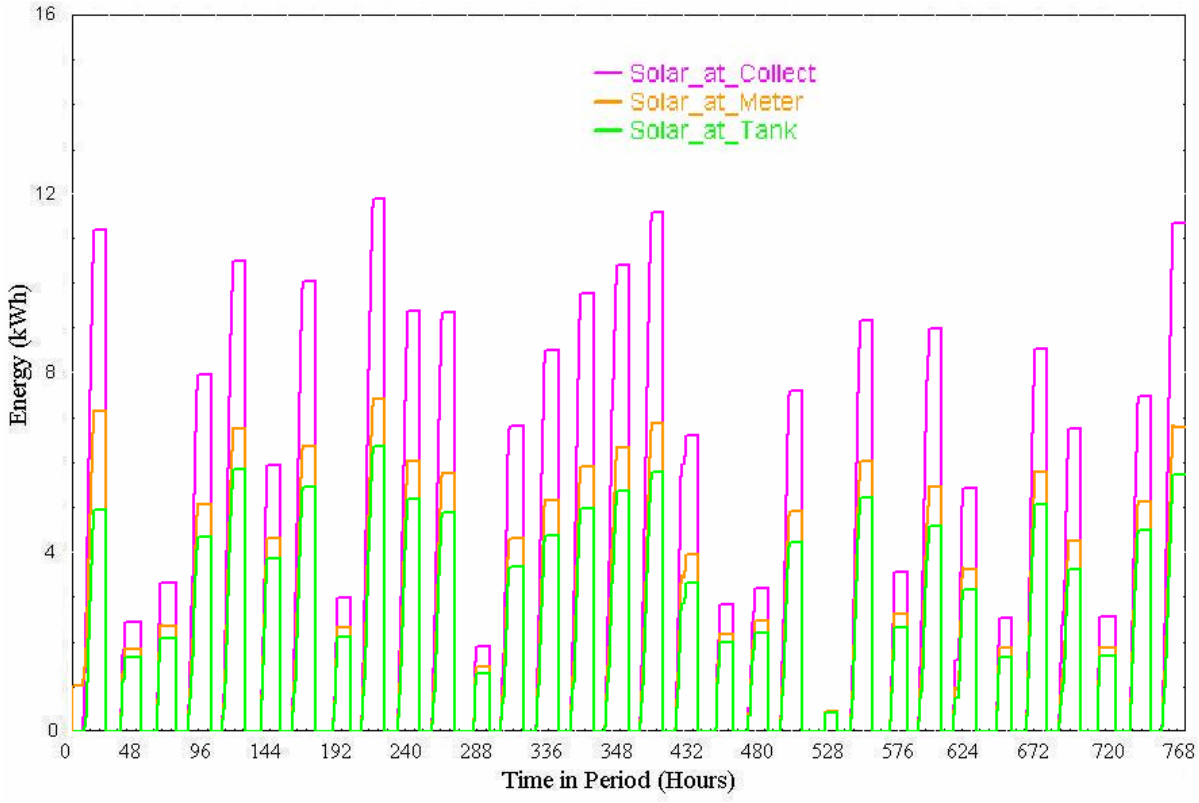

Figure 5.7 Simulation Solar Gain at the Collector, the Meter, and the Tank

5.1.3 Final Model

Both of the methods to model the solar collector produced very good results over the first monitoring period. However, only one of the models was chosen to perform further TRNSYS simulations. Although the experimental collector efficiency model worked well over this period, simulations performed with Raleigh TMY2 data (Typical Meteorological Year) over the other monitoring periods suggested that the fact that it did

not account for seasonal changes in the amount of pipe loss in the unconditioned attic produced slight errors. Therefore, the more detailed model using the SRCC collector efficiency and including the full solar piping loop was used for the all TRNSYS simulations of the system.

For the model to be accurate year round, seasonal changes had to be included in the model. Primarily, the water mains temperature had to be defined. This was accomplished by defining a water mains temperature for the first day in each month and assuming they change linearly. It was much more difficult to account for the seasonal changes in the pipe losses through the unconditioned attic. To do so the pipes between the collector and the solar meter were each modeled as two separate pipe sections, one in the conditioned house and one in the unconditioned attic. The temperature of the surroundings of pipe in the conditioned space was assumed to be a constant 72 °F. The temperature of the surroundings of the pipe in the unconditioned space was defined as a function of the outdoor dry bulb temperature provided in the TMY2 data. This equation was developed based on the assumption that the attic was typically warmer than the outdoor dry bulb temperature during the types the solar system was operating. It was then refined through simulation experiments, which were compared to the actual data from all three periods. The equation developed was simply: T_{attic} (°F) = T_{amb}(°F) +15 °F

5.2 Simulations of Monitoring Periods using TMY2 Data

Next, a simulation was run for each of the three monitoring periods using TMY2 data for Raleigh, NC as the input. The model for the first period was obviously unchanged

from the model described above; however, the other periods required changes in the model draw profile, tank set point, and tempering value temperature setting. The results of all three of these simulations were very pleasing and are displayed below.

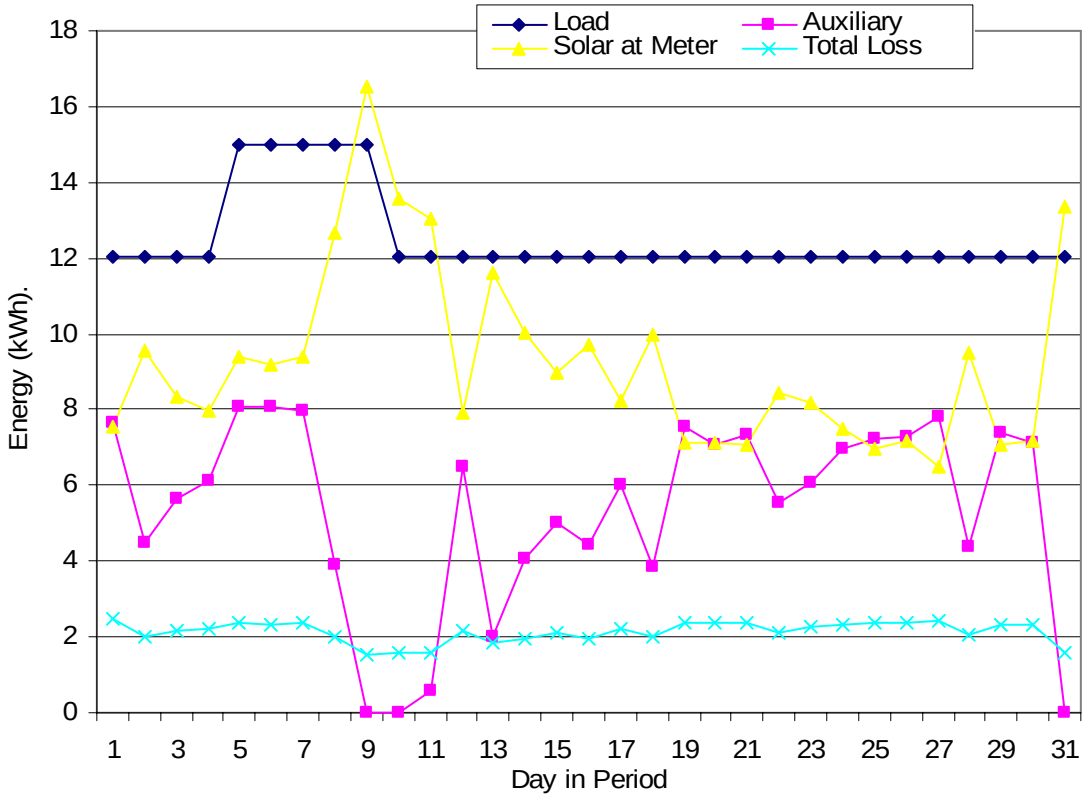

Figure 5.8 Simulation Results for Period 1 using tmy2 data

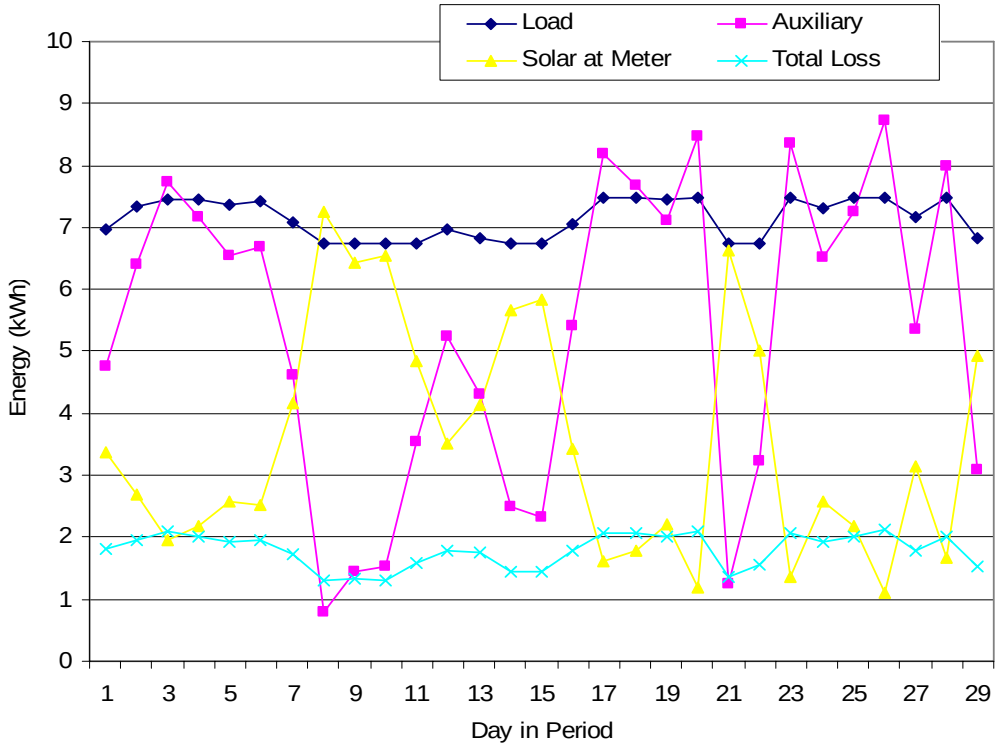

Figure 5.9 Simulation Result using TMY2 Data over Period 2

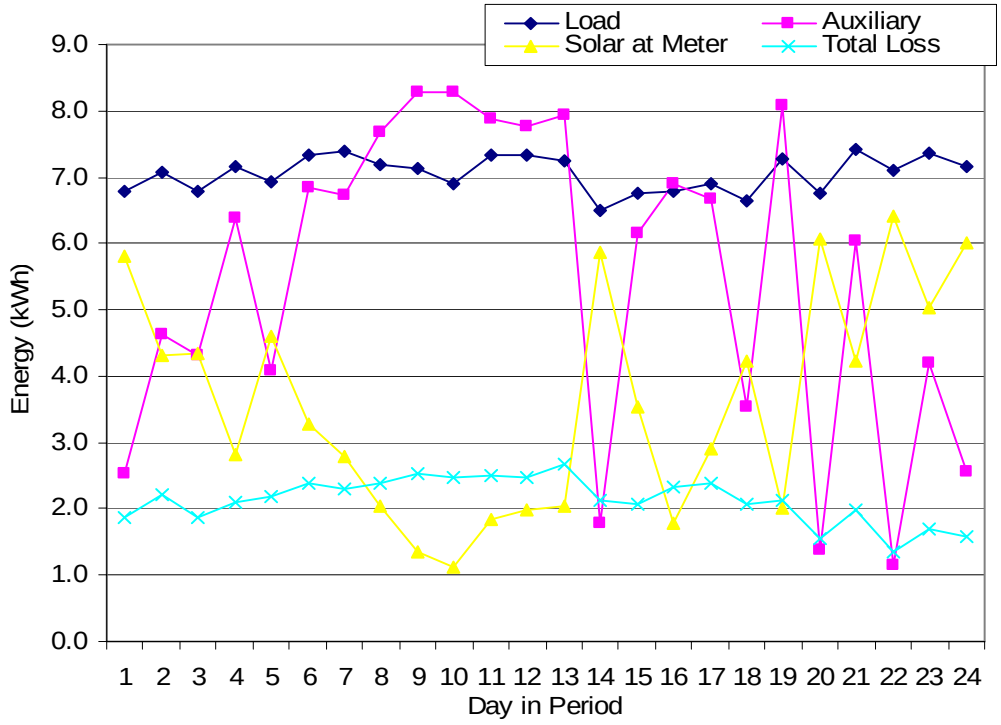

Figure 5.10 Actual Data from Period 2

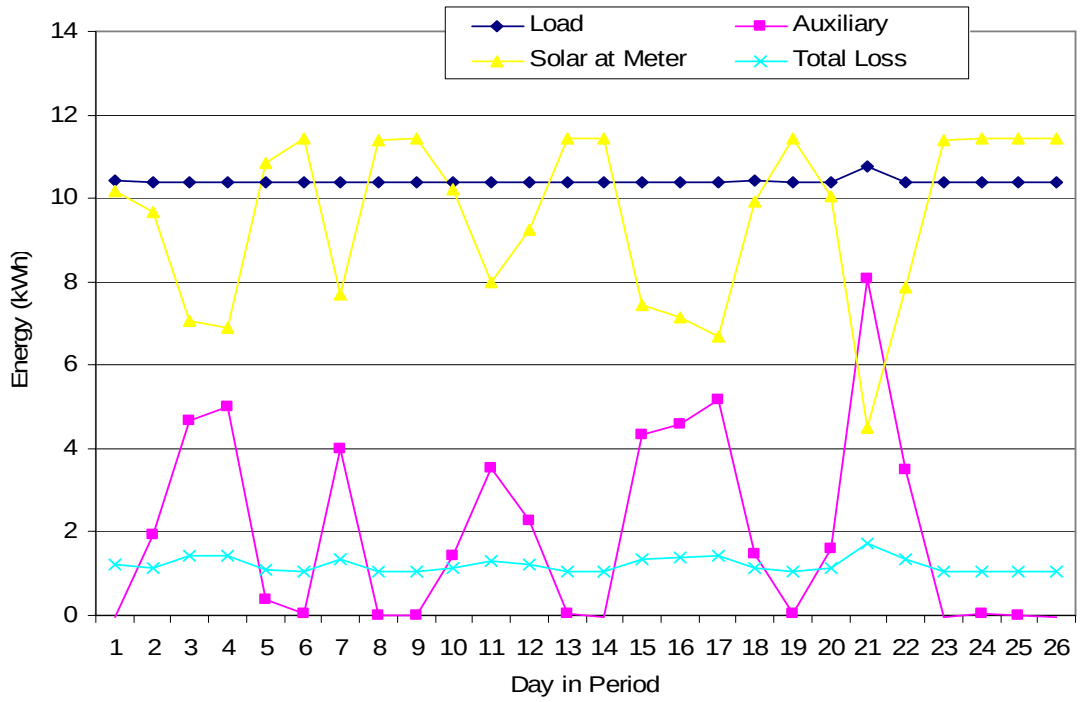

Figure 5.11 Simulation Results using TMY2 Data over Period 3

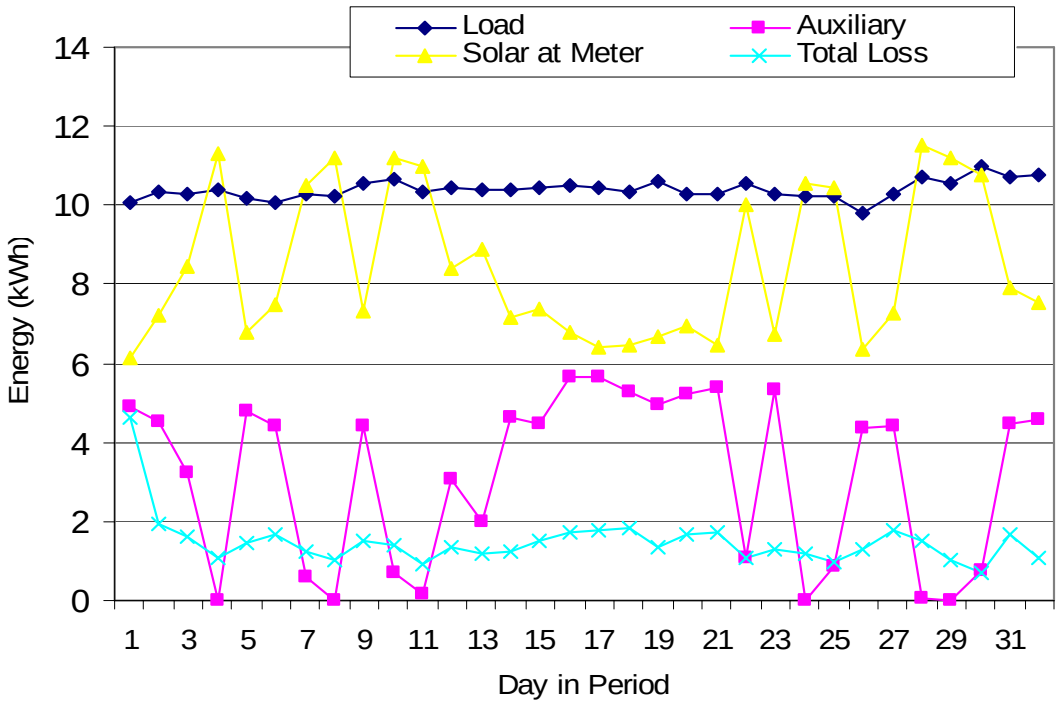

Figure 5.12 Actual Results from Period 3

Comparisons with the actual data over these periods showed that these simulations produced reasonable results over these periods. Note that period 3 was not continuous. It contained two sets of days separated by six days. A simulation was run for the period including these missing days, but these days were not included in the presented graph of results. TMY2 data of the days used did not happen to include any exceptional solar days. One of the excluded days and the day just 4 days after the entire period both produced solar (at the meter) gains of over 6 kWh in the simulation.

5.3 Detailed Draw Profile

The draw profiles used in all the prior experiments and simulations consisted of just six large uniform draws. In an effort to make the simulations as realistic as possible a more realistic hot water draw profile was used. The profile used was produced by ASHRAE [22]. It was produced from a large survey of families and defined the total water drawn per hour. The total daily draw was still approximately the same as the DOE water draw, but this profile included typical morning and evening hot water usage peaks. Each draw was still drawn off at 2 gallons per minute and started at 30 minutes past the hour. Knudsen [12] showed that for a SDHW system similar to the one used here the yearly net utilized solar energy dropped about 10% when a realistic profile was used instead of a simple three uniform draw per day profile. Figure 5.14 displays the results of a simulation using Raleigh TMY2 data and the

DOE water draw profile (set point at 120 °F). Figure 5.15 is the same simulation, but with the ASHRAE water draw profile applied instead of the DOE profile. DOE load tended to be slightly less. This is because the larger draws meant slightly cooler water toward the end of the flow. Also the DOE simulation clearly collected more solar energy, but by less than 10% annually. Note that the model used includes the large losses from the solar pipes leading up to the solar collector. These simulations conservatively predict solar gains because of this. Insulating the exposed pipes would make a noticeable increase in solar gains.

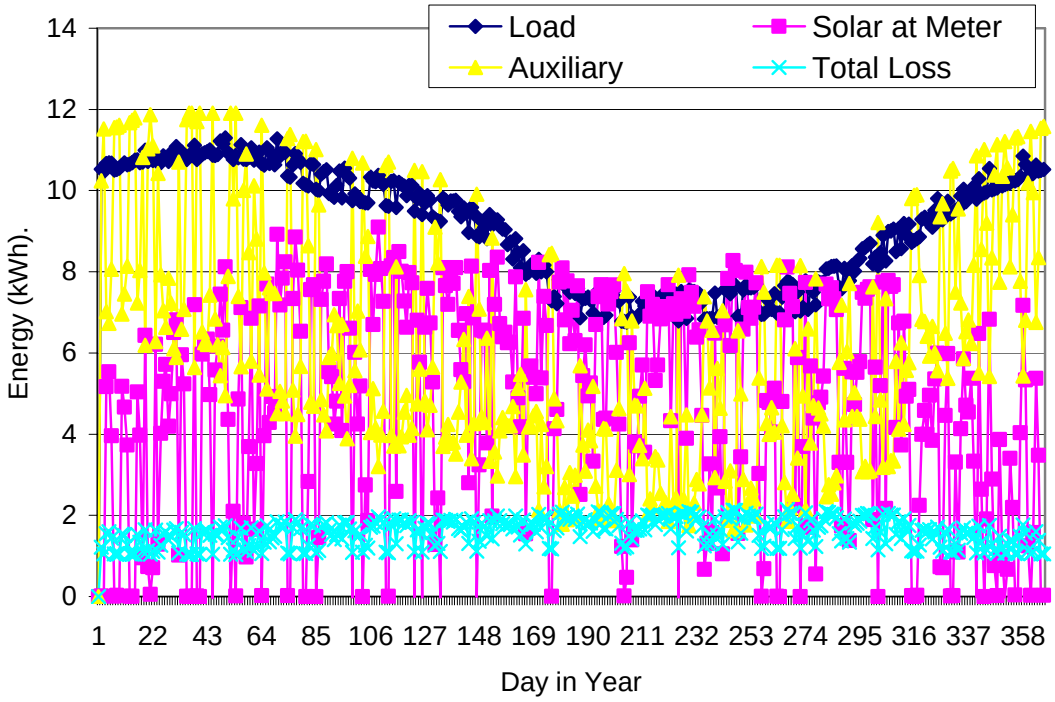

Figure 5.13 Annual Simulation using Raleigh TMY2 Data and DOE Draw Profile

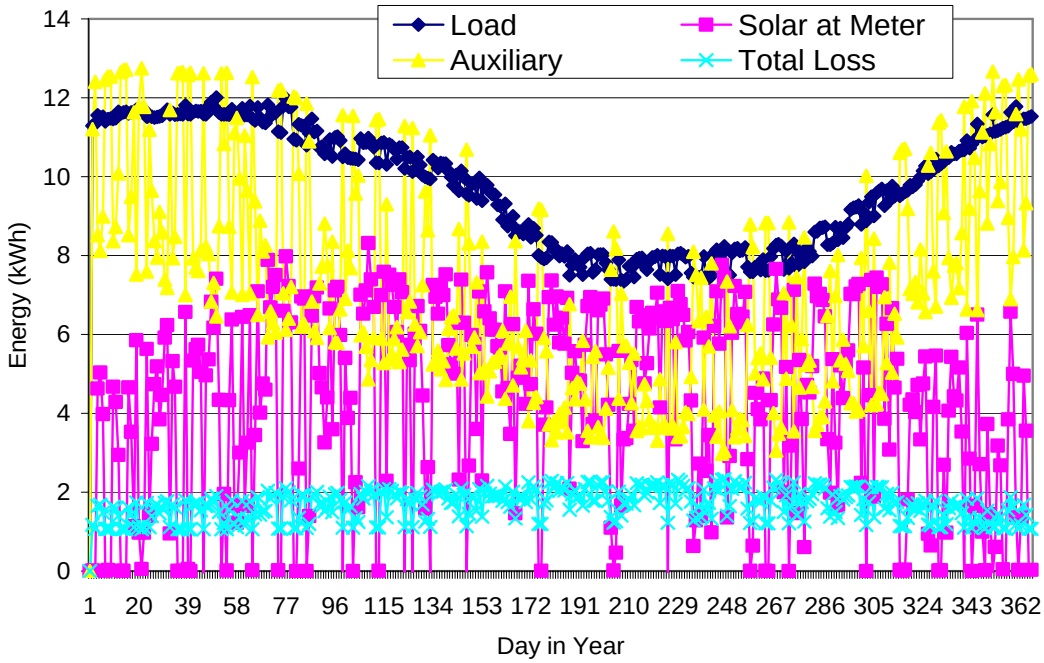

Figure 5.14 Annual Simulation using Raleigh TMY2 Data and ASHRAE Draw Profile

5.4 Other North Carolina Regions

Simulations applying the ASHRAE draw profile were run using the TMY2 for both Asheville and Wilmington, North Carolina. These two cities were chosen to represent the other two regions of North Carolina outside of the piedmont: the coastal plains and the mountains. They were included primarily to demonstrate that SDHW heaters may be utilized with good results across the entire state. This could be a factor in the possible inclusion of SDHW into statewide incentive programs. Again the set point was 120 °F as is recommended for most SDHW systems. Unfortunately, water mains temperature data

was not available for either of these two locations. Instead, the water temperature curve developed for Raleigh was used.

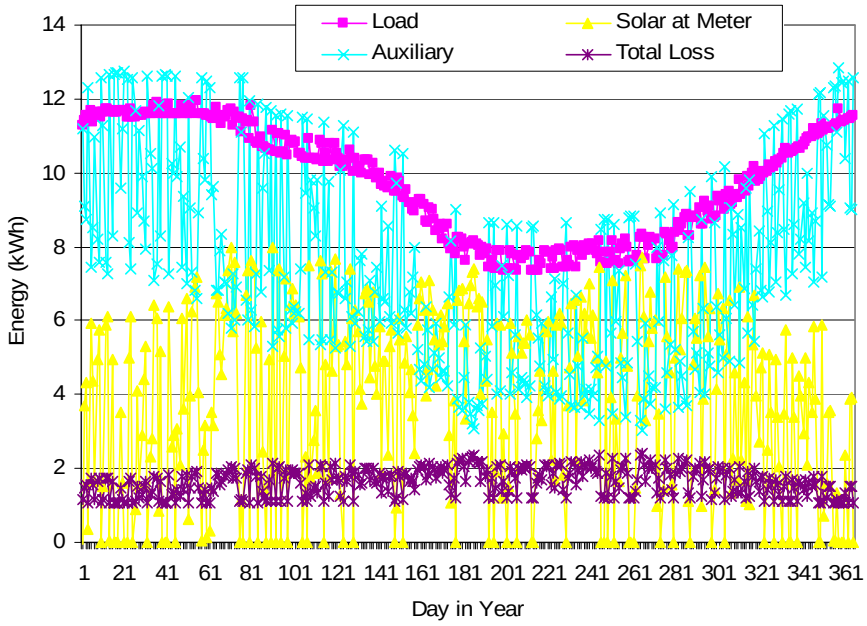

Figure 5.15 Annual Simulation using Ashville TMY2 Data

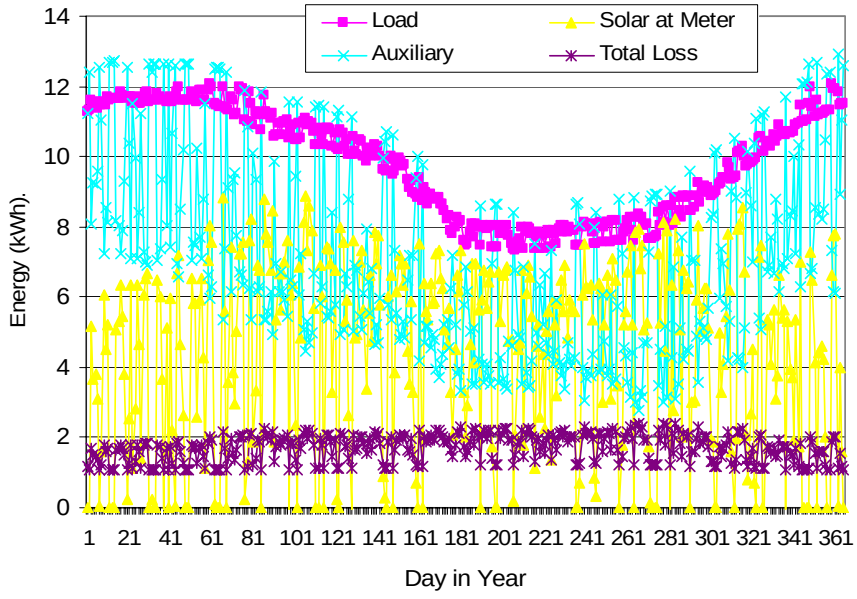

Figure 5.16 Annual Simulation using Wilmington TMY2 Data

5.5 Auxiliary Energy Offset

The goal of metering SDHW systems is to determine the amount of auxiliary energy offset by the solar gain so that this can be rewarded. Simulations were used to help determine the relationship between the system energy flows and the amount of auxiliary energy offset. The results of the simulations in this chapter are presented by month. This was done because one month would presumably be the reward period for production-based incentive programs and because the random daily fluctuations do not appear at this level.

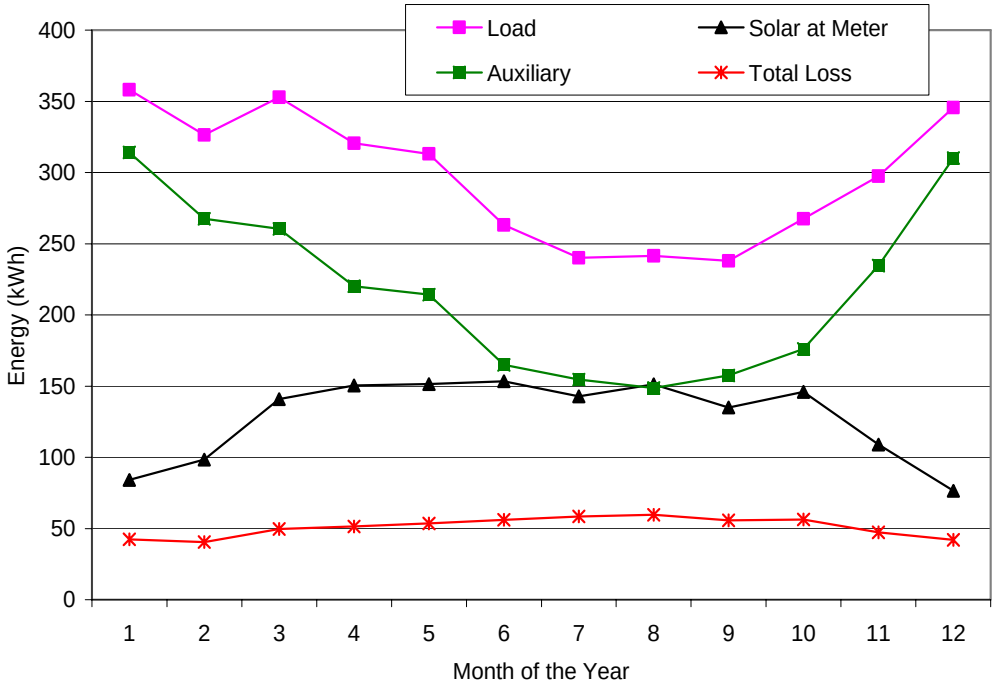

Figure 5.17 Annual Simulation using Raleigh TMY2 Data and ASHRAE Draw Profile, Solar On

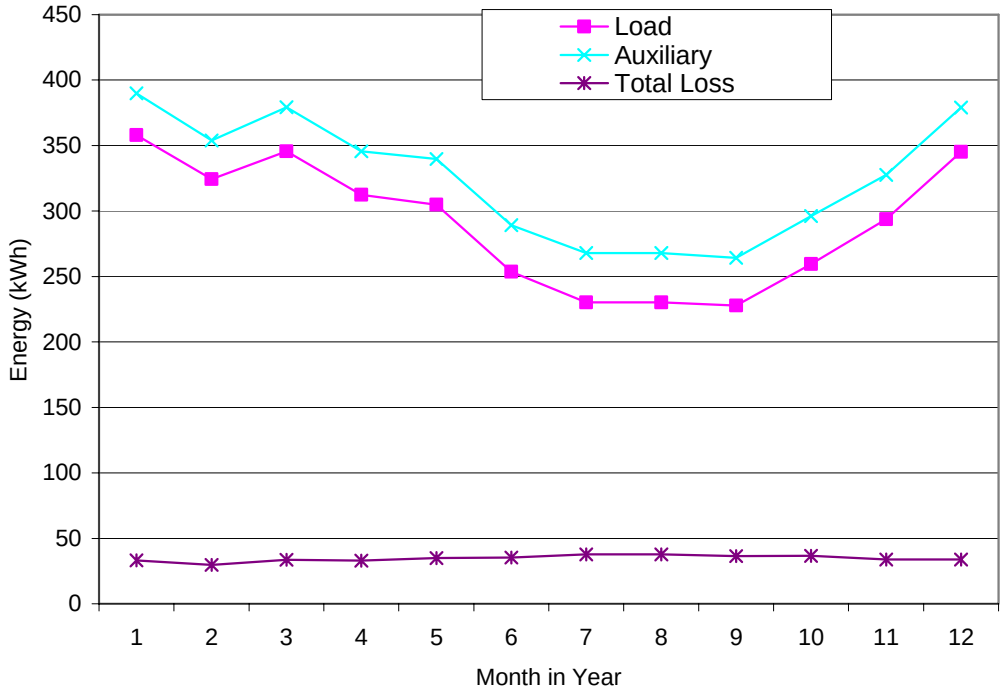

Figure 5.18 Annual Simulation using Raleigh TMY2 Data and ASHRAE Draw Profile, Solar Off

Figures 5.17 to 5.19 all present the results of one pair of simulations. These two simulations both occurred over one year using Raleigh TMY2 data and were performed on systems different in only one way, one of them was a SDHW tank and the other was solely a DHW tank. Their monthly results are seen in Figures 5.17 and 5.18 respectively. Comparisons of the results of these two simulations allowed analysis of which meter, or meters, best represented the electric energy offset by the SDHW system. Table 5.1 displays first how the amount of electric energy offset by the SDHW system was determined. Without manipulating the draw profile the SDHW produced draws of larger energies because at times they rose the temperature of the water in the tank above the tank set point. To greatly simplify the comparisons of these two simulations, the flow rate of each SDHW draw was reduced by roughly 8%. A similar adjustment would often be performed by the hot water

consumer by instinctively adjusting the amount of cold water mixed with the hot water at the faucet to produce the desired temperature. After this correction, the monthly and annual load energies were nearly identical.

Then it was a simple matter to determine the amount of electric energy offset by the addition of a solar thermal collection system. This is shown under the heading "Electric Energy" in Table 5.1. The next two columns in the table display the two metered values considered to represent the electric energy offset values. The "Losses" column is included only as an interesting level for comparison. Note that these losses do not include the drain down loss or the losses from the pipes away from the tank, but are based on the poorly insulated system model.

Table 5.1 Results of Two Simulations: One with Solar one with Solar Unconnected

	Electric Energy				Load Energy Meter	
	SDHW	DHW	offset	Solar Energy Meter	Minus Electric Meter	Losses
Jan	314.2	389.8	75.7	84.2	44.0	42.5
Feb	267.6	354.0	86.4	98.4	58.8	40.6
March	260.5	379.4	118.9	140.8	92.4	49.6
April	220.2	345.6	125.5	150.6	100.3	51.4
May	214.3	339.7	125.4	151.4	98.8	53.6
June	165.1	289.2	124.1	153.4	98.1	56.2
July	154.5	268.1	113.5	142.8	85.6	58.5
Aug	148.8	268.0	119.2	151.3	92.7	59.8
Sept	157.6	264.3	106.6	135.0	80.3	55.7
Oct	176.0	296.1	120.1	146.0	91.4	56.3
Nov	234.6	327.5	92.9	109.0	62.8	47.3
Dec	310.3	379.0	68.7	76.5	35.3	42.1
TOTAL:	2623.6	3900.7	1277.1	1539.3	940.4	613.7
Average Daily	7.19	10.69	3.50	4.22	2.58	1.68

Figure 5.19 display the electric energy offset in black and three other metered quantities considered as possible representations of the offset energy. Clearly the energy

flow labeled "Solar*0.86" most closely represented the offset energy. As expected the solar meter alone overstates the offset energy and the load minus electric in the SDHW system understate the offset energy. Solar* 0.86 represents the amount of solar energy collected as read by a thermal energy meter times the tank Energy Factor. Further simulation and empirical testing would verify their relationship, but the next several simulations suggest that under normal hot water use this value is a very good representation of the offset energy for this system. Figure 5.20 is a simulation of a system without the uninsulated solar pipe sections that existed the tested system. "Solar*0.86" is an even better match with the offset energy in this case. Figure 5.21 displays the results of simulations on an identical to the one presented in Figures 5.17 – 5.19 and Table 1 but with a tank set point of 135 °F. Again, the agreement of the solar energy meter reading times the tank energy factor with the offset electric energy is excellent.

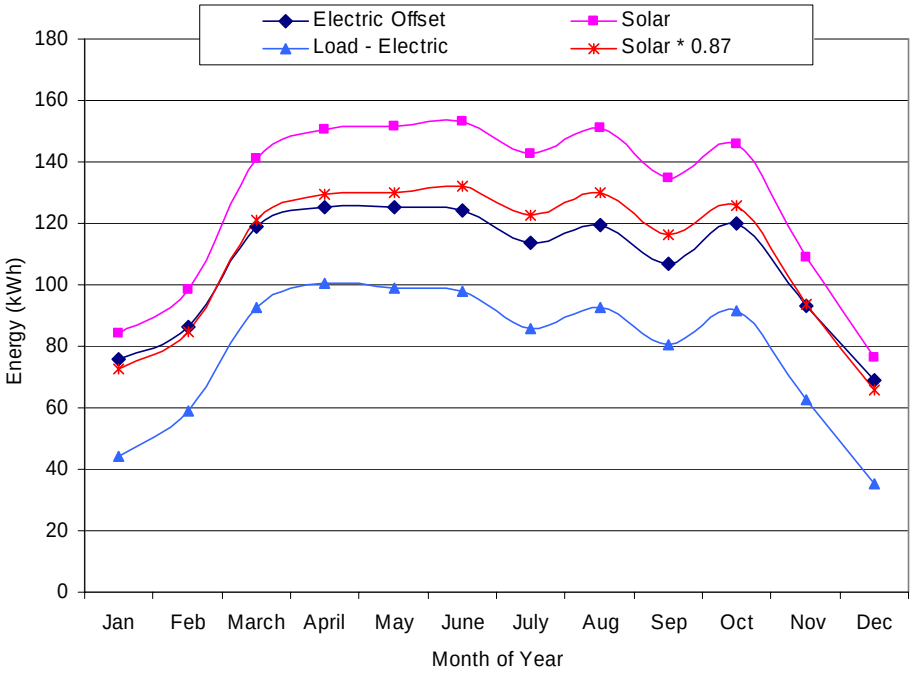

Figure 5.19 Meter Results Compared to the Offset Electric Energy: Raleigh, 120 °F, ASHRAE, Pipe Losses of Solar House System

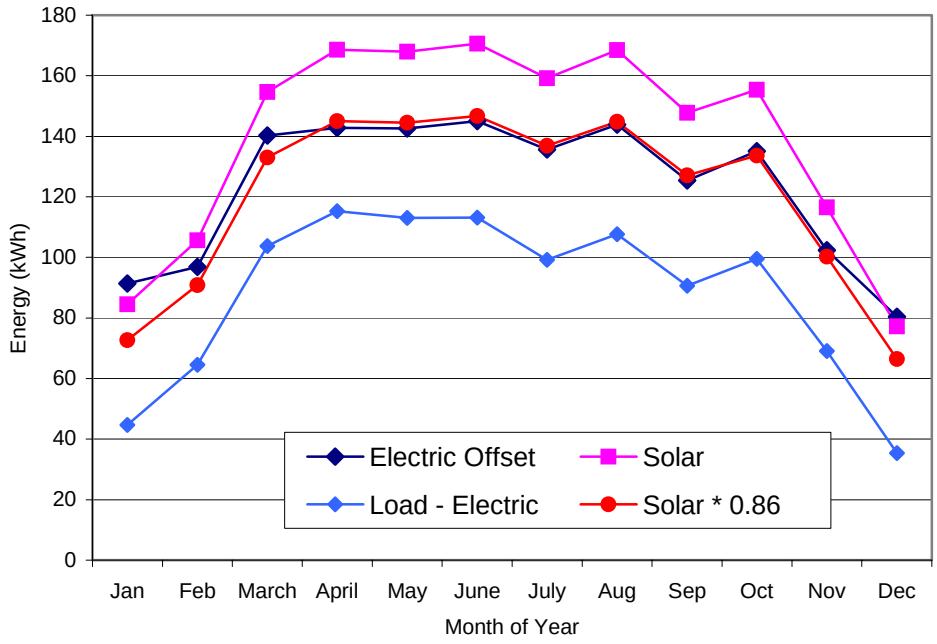

Figure 5.20 Meter Results Compared to the Offset Electric Energy: Raleigh, 120 °F, ASHRAE, Pipe Losses of Solar House System if all pipes were well insulated

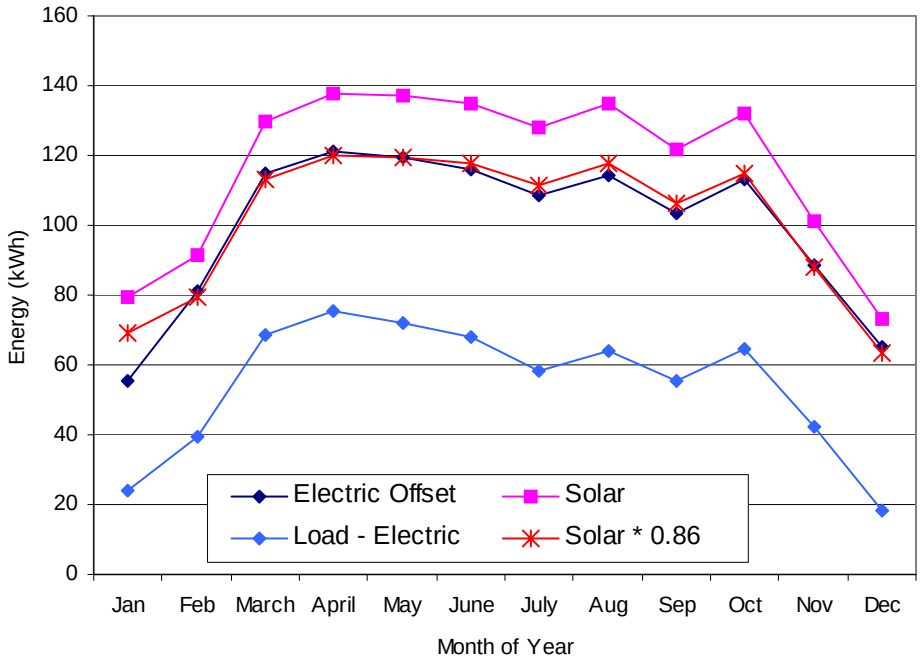

Figure 5.21 Meter Results Compared to the Offset Electric Energy : Raleigh, 135 °F, ASHRAE, Pipe Losses of Solar House System

This nice simple correlation of the electric offset energy and the solar energy meter is a strong function of the losses in the solar system between the solar meter and the tank. It is also dependent on the hot water usage pattern. When simulations were run with a small about of loss between the solar meter and the tank (~3% of tank loss on a sunny day) the offset electric energy is about 95% of the solar meter reading when a standard profile is applied. However, simulations showed that when atypical hot water use profiles are applied to the system (regard of solar piping losses) there is no simple correlation between the solar meter reading and the offset electric energy. This is, however, a simple correlation between the hot water load meter reading minus the electric energy meter reading and the offset electric energy. The correlation is a simple constant offset, seemingly regardless of hot water usage. The following figures show the results of these simulations. The atypical hot water uses shown are a typical hot water load daily total all occurring between 6AM and 9AM in six even draws and hot water use only the last two days out of the week. These two examples represent uses that have a large affect on the functioning of a SDHW system.

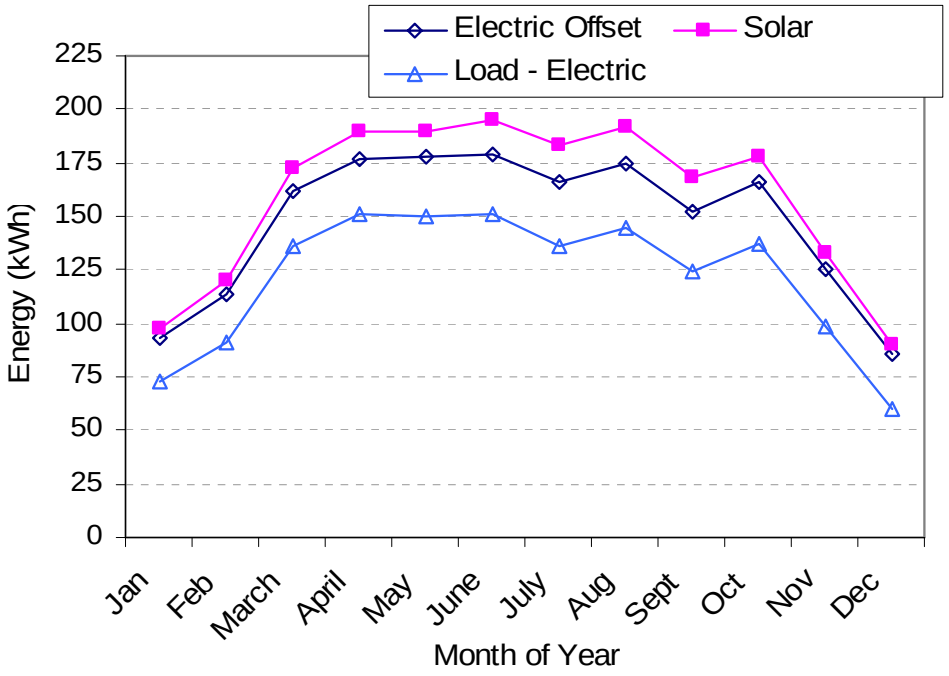

Figure.5.22 Simulated electric energy offset and energy meter readings with small losses between solar meter and tank

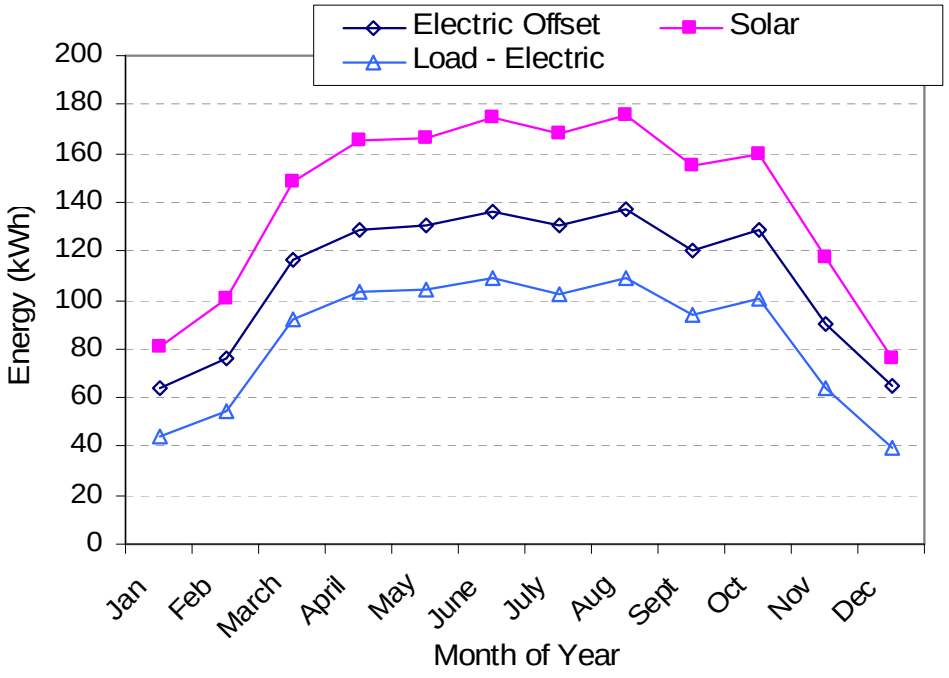

Figure 5.23 Simulated electric energy offset and energy meter readings with full load between 6AM and 9AM

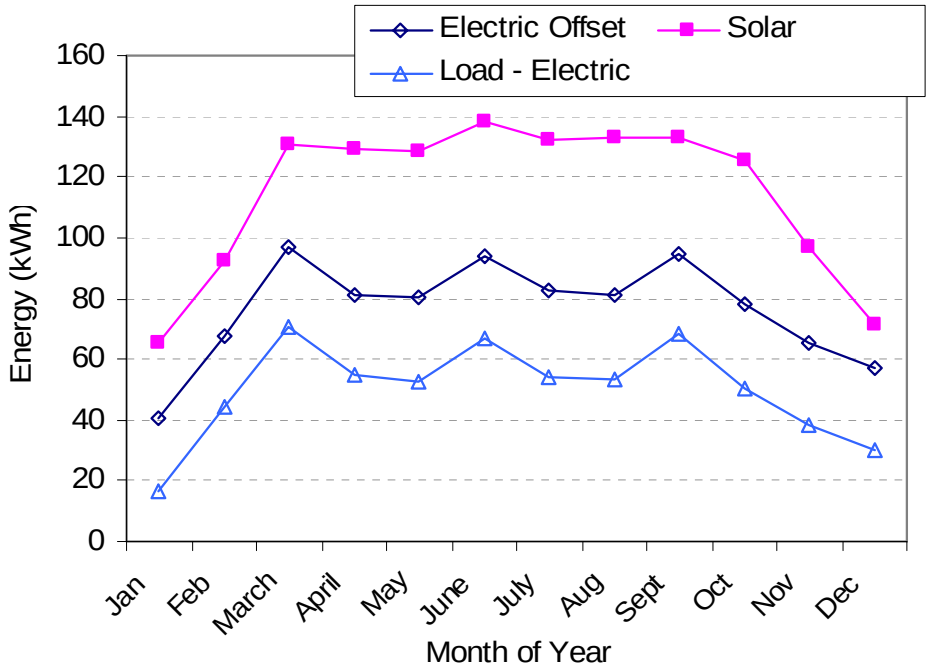

Figure.5.24 Simulated electric energy offset and energy meter readings with only weekend hot water loads

These simulation sets of extreme, but surely not uncommon, hot water draw profiles revealed that there is a simple and quite constant correlation that may be made between the load thermal meter minus the electric meter and the offset electric energy. The metered value plus the daily experimental (24hr) tank loss of the system without the solar system equals the offset electric energy. The table below shows the consistency of this correlation over the range of draw profiles.

Table 5.21 Summary of 'Load minus Electric' Agreement (kWh)

	Daily tank loss (no solar)	Daily tank loss (solar)	Daily average 'Offset' minus 'Load – Electric'	Range of monthly daily averages
ASHRAE	0.88	1.28	0.87	0.67 to 0.95
Morning	0.85	1.88	0.84	0.65 to 0.91
Weekends	0.89	2.17	0.88	0.77 to 0.92

Although, the exact error that would occur over a wide range of actual SDHW systems is not known, but it is believed to be acceptably low. In the case of the modeled system, the error of correlated metered value in determining the electric offset energy was less than 2% in all cases. Most solar systems have a similar ratio of collector area to tank volume (0.64 ft^2/gal) (15.7 m^2/m^3) to the tested system. The tested system was a one-tank system, but many SDHW systems include two hot water tanks. In a two-tank system, the hot water load and the auxiliary electric energy are metered in the same way, and the metering results are expected to be very similar. In an indirect system, this metering strategy would not require any fluid to be measured other than water. This is a definitive advantage over metering the solar gain added to the tank, because fluids other than water would need to be metered for one-tank indirect SDHW systems. In North Carolina the weather will not permit integral collector storage (ICS) systems, but this general metering strategy is applicable to them as well. Further work needs to be done in order to fully develop and verify this metering methodology for all types of SDHW systems.

Chapter SIX ANALYSIS OF METERING SCHEMES

The goal of the each metering scheme is to meter the electric energy offset. This is impossible to do directly, so allowances must be made. The final TRNSYS simulations suggested that the best metering strategy to represent the electric energy offset is a hot water load thermal energy meter and an auxiliary electric energy meter. The metered value is then the load meter value minus the electric meter value plus an experimentally determined daily tank loss for the system times the number of days in the metering period. This daily tank loss is effectively independent of season and hot water use. In this chapter, each scheme is applied to the data from the three monitoring periods in order to determine the accuracy of each scheme (compared to the most reliable metered values available). However, there is more to choosing the most effective metering scheme than this one factor alone, especially when the logistics of incorporating the chosen method into a state or nationwide program are considered.

The goal of this analysis was to determine 'the best' metering scheme for metering SDHW systems for inclusion in NC Green Power. All analysis was conducted with this goal, so the results are therefore specific to North Carolina. Obviously, North Carolina contains a range of locations and even climates. It is believed that in regard to the analysis of SDHW system metering, Raleigh serves as a more than adequate representation of the entire state, so this data was used to represent the whole of North Carolina. With this said,

climatic effects are significant in only a few of the considered schemes. These effects are discussed in this chapter, therefore allowing the adaptation of this analysis to locations outside of North Carolina.

The metering schemes, or metering methodologies, under consideration were described in Chapter 2.2.7. They are as follows:

- Solar-Loop Thermal Energy Meter
- Hot Water Load Thermal Energy Meter and Electric Meter
- Electric Meter and the Load Cold Water Flow Meter with Temperature Estimates
- The Solar Loop Flow Meter and Temperature Difference Estimate
- Solar Loop Temperature Difference with Watt-Hour Meter to Determine Flow Rate

6.1 Comparison Criteria

Before any actual analysis took place, the criteria of the desired final scheme were carefully considered. Much time and effort was expended to ensure the accuracy of each scheme was well understood and well represented. The accuracy of each scheme was the primary design criteria. In order for any metering scheme to have merit it must be accurate enough for all parties involved to be satisfied the metered values are a fair representation of the actual energy collected, and further, the energy offset. Once all parties are satisfied of this, the other criteria become important as well. The level of accuracy required to satisfy all parties is subjective and perhaps even flexible when other benefits and drawbacks of

each scheme are considered. Obviously, the accuracy must be balanced with the other characteristics of each scheme, but there is some level of accuracy below which the scheme is of no value. Further discussion of the required level of accuracy is included below in the analysis of each considered scheme.

The second most important criteria in the selection process was the cost of each system. The lower the cost of a metering scheme the more economically beneficial its use will be and the more interest it will invoke. The thermal meters used in most of the schemes are quite expensive. A high initial cost may cancel much of the rewards paid by the NC Green Power program and cause a very long payback period. Too high of an initial cost would make the payback period so long that implementation would not make economic sense. All prices and price ranges quoted are rough. There is a large worldwide market of metering components and only a small amount of time was spent on obtaining price estimates. The detailed economics were too involved for the scope of this paper. However, the consideration of relative prices was considered of utmost importance when considering the metering schemes.

For the most part, the rest of the criteria take a back seat to these first two; accuracy and cost. With one possible exception, if only one final metering scheme is chosen, it must be robust enough to work well on all of the various styles of SDHW systems in North Carolina and in all regions of North Carolina. This is discussed further later in the analysis. The other minor criteria are ease of installation, ease of use, and tamperproof. Ease of installation is closely related to cost, but also refers to the difficulty of correctly installing the system for accurate results. The final criteria are easily described by considering a standard electric meter. Meaning that the metering scheme must provide a number (or two,

or three numbers) that may be easily read by a meter reader and that the device is relatively tamperproof to the owner of the SDHW system.

6.2 Metering Schemes on Different Types of SDHW Systems

All of the experiments performed were on the same one-tank draindown system. Across North Carolina most SDHW systems are different than this one. The metering of other types of SDHW systems would obviously differ in some aspects. For example, no other type of system has to deal with the issue of drain down losses. However, the most relevant differences are that some systems contain two tanks and that some systems are indirect. The two tank systems have a preheat tank that is connected directly to the cold water supply. It is heated solely by the solar thermal gain. From this tank, the water passes on to the final tank which is always kept at least at its set point with backup power. This all has the implication that the solar gain can be metered in two different places, across the solar loop as mentioned before, or across the preheat tank.

The first of these options is straightforward. The second essentially meters only the solar energy that makes its way into the final tank. In other words, this is the solar loop energy value minus any losses that occur from the preheat tank. It is the author's belief that this second value is the one that should be metered. This is because this energy is entering the system at the same place as the backup energy. In other words, this energy is equivalent to the backup energy in usefulness. The energy metered in the solar loop is less useful because some extra percentage of it will be lost to the surroundings. For simplicity

sake, when metered solar energy is mentioned elsewhere in the paper it is referring to the solar energy entering the final tank. In addition, the schemes that meter the hot water load energy and the electric energy consider the solar energy that enters the final tank and not the energy entering the preheat tank.

Indirect systems that use distilled water cause no concerns about the application of any of the mentioned metering schemes, however those that use glycol as the solar collection liquid do cause some concerns. This is only a concern in a single tank system because otherwise the thermal meter measuring the solar energy is measuring the flow rate of the cold water into the preheat tank, and there is no problem. However, in the one tank indirect system a thermal energy meter directly measuring the solar gain would have to be in the solar-loop containing glycol, or some other heat transfer liquid. The problem is the electronics in the thermal energy meter that calculate energy from the flow rate and temperature inputs does so by using the specific heat and density of water. In order for such a meter to work with a liquid other than water these two values must be either changeable or preset for the liquid in use. The thermal energy meters on the market that are capable of this are more expensive than meters that work only with water. There is an one upside to placing a thermal meter into glycol rather than water. This is that glycol does not cause the same scaling and corrosion problems that water can cause, thus leading to a potentially more reliable meter.

6.3 Analysis of Each Scheme

Each of the metering schemes under consideration is described and its strengths and weaknesses as they are understood are discussed. Then, the results of the experimental accuracy study are displayed and analyzed. These accuracy studies were performed on the data recorded by the detailed monitoring system during the three monitoring periods. The completeness of the sets of data made it possible to compare the actual energy flows to the value that each individual metering scheme would have returned, thus making it possible to test the accuracy of each scheme over three different month long periods. These periods represent winter and summer, with different draw profiles and set points. When a temperature estimate was required it was made with the help of both the actual data and simulations. If only the actual data was used the results of this analysis would be deceiving because a form of the results would be the only input.

The values returned by each would-be scheme were calculated based on the calculated thermal meter values. This was done because it is believed the time response problem experienced in this project would not typically exist, especially after the level of the problem was revealed here. However, the false load meter readings caused by the filling of the solar collector were not corrected for, because although they only happen in direct systems, they are practically unavoidable in such systems. The pipe losses between the meter and the tank were also not corrected for because some actual systems would be no better insulated than the original SDHW system in this experiment. However, the performance of the SDHW system is clearly improved when this region is better insulated. The same logic was used when it came to the pipe losses between the tank and the

collector. No adjustments were made to the data to attempt to correct for some of these losses. Although, better insulation of these pipes would clearly improve the functionality of the SDHW system. In addition, drain down looses are impossible to correctly meter with a typical thermal meter. On most days the drain down loss was metered as very little or no energy by the solar loop thermal meter. This is convenient because it does not significantly affect the solar energy meter value, as should be the case. No adjustments were made to the data to correct for any energy gain that was falsely recorded.

6.3.1 Solar-Loop Thermal Energy Meter

This is the most straightforward of all the schemes. There is simply one thermal meter installed on the solar loop that directly meters the amount of energy collected by the solar collector. This scheme is by far the most intuitive. It also has the potential to be the most accurate because there is not the problem of false readings during collector fillup. The thermal meter used in this position during the three monitoring periods performed much better than the thermal meter monitoring the hot water load energy use. This is because the time response problem experienced was a much larger problem for the hot water load meter because the flows were much shorter and intermittent. The temperature probes often needed to register large temperature changes over a very short time. Although higher temperatures were reached in the solar loop than in the house pipes, the temperatures at the onset of a flow in the solar loop were typically much closer to room temperature, and then rose higher quite slowly. However, when the temperatures from the

very fast responding thermocouples were used in place of the sluggish temperature probes the accuracy of this thermal meter was excellent. In fact, it was used as the standard for comparison when testing the accuracy of other metering schemes. Because of this, the accuracy tests of this method during the monitoring periods always returned a perfect match.

The cost of this scheme is the only real drawback. The thermal meters are quite expensive, but very accurate (particularly when they have fast temperature reactions), durable, robust/straightforward (they measure just what we want, so they will work simply on any system), easy to use (just one number to read), and they are tamperproof. The cost of the meter used in the experiments was ~$500. The installation of the meter would increase the installation cost of the SDHW system by $50 to $150.

Table 6.1 "Solar Loop Metering" Applied to Data

	Period 1		Period 2		Period 3	
	1: Solar Meter (solar alone)	actual solar (kWh)	1: Solar Meter (solar alone)	actual solar (kWh)	1: Solar Meter (solar alone)	actual solar (kWh)
Daily Avg.	4.24	4.24	5.5	5.5	3.1	3.1
Total	131.3	131.3	131.8	131.8	85.4	85.4
Percent Error	0%	0%	0%	0%	0%	0%

6.3.2 Hot Water Load Thermal Energy Meter and Electric Meter

This is the metering scheme used by Lakeland Electric and the one able to be easily correlated to the offset electric energy for a wide range of hot water use profiles.. This utility in Lakeland Florida has installed utility-owned SDHW systems onto customers' homes and charges them monthly for the energy it produces. In this scheme, one thermal energy meter is installed across the hot water heater. A second meter, an electric watt-hour meter, is installed inline with the electric heating elements in the tank. The metered value is obtained by subtracting the electric energy used, read on the Watt-hour meter, from the total energy used in the form of hot water, read on the thermal meter. The value this gives is the amount of solar energy collected minus the thermal losses from the tank and the pipes before the thermal meter. This obtained value could be used directly, as Lake Land Electric does, or to determine the electric energy offset of the SDHW system the tank loss estimate could be added to the metered value.

A problem experienced with this meter over the course of the experiments was mentioned in the discussion of the first scheme. The problem had to do with the speed at which the thermal meter temperature probes could respond to the temperature of the water when a flow started. In the winter time this lead to large errors because the water in the pipes between flows would warm up above room temperature due to heat loss from the tank and then take some time to correctly report the cold temperature of the new water flow. This problem was bad enough that the temperature probes did not appear to read the correct temperatures until about 5 gallons had flowed past. During the 3rd monitoring period this meter experienced a nearly 16% percent error due to this effect. Assuming a

thermal meter could by installed in a way to avoid this problem this scheme still has other downsides.

The more difficult problem to correct with this scheme is the problem of false hot water use readings caused when the solar collector was filled. These errors were significant if the pipes were still hot from a recent draw when the collector filled. This problem could be avoided if the flow meter was placed in the hot water line. The flow meter included with the thermal meters used was specified to be placed in the cold water line and can be damaged by water over 104 °F (40 °C), but other thermal meters could be chosen that would allow for the flow meter to be placed in the hot water line. In the following table, this error was not been corrected for, thus the larger error in the winter monitoring period when this was more of a problem. The errors presented are the unrelated to the error of the method at representing the offset electric energy. Remember that this would not be a problem in an indirect system, or if the flow meter was moved to the hot water line. This scheme appears to be very accurate barring this problem.

The cost of this scheme is larger than that of the solar thermal meter alone. In the experimental system, as would be the case in most SDHW systems, the flow rates through the house thermal meter are greater than those through the solar thermal meter. This difference meant different pipe sizes and different sized thermal meters. Therefore, the thermal meter measuring the house hot water use was larger and somewhat more expensive than the one on the solar loop. In addition, this scheme also requires an electric meter. This would add up to an extra $100 onto the price of the metering package.

Table 6.2 "Load and Electric Metering" Applied to Data

	Period 1		Period 2		Period 3	
	2: load meter and electric meter (solar minus losses)	actual solar minus losses (kWh)	2: load meter and electric meter (solar minus losses)	actual solar minus losses (kWh)	2 load meter and electric meter (solar minus losses)	actual solar minus losses (kWh)
Daily Avg.	2.01	1.87	3.35	3.28	1.84	1.65
Total	62.38	58.04	83.9	81.7	51.5	46.2
Percent Error	7.5%		2.7%		14%	

6.3.3 Electric Meter and the Load Cold Water Flow Meter with Temperature Estimates

This scheme is a modified version of the previous scheme. It replaces the expensive thermal energy meter with a flow meter and average monthly estimates of the temperature of the cold city water and the hot water used in the house. Both of these numbers are relatively constant over a period of one month. The temperature of the hot water experiences only small fluctuations because the tempering valve limits the maximum value and the auxiliary heating elements limits the minimum value. The cold-water temperature varies significantly from season to season, but from year to year the average cold-water temperature in any given month is more or less constant. This results in a cheaper, possibly as accurate version of the above metering. The cost savings of this scheme, with only the flow meter and not the other components of the thermal energy meter, is significant, however because of the very wide range of flow meter manufactures

an suppliers this is not attempted to be quantified. Again, the slow response error was not accounted for in the following table.

This scheme requires more work to take a reading than the schemes discussed so far. The total flow must be multiplied by the heat capacity of water, the density of water, the monthly average temperature difference, and a unit conversion factor to determine the amount of energy in kWh used in the form of hot water. Then the electric meter value must be subtracted from the first product to determine the final 'metered' value. This process could be made very simple with a small computer program.

Table 6.3 "Load Temperature Estimates Metering" Applied to Data

	Period 1		Period 2		Period 3	
	3: Electric meter, cold flow, and temp. estimates (solar minus losses)	actual solar minus losses (kWh)	3: Electric meter, cold flow, and temp. estimates (solar minus losses)	actual solar minus losses (kWh)	3: Electric meter, cold flow, and temp. estimates (solar minus losses)	actual solar minus losses (kWh)
Daily Avg.	2.11	1.87	3.42	3.28	1.95	1.65
Total	65.4	58.0	85.2	81.7	54.6	46.2
Percent Error	13%		4%		18%	

6.3.4 The Solar Loop Flow Meter and Temperature Difference Estimate

This scheme originally looked very promising, no expensive thermal meter, only one number to estimate, and the final result is the solar energy collected. The scheme is quite simple. A flow meter is installed on the supply line to the solar collector to meter the

amount of water flow going through the solar loop. This total flow is used along with a monthly estimate of solar-loop temperature differences to calculate the total solar energy collected. The accuracy of the flow meter is excellent, so the final accuracy of the metering system is determined by the accuracy of the temperature difference estimate. Without more data than was recorded for the experimental system, it is very difficult to produce accurate monthly solar-loop temperature difference estimates. Even during some of the months when data is available, the mass-weighted average temperatures of both the supply and return flows do not produce an accurate monthly average temperature difference. This method produced percent errors for the three monitoring periods of 4%, -5%, and 14%. If more data were available, preferably several years for the same system and location, then it is possible that accurate monthly temperature difference estimates could be produced.

The cost of this method is lower than the two prior reviewed schemes. The only cost is a flow meter and its installation. This scheme is also rather easy to read. One number is read from the physical system (flow volume), and this is multiplied by a couple of constants (the heat capacity of water and the density of water), and the estimated monthly average temperature difference. This system is also rather tamperproof; it would be possible although quite difficult to falsely run up the flow meter value.

Despite the advantages of this scheme, there would be large amounts of work and bureaucracy required to develop a suitable system able to determine accurate average monthly solar-loop temperature differences. Until this problem is solved and a universal procedure developed, the difficulties producing accurate temperature differences are too great for this scheme to be used in a consumer program such as NC Green Power.

Table 6.4 "Solar Temperature Difference Metering" Applied to Data

	Period 1		Period 2		Period 3	
	4: Solar flow and temp. diff. estimates (solar alone)	actual solar (kWh)	4: Solar flow and temp. diff. estimates (solar alone)	actual solar (kWh)	4: Solar flow and temp. diff. estimates (solar alone)	actual solar (kWh)
Daily Avg.	4.04	4.24	5.3	5.5	2.7	3.1
Total	125.3	131.3	127.8	131.8	75.0	85.4
Percent Error	5%		3%		12%	

6.3.5 Solar Loop Temperature Difference with Watt-Hour Meter to Determine Flow Rate

This scheme does not rely on any estimates or monthly averages and has the potential to be less expensive than the other schemes that use no estimates. However, it would require the development of a new product and therefore is purely academic at this time. This method would essentially replace the flow meter of a thermal meter with a watt-hour meter connected to the solar pump. Colon and Long [23] showed that in a typical solar loop the flow rate can be accurately determined from the power being used by the solar pump. The main disadvantage of this system is that each meter would have to be calibrated to the specific solar system. It is not clear at this time the best way to perform such a calibration, but this could potentially be difficult and make accuracy hard to quantify. The temperature difference of the solar-loop is measured with thermocouples, which can give very accurate results when measuring temperature differences. No table of

results was included for this scheme because no such flow meter was installed from which to collect the needed data.

If the calibration issue were overcome, it is believed that a large production level of these meters would cost considerably less than the currently available flow-meter equipped thermal energy meters. If the cost of this specially designed meter was much less than the current thermal meters and any problems with calibration and accuracy were overcome this could prove to be the preferred metering scheme solely because of the affordability, even if this meant a convoluted correlation between the metered value and the offset electric energy. This would only be the case if the hardware was greatly less expensive than a physical flow meter based thermal meter.

Chapter SEVEN CONCLUSIONS

The SDHW system monitoring allowed for a very good understanding of the general dynamics of the entire SDHW system. Since a large portion of this monitoring was performed with thermal meters their reactions to the system dynamics was also gathered. Primarily of note was the slow time response of the thermal meter temperature probes as they were required to be installed due to incompatibility of the probes' mounting sleeve and piping available in the US.

System losses were shown to be significantly larger than expected. This was due in part to minor thermal short circuits and pipe thermosiphoning, both of which cause hot water tanks to lose more heat than most consumers realize. It was also due in part to several uninsulated sections of the solar loop, both near the tank and near the solar collector. It was determined that the losses from the solar pipes alone were often higher than the amount of solar gained by the tank that day.

After a heat transfer model of the system was developed, a TRNSYS computer simulation model was also developed. The heat transfer model was crucial in the understanding of the accuracy of each energy meter. The model calculated all of the losses from the system, and showed good agreement with the experimental results. The TRNSYS model was then validated with the correct data. This model was used to generally show the effect of a more realistic draw profile than the one implemented during the majority of the testing. It also served to demonstrate the effectiveness of a SDHW system at each end of

North Carolina. More importantly, the model was used to examine the relationship between the two major metering schemes and the amount of electric energy offset by the use of the solar system.

The goal of this project was to develop an experimentally verified metering methodology for SDHW systems that was able to well represent the amount of auxiliary energy offset by the solar energy collected. The analysis suggests that the only meterable quantity able to consistently represent the amount of offset energy is the hot water load meter minus the electric meter plus the experimentally determined standard tank losses. The solar energy metered alone was found to not have a consistent relationship with the amount of offset electric energy, thus making it nearly impossible to correlate the metered value to the desired value of the amount of electric energy offset by the solar system. Although the scheme using both the hot water load thermal meter and the electric meter showed it was able to effectively 'meter' the amount of electric energy offset, it does have some drawbacks. In particular, the high cost of the two meters and potential erroneous load readings when used in a direct SDHW system. Perhaps the first problem may be overcome with a different style of thermal meter unknown to the author, barring this, the cost of this system may make resistance to it use too high for widespread use. The second problem may be overcome by the selection of a thermal meter containing a flow meter capable of being installed in the hot water line

Literature Citations

[1] Anonymous, 2003, "Solar Decathlon, Energy Facts and Figures," Available at: http://www.eere.energy.gov/solar_decathlon/energy_facts.html

[2] Grillot, M.J., 2003, "International Energy Annual 2001," Energy Information Administration, Washington, D.C., p. 183

[3] Latta, R, "A Look at Residential Energy Consumption in 2001," U.S. Department of Energy, Energy Information Administration

[4] Shirley, L., June, 2003, *State Energy Plan,* State Energy Office and Appalachian State University Energy Center, pp. 47-48

[6] Cragan, K.E., Klein, S.A., and Beckman, W.A., 1995, "Impact on a Utility, Utility Customers and the Environment of an Ensemble of Solar Domestic Hot Water Systems," Proceedings, 1995 ASES Conference

[7] Carlisle and Barrett, 1992, "Opportunities for Utility Involvement with Solar Domestic Hot Water," Proceedings, 1992 ASES Conference

[8] Anonymous, 2002, "Florida Sunshine – Natural Source for Heating Water," National Renewable Energy Laboratory

[9] Rader, N. and Hempling, S. 2001, "The Renewable Portfolio Standard, A Practical Guide," National Association of Regulatory Utility Commissioners

[10] Anonymous, 2004, "www.ncgreenpower.org"

[11] Anonymous, 1999, *CR10X Handbook,* Campbell Scientific Inc.

[12] Knudsen, S., 2002, "Consumer's Influence on the Thermal Performance of Small SDHW Systems – Theoretical Investigations," Solar Energy Vol. 73, No. 1, pp. 33-42

[13] Anonymous, 1995, fact sheet, "Energy Efficient Water Heating," National Renewable Energy Laboratory (NREL)

[14] Anonymous, 1998, "Energy Conservation Program for Consumer Products: Test Procedure for Water Heaters; Final Rule," *Federal Register*, Vol. 63, No. 90. pp. 260005-260006

[15] Incoperia and DeWitt, 1996, *Introduction to Heat Transfer,* John Wiley & Sons, New York

[16] Bejan, A., 1995, *Convection Heat Transfer,* John Wiley & Sons, New York, pp. 198-200

[17] Kreith, F. and Bohn, M.S., 1986, Principles of Heat Transfer, 4th Edition, Haper & Row, New York

[18] Burch, J. and Murley, C.S., 1995, "Field monitoring of Solar Domestic Hot Water Systems Based on Simple Tank Temperature Measurement," Proceedings, 1995 ASES Conference

[19] Burch, J.D., Wood, B.D., Huggins, J.C., and Thornton, J.W., 1992, "Simulation-Based Ratings for Solar Hot Water Systems," Proceedings, 1993 ASES Conference

[20] Song, J. and Wood, B.D., 1999, "Effects of Pluming Attachments on Heat Losses From Solar Domestic Hot Water Storage Tanks," Proceedings, 2000 ASES Conference

[21] Anonymous, 2001, "Energy Conservation Program for Consumer Products: Energy Conservation Standards for Water Heaters," *Federal Register*, Vol. 66, No. 11, pp. 4475-4485

[22] Anonymous, 1999, *1995 ASHRAE Applications Handbook*, pp. 48.9-48.11

[23] Colon, C.J. and Long, S.M. 1998, "A Non Invasive Experimental Method for the Determination of Flow Rate in a Photovoltaic Pumped Solar Domestic Hot Water System." Proceedings, 1998 ASES

[24] Solar Energy Laboratory, "TRNSYS version 15 Users Manual," University of Wisconsin-Madison, Madison, WI,